U.S. Department of Transportation

Federal Railroad Administration

Heavy Point Frog Performance under Passenger Vehicles

Office of Research, Development, and Technology
Washington, DC 20590

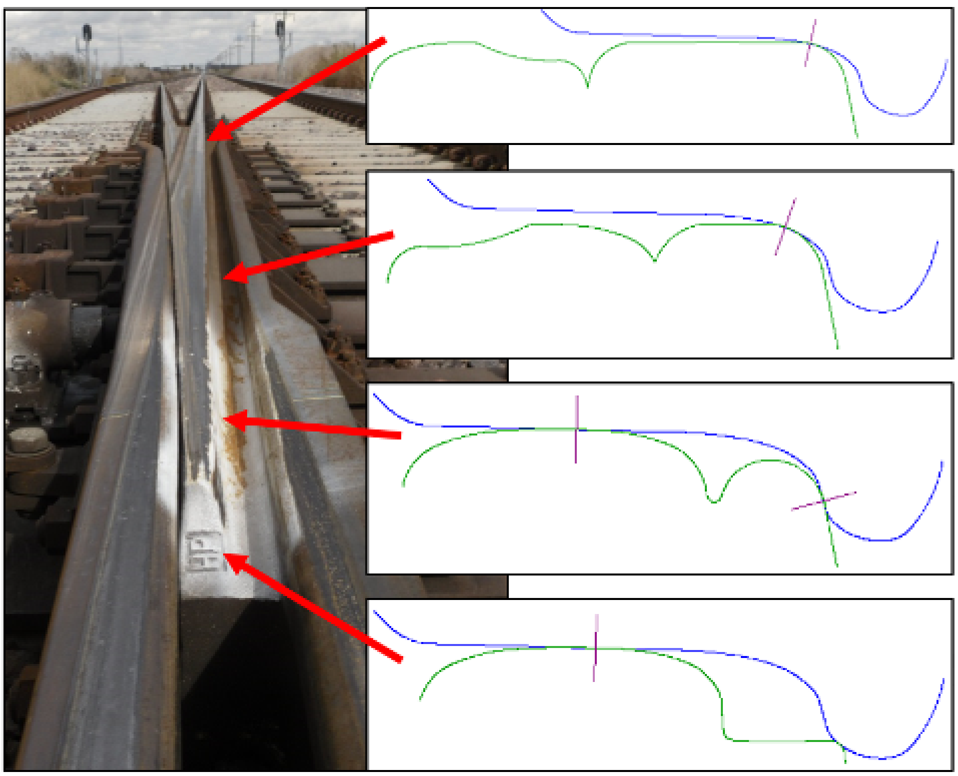

DOT/FRA/ORD-16/19

Final Report
June 2016

REPORT DOCUMENTATION PAGE			*Form Approved OMB No. 0704-0188*

1. AGENCY USE ONLY (Leave blank)	2. REPORT DATE	3. REPORT TYPE AND DATES COVERED
	June 2016	Technical Report – July 2014

4. TITLE AND SUBTITLE Heavy Point Frog Performance	5. FUNDING NUMBERS DTFR53-11-D-00008 Task Order 347
6. AUTHOR(S) Anna Rakoczy, Xinggao Shu, David Davis, Dingqing Li	
7. PERFORMING ORGANIZATION NAME(S) AND ADDRESS(ES) Transportation Technology Center, Inc. P.O. Box 11130 55500 DOT Road Pueblo, Colorado 81001	8. PERFORMING ORGANIZATION REPORT NUMBER
9. SPONSORING/MONITORING AGENCY NAME(S) AND ADDRESS(ES) U.S. Department of Transportation Federal Railroad Administration Office of Railroad Policy and Development Office of Research and Development Washington, DC 20590	10. SPONSORING/MONITORING AGENCY REPORT NUMBER DOT/FRA/ORD-16/19
11. SUPPLEMENTARY NOTES COR: Ali Tajaddini	
12a. DISTRIBUTION/AVAILABILITY STATEMENT This document is available to the public through the FRA Web site at http://www.fra.dot.gov.	12b. DISTRIBUTION CODE

13. ABSTRACT (Maximum 200 words)

Federal Railroad Administration contracted with the Transportation Technology Center, Inc., Pueblo, Colorado, to conduct an investigation of passenger vehicle performance running through heavy point frog (HPF) up to speeds of 110 mph. A NUCARS® simulation study was performed with various conditions of the track and vehicle systems, and for each case the results demonstrated that the HPF can be used successfully for Class 6 track speed with passenger equipment. The work has produced the following railroad impacts:

- Analytical results of HPF performance with passenger equipment traveling over these sections at speeds up to 120 mph
- Results contribute to assessment of the potential risks and dynamic effects of HPFs
- Evaluation of HPF application to high-speed rail (HSR) operations

The work has produced the following recommendations:

- The limited test data performed on the Chicago – St. Louis HSR line provided good validation of NUCARS simulation models. However, the test was run at 79 mph. It is recommended to perform dynamic testing with passenger equipment and test the vehicle response and wheel/rail forces going through the HPFs at speeds up to 110 mph.

14. SUBJECT TERMS Heavy Point Frog (HPF) FRA Vehicle Track Interaction (VTI) safety criteria High-speed Rail (HSR) operations	15. NUMBER OF PAGES 112
	16. PRICE CODE

17. SECURITY CLASSIFICATION OF REPORT	18. SECURITY CLASSIFICATION OF THIS PAGE	19. SECURITY CLASSIFICATION OF ABSTRACT	20. LIMITATION OF ABSTRACT
Unclassified	Unclassified	Unclassified	

NSN 7540-01-280-5500 Standard Form 298 (Rev. 2-89)

Prescribed by ANSI Std. 239-18
298-102

METRIC/ENGLISH CONVERSION FACTORS

ENGLISH TO METRIC

LENGTH (APPROXIMATE)

1 inch (in)	=	2.5 centimeters (cm)
1 foot (ft)	=	30 centimeters (cm)
1 yard (yd)	=	0.9 meter (m)
1 mile (mi)	=	1.6 kilometers (km)

AREA (APPROXIMATE)

1 square inch (sq in, in^2)	=	6.5 square centimeters (cm^2)
1 square foot (sq ft, ft^2)	=	0.09 square meter (m^2)
1 square yard (sq yd, yd^2)	=	0.8 square meter (m^2)
1 square mile (sq mi, mi^2)	=	2.6 square kilometers (km^2)
1 acre = 0.4 hectare (he)	=	4,000 square meters (m^2)

MASS - WEIGHT (APPROXIMATE)

1 ounce (oz)	=	28 grams (gm)
1 pound (lb)	=	0.45 kilogram (kg)
1 short ton = 2,000 pounds (lb)	=	0.9 tonne (t)

VOLUME (APPROXIMATE)

1 teaspoon (tsp)	=	5 milliliters (ml)
1 tablespoon (tbsp)	=	15 milliliters (ml)
1 fluid ounce (fl oz)	=	30 milliliters (ml)
1 cup (c)	=	0.24 liter (l)
1 pint (pt)	=	0.47 liter (l)
1 quart (qt)	=	0.96 liter (l)
1 gallon (gal)	=	3.8 liters (l)
1 cubic foot (cu ft, ft^3)	=	0.03 cubic meter (m^3)
1 cubic yard (cu yd, yd^3)	=	0.76 cubic meter (m^3)

TEMPERATURE (EXACT)

[(x-32)(5/9)] °F = y °C

METRIC TO ENGLISH

LENGTH (APPROXIMATE)

1 millimeter (mm)	=	0.04 inch (in)
1 centimeter (cm)	=	0.4 inch (in)
1 meter (m)	=	3.3 feet (ft)
1 meter (m)	=	1.1 yards (yd)
1 kilometer (km)	=	0.6 mile (mi)

AREA (APPROXIMATE)

1 square centimeter (cm^2)	=	0.16 square inch (sq in, in^2)
1 square meter (m^2)	=	1.2 square yards (sq yd, yd^2)
1 square kilometer (km^2)	=	0.4 square mile (sq mi, mi^2)
10,000 square meters (m^2)	=	1 hectare (ha) = 2.5 acres

MASS - WEIGHT (APPROXIMATE)

1 gram (gm)	=	0.036 ounce (oz)
1 kilogram (kg)	=	2.2 pounds (lb)
1 tonne (t)	=	1,000 kilograms (kg)
	=	1.1 short tons

VOLUME (APPROXIMATE)

1 milliliter (ml)	=	0.03 fluid ounce (fl oz)
1 liter (l)	=	2.1 pints (pt)
1 liter (l)	=	1.06 quarts (qt)
1 liter (l)	=	0.26 gallon (gal)
1 cubic meter (m^3)	=	36 cubic feet (cu ft, ft^3)
1 cubic meter (m^3)	=	1.3 cubic yards (cu yd, yd^3)

TEMPERATURE (EXACT)

[(9/5) y + 32] °C = x °F

QUICK INCH - CENTIMETER LENGTH CONVERSION

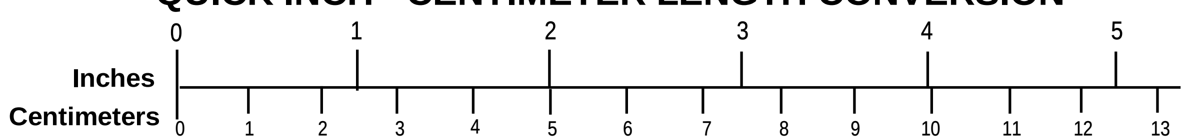

QUICK FAHRENHEIT - CELSIUS TEMPERATURE CONVERSIO

°F	-40°	-22°	-4°	14°	32°	50°	68°	86°	104°	122°	140°	158°	176°	194°	212°
°C	-40°	-30°	-20°	-10°	0°	10°	20°	30°	40°	50°	60°	70°	80°	90°	100°

For more exact and or other conversion factors, see NIST Miscellaneous Publication 286, Units of Weights and Measures. Price $2.50 SD Catalog No. C13 10286

Updated 6/17/98

Acknowledgements

The research described in this report was funded by the Federal Railroad Administration Research and Development program.

Thanks go to Union Pacific Railroad for allowing the Transportation Technology Center, Inc. team to take measurements of heavy point frogs on Chicago – St. Louis line. Special thanks go to Dwight W. Clark, Stephen J. Ashmore, Christopher G. Rewczuk, and Christopher Roop for their direct involvement.

Thanks also go to the Voestalpine Nortrak manufacturer and supplier of trackwork and materials in North America for providing necessary HPF drawings and other files. Special thanks go to Gary Click, Brian Charles, and Gregory Wong for their time and help.

Contents

Illustrations

Tables

Executive Summary

The Federal Railroad Administration (FRA) contracted with the Transportation Technology Center, Inc. (TTCI) in Pueblo, Colorado, to investigate the performance of passenger vehicles passing through heavy point frogs (HPF) at speeds up to 110 mph. The study was performed using computer simulations with various conditions of the track and vehicle systems, and for each case the results demonstrated that the HPFs can be used for Class 6 track speed with passenger equipment.

The study did the following:

- Generated analytical results of HPF performance using passenger equipment traveling over HPF sections at speeds up to 120 mph
- Created results that contributed to assessment of the potential risks and dynamic effects of HPFs
- Evaluated the application of HPF to higher speed operations

The work has produced the following recommendations:

- The limited test data performed on the Chicago – St. Louis high-speed rail (HSR) line provided good validation of NUCARS®[*] models. However, the test was run at a speed of 79 mph. It is recommended to perform dynamic testing with passenger equipment and test the vehicle response and wheel-rail forces going through the HPF at speeds up to 110 mph.

[*] NUCARS® is a registered trademark of Transportation Technology Center, Inc., Pueblo, CO

1. Introduction

Heavy point frogs (HPFs) reduce the standard guard check distance from 4 feet 6 5/8 inches (54.6250 inches) to 4 feet 6 29/64 inches (54.4531 inches), which does not comply with the safety standards for Class 5 track and above. The Association of American Railroads (AAR) obtained a waiver from FRA to use these frogs in class 5 track. Since then, HPFs have been operated in Class 4 and 5 tracks with good results for many years.

This study provides analytical results for passenger equipment traveling over HPF at speeds up to 120 mph. The purpose of this study is to assess the safety performance of HPFs on Class 6 track.

1.1 Background

HPFs are used extensively by North American railways in freight service. They have a long history of service, dating back to the 1980s. The design has provided significant service life benefits for heavy haul operations. The HPF is a unique design, which has a thicker (i.e., wider) frog point. It offers safety benefits over a traditional frog because there is more mass to reduce metal fatigue from impact loading, greater durability, reduced susceptibility to point rollover, and better ability to guide the wheel flange toward the proper flangeway. The thicker point creates a deviation from the theoretical gage line in each route through the frog for a distance of about 4 feet for mainline No. 20 and No. 24 frogs. The maximum gage line deviation is at the theoretical 5/8 inch thickness point of the frog and reduces back to the theoretical gage line at about 4 feet into the frog point. Thus, the maximum gage line deviation is 11/64 (0.1719) inch for each route (Figure 1).

Application to higher speed operations will require assessment of the potential risks and dynamic effects of HPFs. Guard rails are positioned to account for the alignment deviation on the frog side. The larger ride quality issue for HSR HPF operations is the arrangement of the guard rails. In current operations, the guard rail is moved 3/16 inch laterally to account for the heavy points. This may result in more wheelsets striking the guard rail than would occur for standard points. The flangeway between the running rail and the guard rail is narrower. Thus, a study of the length and entry configuration of the guard rail for HSR operations is needed.

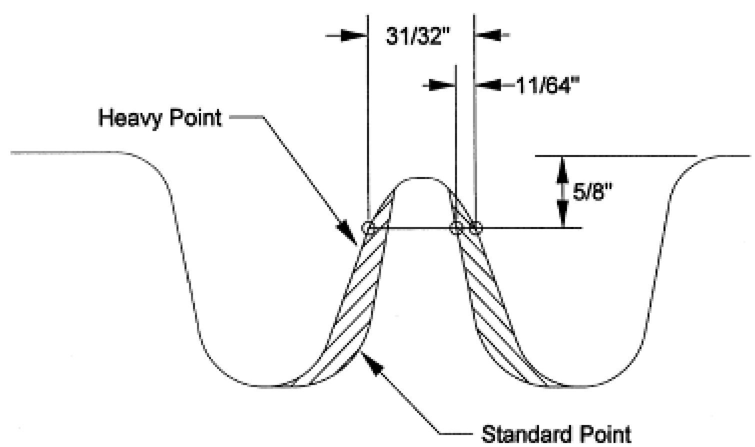

Figure 1. Section 5/8-inch (0.625-inch) point of HPF and standard frogs

1.2 Objectives

The primary aim of this research work was to investigate how the HPF will perform in operations up to 110 mph and if there is any risk for operation at up to Class 6 track speed for passenger equipment.

1.3 Overall Approach

- Model mainline operations on HPFs for HSR operations from 20 to 120 mph and investigate the effects of track parameters including rail profiles of HPFs.
- Conduct NUCARS® simulations on a selected passenger vehicle and locomotive deemed to be representative for HSR operations.
- Use FRA Vehicle Track Interaction (VTI) safety criteria to examine the safety of the equipment based on NUCARS® simulation results.
- Present a comprehensive summary of key findings regarding HPFs and how they relate to vehicle performance.

1.4 Scope

The simulation work only concerned HPF: operation through switches was not studied.

Both new and worn HPFs were modeled. The worn frogs were measured using a portable electronic profile measurement device (MiniProf) on typically worn HPFs on the Chicago – St. Louis HSR line.

A locomotive and a passenger with two alternative wheel profiles were modeled.

1.5 Organization of the Report

TTCI separated the work in this project into several tasks. Figure 2 shows the work breakdown structure. The subsequent chapters describe each of the tasks in detail.

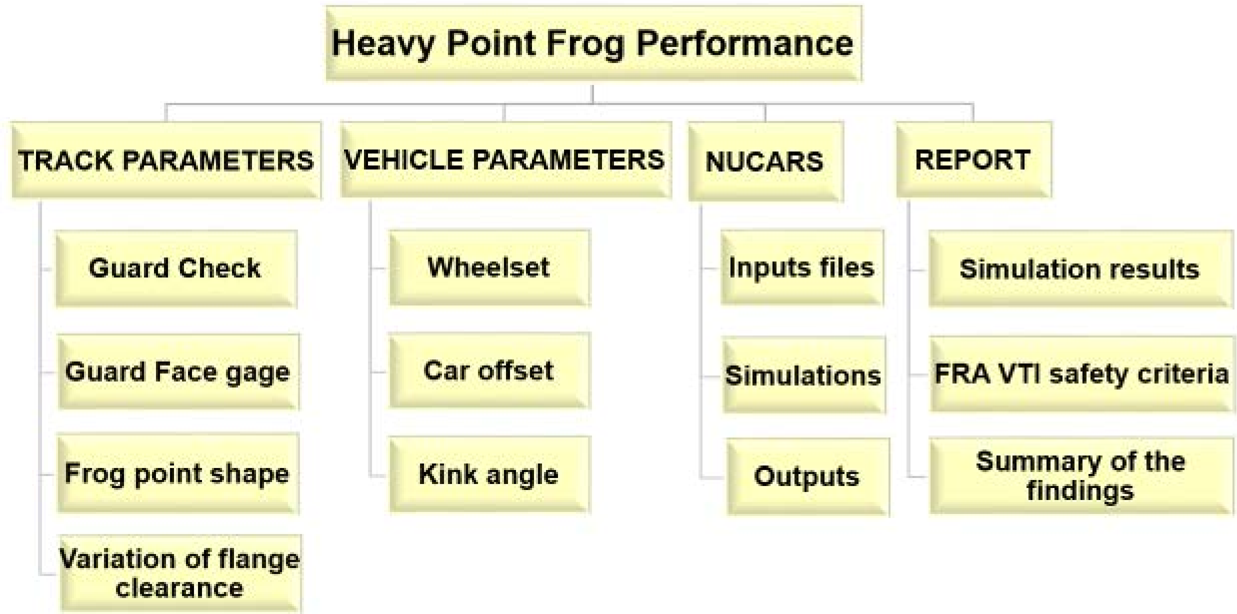

Figure 2. Work Breakdown Structure

Chapter 1 of this report presents the introduction, problem statement, objective, and scope of the research. Chapter 2 reviews the principles of the NUCARS® modeling that was used in the study. Basic information of vehicle and track models, track perturbations, and simulation matrixes for parametric study are introduced. The combinations of parameters for modeling are provided for measured and design HPFs.

Chapter 3 describes the measurements of in-service HPFs. The equipment, requirements, and procedures of measurement are described. Post-processing algorithm of measured rail profiles is presented, and examples of measured profiles are plotted. Chapter 4 presents two types of the design HPFs that were modeled in this study. The process of developing input files for design HPFs is described.

Chapter 5 compares the simulation results with FRA Track Safety Standards to identify wheel-rail forces and accelerations of vehicles that are outside the limiting conditions for a particular class of track. The limited test data performed on the Chicago – St. Louis HSR line is compared with simulation results to verify validation of NUCARS® models.

Chapter 6 presents the summary and conclusions of the research performed for the scope of this project.

2. NUCARS® Modeling

NUCARS® is a computer program developed by TTCI, a subsidiary of AAR, for modeling rail vehicle transient and steady-state response. It belongs to a class of programs commonly termed multi-body simulations. The NUCARS® simulations assess different scenarios of vehicle response to track geometry.

In this study, NUCARS® was used to evaluate the effects of HPF in HSR operations from 20 to 120 mph for FRA Class 6 track. Simulations of two car models (generic power and coach cars) with alternative wheel profiles running on the mainline route of the proposed No. 24 straight HSR frog were conducted.

2.1 Vehicle and Track model

Two vehicles were modeled: a GP 40 locomotive and the DOTX 216 (T16) passenger car.

GP 40 Locomotive car geometry and connections:

- Truck center spacing: 408 inches
- Axle spacing: 108 inches
- Wheel diameter: 40 inches
- Wheel profiles: APTA 340 and APTA 140
- Traction rod between carbody and truck frame
- Yaw damper between carbody and truck
- Carbody roll stabilizer
- Coil spring secondary suspension
- Primary suspension: radial arm with coil spring and bushing element
- Vertical and lateral damper in primary and secondary suspension
- Vertical damper in primary suspension
- Motor and gear connections with axles

T16 car geometry and connections:

- Truck center spacing: 720 inches
- Axle spacing: 102 inches
- Wheel diameter: 36 inches
- Wheel profiles: APTA 340 and APTA 140
- Anchor rod between carbody and truck bolsters
- Simple gap-type side bearings between the bolster and the truck frame
- Coil spring secondary suspension between the carbody and truck bolster
- Bolster connected to truck frame through a center plate
- Coil spring primary suspension supported by equalizer beams

- Equalizer beams rest on the bearing boxes
- Vertical and lateral rotary dampers in the secondary suspension

The carbody was modeled as a rigid body. Equalizer beams were modeled as flexible bodies with torsional modes. Each truck was modeled using separate bodies for the truck bolster, truck frame, both equalizer beams, and both axles.

The vehicle model parameters were measured through characterization tests or calculated based on manufacturer's drawings (1). APTA wheel profiles and 0.5 wheel-rail friction coefficients were used in the simulations.

Two types of wheel profiles, APTA 340 and APTA 140, were used in the NUCARS® simulation. Figure 3 compares these two wheel profiles and also shows the standard wheel profile, AAR 1-B. The wheel back-to-back distance of the APTA 340 wheelset is 53.375 inches (1,355.7 millimeters). A 53.0 inches (1,350.9625 mm) wheel back-to-back distance was used for APTA 140 wheel simulations for comparison with APTA 340 wheel profiles.

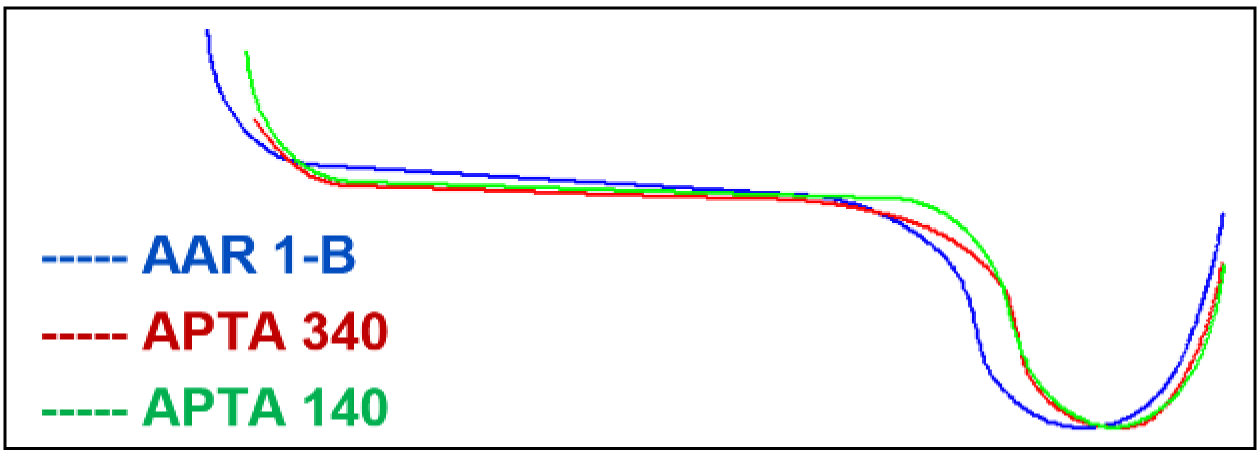

Figure 3. Wheel profiles

Rail profiles through frogs are significantly different to those in open track. Turnout rail profiles and contact geometries were varied along the track through the HPF in the simulations. The NUCARS® wheel-rail penetration contact model was used to calculate the wheel-rail contact geometry and forces. The rail was connected to ground with track stiffness and damping.

Wheel and rail profiles were preprocessed as inputs for NUCARS® simulations. One of the biggest challenges of this project was developing a series of rail profiles for all sections of HPF. The process of developing these files is described in section 3.4 for measured profiles and in section 4.2 for as-designed profiles.

A turnout generally consists of three sections: the switch, closure, and frog. However, this study focused only on the frog section. NUCARS® simulations were performed on a selected passenger vehicle and a locomotive deemed to be representative for HSR operations. The design and measured rail profiles were used in the simulations. The NUCARS® simulations were performed on mainline tangent track.

2.2 Track Perturbations

The allowable 31-foot, alinement mid-chord offset for Class 6 track is 0.5-inch (49 CFR §213.327). However, the track gage must be at least 56 inches and not more than 57.25 inches (49 CFR §213.323). Thus, for nominal track gage (56.5 inches) the maximum perturbation allowed is 0.5 inch on one rail to the inside. For narrow gage (56 inches) no lateral perturbations are allowed. (2)

The allowable 31-foot, surface mid-chord offset for Class 6 track is 1 inch on either rail (49 CFR §213.331). (2) The difference in cross level between any two points less than 62 feet apart may not be more than 1.5 inches (49 CFR §213.331). (2) Therefore, the perturbation used for simulations are: vertical perturbation – left rail (running rail) up 0.5 inch and right rail (including HPF) down 1 inches; lateral perturbation – left rail 0 inch and right rail to inside 0.5 inch. The perturbation was assigned to the model as sinusoidal waves of 31 inches and 62 inches in length, as Figure 4 shows.

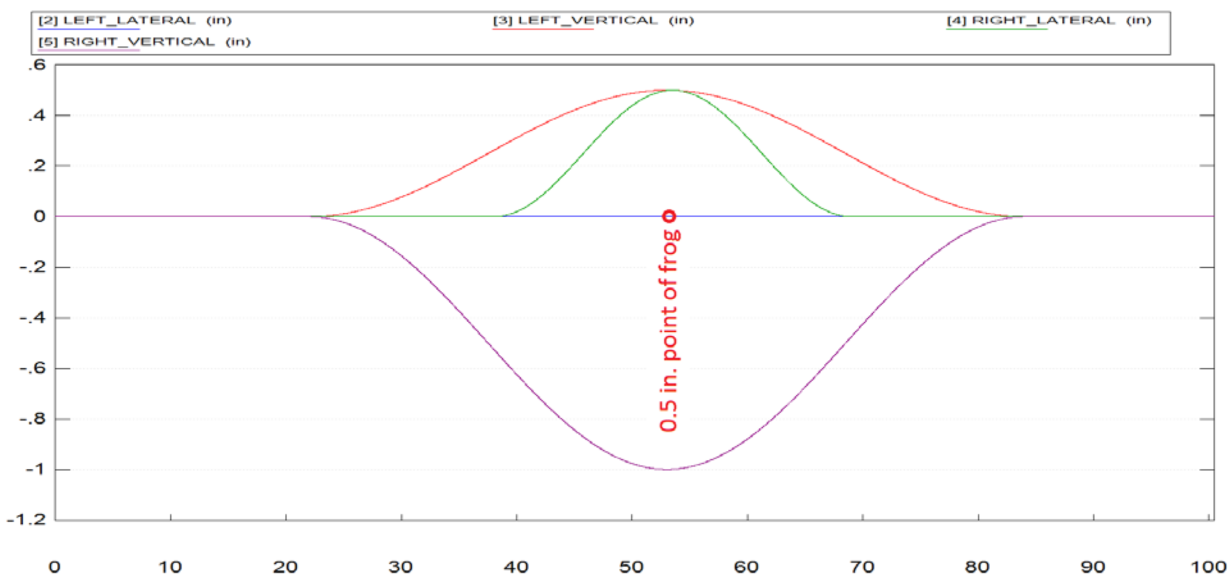

Figure 4. Plot of the extreme perturbations defined for the simulation

2.3 Simulation Matrix

The matrix of simulation included design and measured HPFs. The vehicles used for simulations were the T16 passenger car and a GP40 locomotive. The simulations were run with speeds from 20 mph to 120 mph.

All measured HPFs were moveable wing, fixed point frogs. They are commonly known as "spring" frogs due to the spring that holds the moveable wing against the frog point for mainline operations. For measured HPFs, track gage and flangeway were not varied for the parametric studies. These properties were used in the simulations as they were measured. The vehicle variables were: positive and negative car lateral offsets and two wheelsets: APTA340 with

53.3750 inches back-to-back spacing, and APTA140 with 53 inches back-to-back spacing. Table 1 summarizes the simulation cases for the measured HPFs.

Table 1. Modeling Matrix for Measured HPFs

Speed	**20 mph - 120 mph**			
Vehicle	**T16 and GP40**			
Location of HPFs / **Case**	**Pontiac 92.48**	**Pontiac 94.98**	**Ballard 108.83**	**Normal 121.4**
1. Wheelset APTA340	x	x	x	x
2. Wheelset APTA140	x	x	x	x
3. Wheelset APTA340 with lateral offset of the car to the left (positive offset)	x	x	x	x
4. Wheelset APTA340 with lateral offset of the car to the right (negative offset)	x	x	x	x

For as-designed HPFs, two types were considered in the modeling: moveable wing (spring) frogs, and rail bound manganese frogs (RBM). Section 4.1 briefly describes the two frog types modeled.

For as-designed HPFs, the track gage, flangeway, track perturbations, and car offsets were varied. Two track gages were considered: nominal 56.5 inches and narrow track gage 56.0 inches. For nominal gage track, the following guard-rail flangeways were simulated: 1.625 inches, 1.875 inches, and 2.0 inches. Nortrak's design values for the HPF point-wing flangeway were used: 1.875 inches for the RBM frog, and 2.0 inches for the spring frog. This dimension relates to the distance between the theoretical point and the wing, which is not the same as the clearance between the frog and the wing. This clearance changes along the frog. Appendix B presents some sections and dimensions of the as-designed HPF.

Various track conditions were modeled: no perturbation, vertical and lateral perturbation, and kink angle of the carbody. The lateral and vertical perturbations were simulated according to the maximum perturbations allowed by FRA's Track Safety Standard.

Lateral offsets of the car bodies were modeled. Based on calculations and expert opinion, the offsets used for the simulation were 3 inches for the T16 car and 6 inches for the GP40 locomotive. The simulations were run with positive and negative offsets.

Most of the parametric studies were performed with wheelset APTA 340 with 53.3750 inches back-to-back spacing, but wheelset APTA 140 with 53 inches back-to-back spacing was also examined. All simulations were run on tangent track. Table 2 presents the matrix of simulations for as-designed HPFs.

Table 2. Modeling Matrix for Design HPFs

	Speed	**20 mph - 120 mph**			
	Wheelset	**APTA340**			
	Design/Theoretical HPF	**RBM**		**Spring**	
	Vehicle	**T-16**	**GP40**	**T-16**	**GP40**
Standard gage 56.5 inches	1. Nominal track gage with 1.875-inch flangeway - Theoretical conditions	x	x	x	x
Standard gage 56.5 inches	2. Nominal track gage with 1.875-inch flangeway with extreme perturbations - left rail up 0.5 inch and right rail down 1inch. Lateral perturbation - left rail 0 inch and right rail to inside 0.5 inch.	x	x	x	x
Standard gage 56.5 inches	3. Nominal track gage with 1.625-inch flangeway with extreme perturbations - left rail up 0.5 inch and right rail down 1 inch. Lateral perturbation - left rail 0 inch and right rail to inside 0.5 inch.	x	x	x	x
Standard gage 56.5 inches	4. Nominal track gage with 2.0-inch flangeway with extreme perturbations - left rail up 0.5 inch and right rail down 1 inch. Lateral perturbation - left rail 0 inch and right rail to inside 0.5 inch.	x	x	x	x
Standard gage 56.5 inches	5. Nominal track gage with 1.875-inch flangeway and Kink angle of 0.25 degree in direction to the HPF	x	x	x	x
Standard gage 56.5 inches	6. Nominal track gage, 1.875–inch flangeway, perturbations, and the lateral offset of the car to the left (positive offset)	x	x	x	x
Standard gage 56.5 inches	7. Nominal track gage, 1.875-inch flangeway, perturbations, and the lateral offset of the car to the right (negative offset)	x	x	x	x
Standard gage 56.5 inches	8. Nominal track gage with 1.875-inch flangeway, extreme perturbations, and APTA140	x	x	x	x
Narrow gage 56.0- inches"	9. Narrow track gage - Theoretical conditions	x	x	x	x
Narrow gage 56.0- inches"	10. Narrow track gage and extreme vertical perturbations - left rail up 0.5 inch and right rail down 1 inch.	x	x	x	x
Narrow gage 56.0- inches"	11. Narrow track gage and extreme vertical perturbations and Kink angle of 0.25 degree in direction to the HPF	x	x	x	x
Narrow gage 56.0- inches"	12. Narrow track gage and extreme vertical perturbations and the lateral offset of the car to the left (positive offset)	x	x	x	x
Narrow gage 56.0- inches"	13. Narrow track gage and extreme vertical perturbations and the lateral offset of the car to the right (negative offset)	x	x	x	x
Narrow gage 56.0- inches"	14. Narrow track gage, extreme vertical perturbations, and APTA140	x	x	x	x

2.4 Modeling Assumptions

The models for HPFs were developed to represent field situations. The following assumptions were made for all simulation cases:

- Tangent track.
- Both rails are straight and minimum gage occurs at the 5/8-inch point below the top of the rail.
- HPF is located on the right side (i.e., this is a right-hand turnout).
- Guard rail is positioned to create a specific (1.625-, 1.875-, or 2.0-inch) flangeway at the 5/8-inch point below the top of the rail.
- For design HPF, restraining rails are used instead of the actual wing and guard rail profiles.

Measured HPF profiles included the guard rail and the wing of the frog. The contact angle between the back of wheel and the guard rail was approximately 85.5 degrees, as shown in Figure 5 for APTA 340 and in Figure 6 for APTA 140. The contact angle between wheel back of flange and the frog wing is approximately 80 degrees, as shown in Figure 7 for APTA 340 and in Figure 8 for APTA 140.

Table 3 summarizes the contact angles for measured HPFs.

Table 3. Modeling Matrix for Design HPFs

Measured Locations	Contact Angle between Back of Wheel and	
	Guard Rail	HPF Wing
N Normal 121.4	85.6–86.4	72.0–78.3
S Ballard 108.83	85.5–86.6	75.0–81.0
S Pontiac 94.98	85.6	74.9–77.9
N Pontiac 92.49	83.0–86.4	71.0–73.0

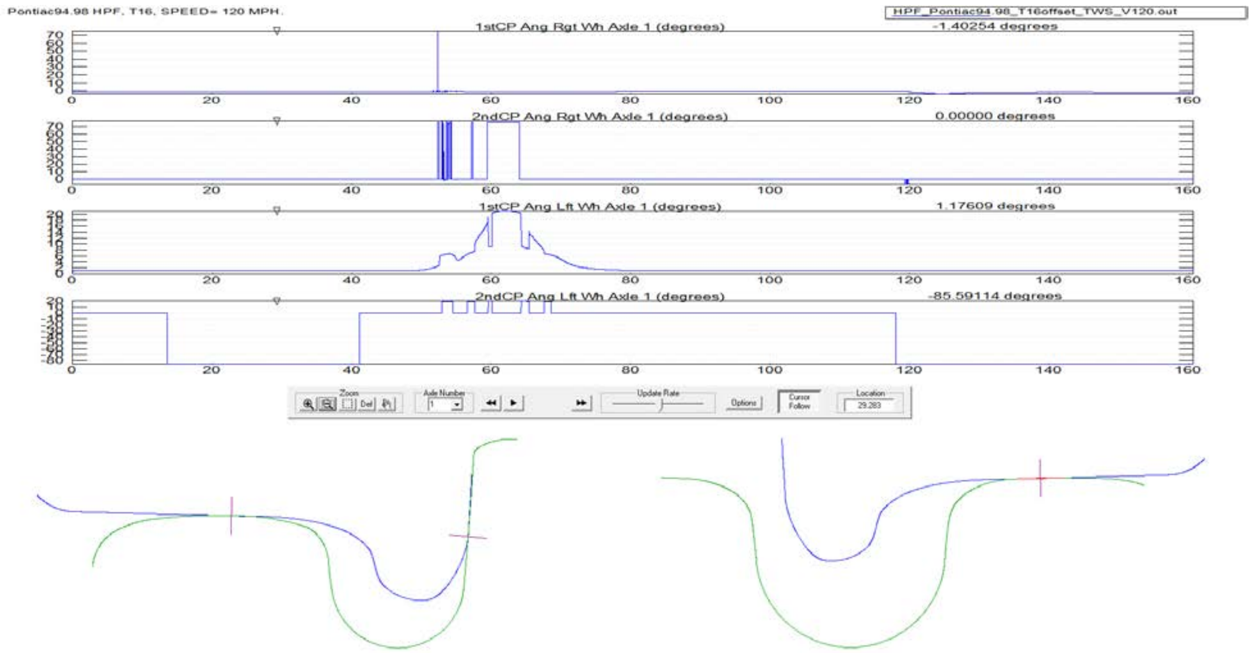

Figure 5. Contact on the guard rail with APTA 340

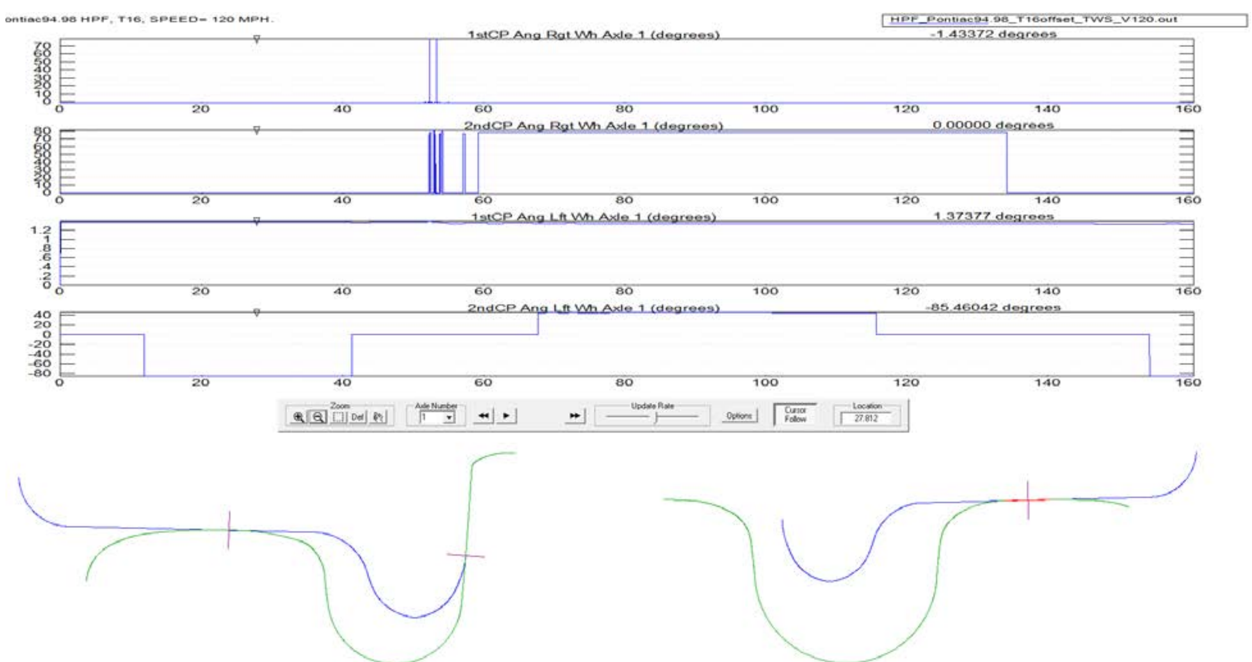

Figure 6. Contact on the guard rail with APTA 140

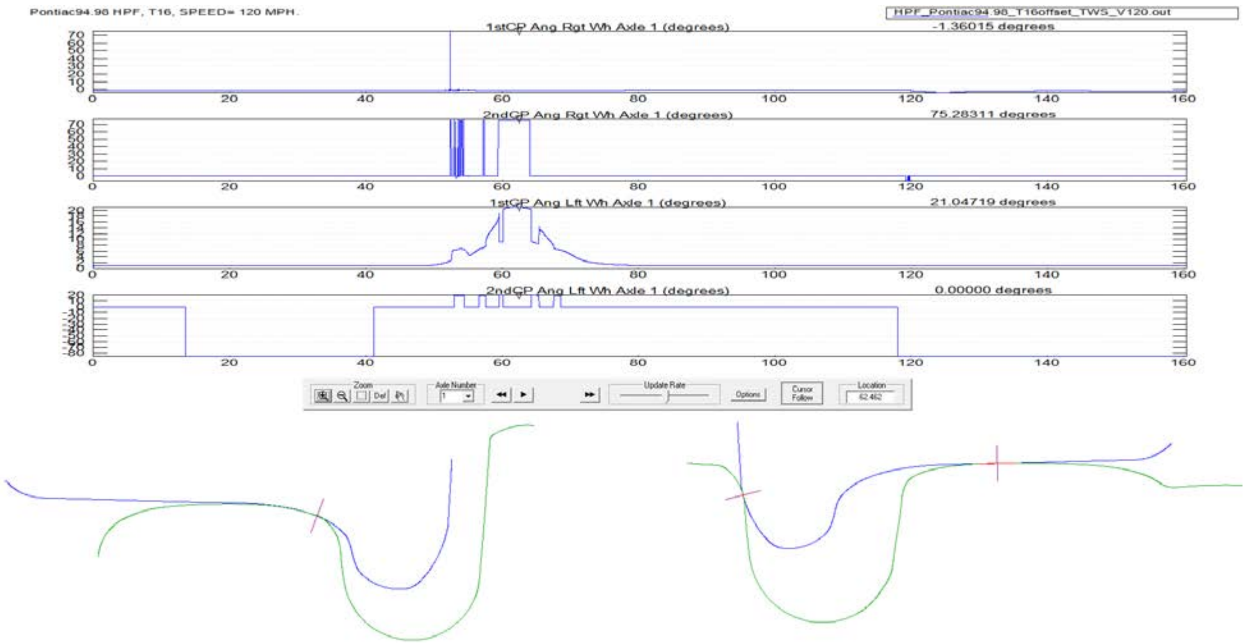

Figure 7. Contact angle on the back flange with APTA 340

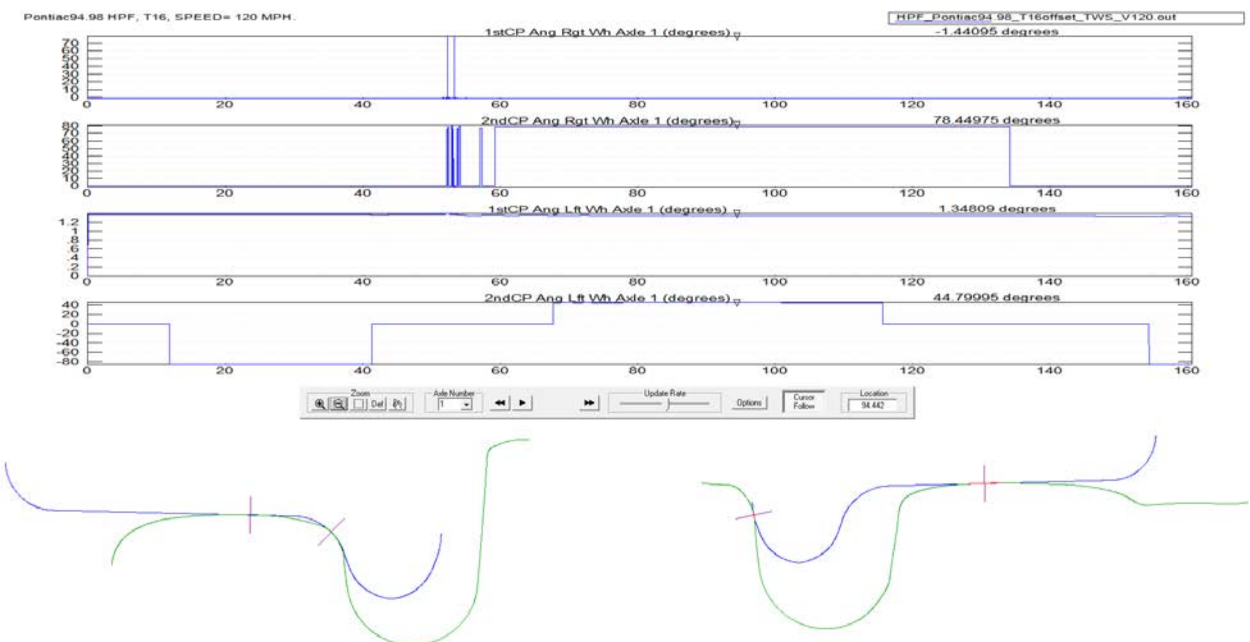

Figure 8. Contact angle on the back flange with APTA 140

For the as-designed HPF (RBM and spring) the frog rail profiles did not include wing rail profiles, instead, the restraining rails were used to simplify the frog profile variations. The wheel back contact angle on the wing rail was approximately 80 degrees, while the wheel back contact angle on the restraining rail was close to 90 degrees. Figures 9 and 10 illustrate the contact of the back of the wheel with the restraining rail. The effects of the contact angle differences on dynamic performances are discussed in Section 5.8.

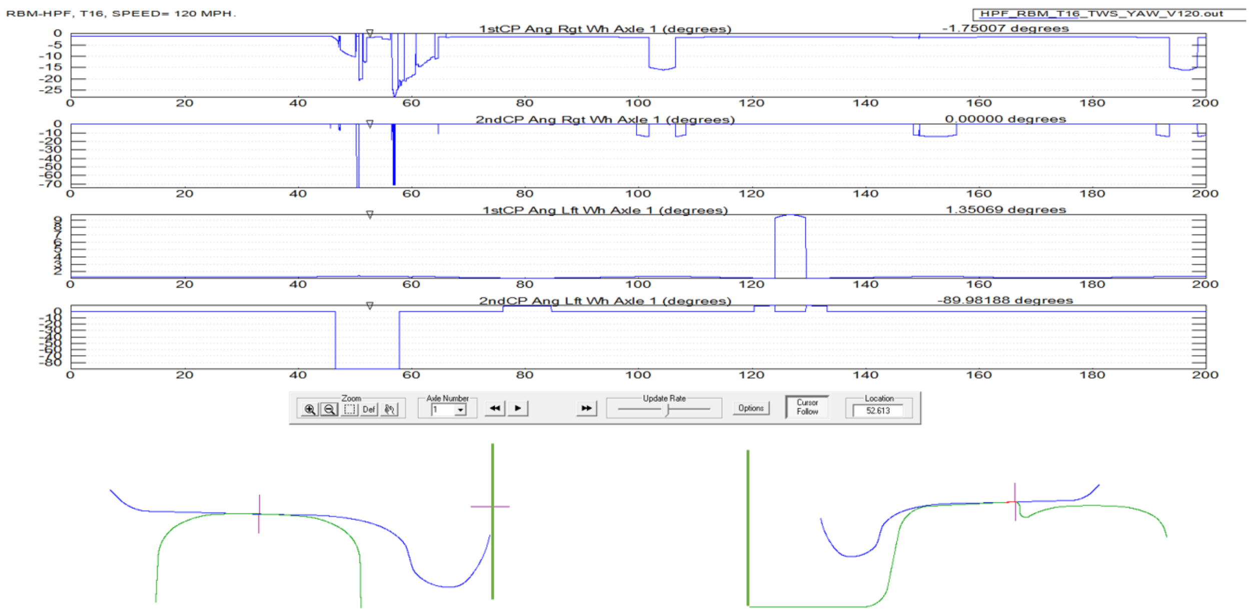

Figure 9. Contact of the back wheel with restraining rail, which represents guard rail

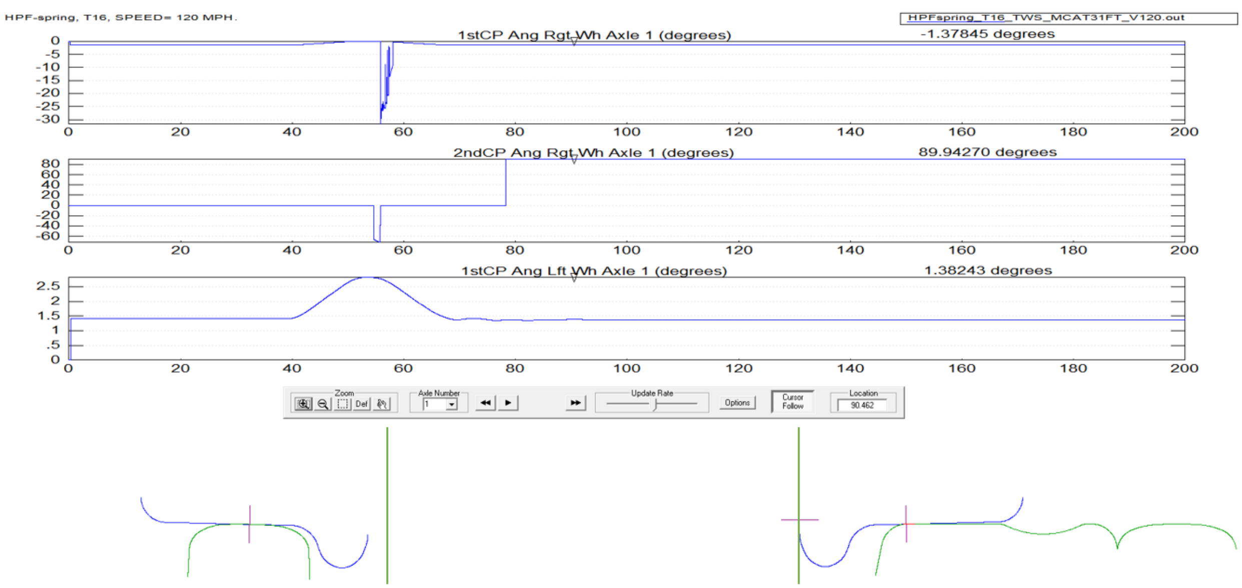

Figure 10. Contact of the back wheel with restraining rail, which represents back flange

3. In-service HPF

When a vehicle runs on special trackwork, such as frogs, a wheel may contact on several rail surfaces. This is the case with either one piece castings or when several separate rails are bolted together. The NUCARS® simulations are more realistic if measured rail profile shapes are used from the actual track being simulated. For measured HPFs, the first step was to collect the track parameters by making MiniProf measurements (3). Then the measured profiles were used to create input files for the NUCARS® simulations.

3.1 Track Parameters

The portable MiniProf instrument can measure both wheel and rail profiles. Measurements of HPF profiles for this project were taken at several locations through each HPF.

The following characteristic dimensions were also measured :

a. Guard Check — The distance between the gage line of a frog to the guard line of its guard rail or guarding face, measured across the track at right angles to the gage line
b. Guard Face gage — The distance between guard lines, measured across the track at right angles to the gage line
c. Frog point shape — Including the frog number (the ratio of its length to its breadth) and the frog angle (the angle formed by the gauge lines of the rails, which form its tongue)
d. Guard rail length and entry
e. Variation of flange clearance

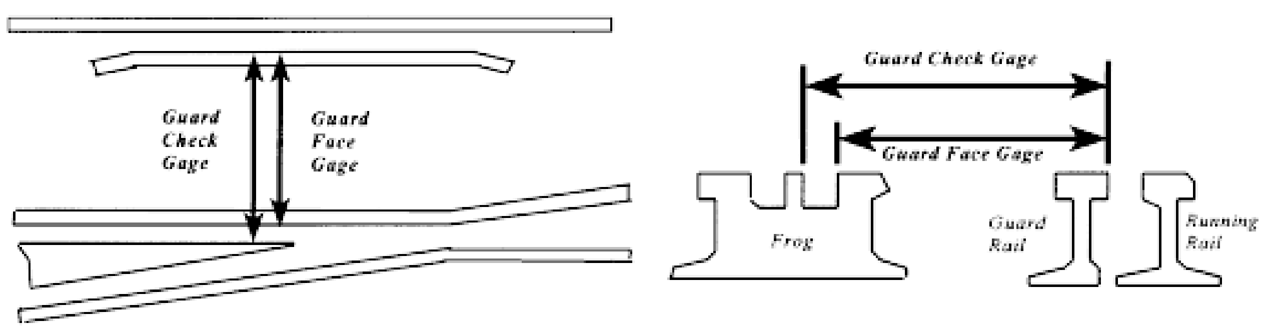

Figure 11. Description of characteristic dimensions

3.2 MiniProf

The MiniProf (from Greenwood Engineering) measuring system is a handheld tool for monitoring the cross-sectional profile of wheels, rails, and brakes. The standard MiniProf instrument for rails can be used on many different types of track and also on grooved rails. The rail unit is magnetically attached to the top of the railhead and uses the opposite rail as a reference through a telescopic rod. It can be modified to work on special profiles if required. (3)

3.2.1 Equipment

MiniProf measurement of the rail requires the following:

- MiniProf instrument
- Gage rod (rail bar)
- Custom plates
- Data acquisition system

Frog castings are nonmagnetic and may be too wide to measure all running surfaces in a single profile. Thus, custom platework is used, as Figure 12 shows. This allows a stable and secure base for the MiniProf instrument to be attached magnetically. In addition, it ensures the partial profiles are taken in the same plane, facilitating combination into a single, undistorted profile.

Figure 12. Photographs of MiniProf device (www.railway-technology.com /contractors/track/greenwood)

3.2.2 General Requirements for MiniProf Users

The following key procedures need to be applied before and during taking profile measurements:

- Ensure the MiniProf is calibrated and the correct calibration file is used.
- Clean the back of the measurement surface.
- Ensure the MiniProf is correctly located on the frog to be measured. It should be square and secure.
- If the profile measurements are carried out in separate parts (main wing, point, and branch wing) the individual measured parts should overlap to allow a proper fit (Figure 13).

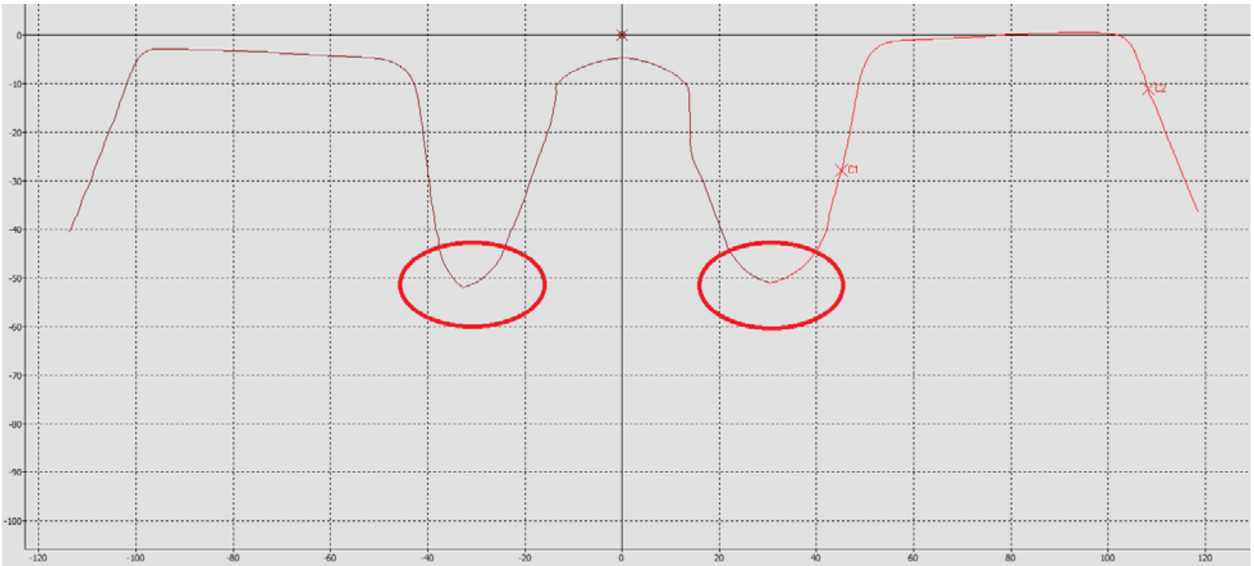

Figure 13. Marked locations of overlap of individual parts

3.2.3 Data Collection Sheet

The following information, if available, is included in the header of the measurement data file:

- Measurement date
- Measurement time
- Measurement location (shop/yard/line)
- Time in service (since installation)

A plan was followed when the cross sectional running surface profiles for the mainline route through the frog and its matching running rail were measured. At each frog, 21 locations (from 16 inches behind the 0.5-inch point and 36 inches ahead of the 0.5-inch point) were marked and running surface profiles were collected. Figure 14 shows a No. 20 HPF marked for profile measurements.

Figure 14. Marked sites for measurements

3.3 Field Measurements

The worn point frogs were measured on the Chicago – St. Louis HSR line. The measured frogs are listed in Table 4 and the locations are shown in Figures 15 and 16. All four HPFs were measured to provide a range of field conditions and for better interpretation of the simulation results.

Table 4. Locations of measured frogs

Location	Name	Size	Mile Post (MP)	Guard Check Gauge (inch)
1	N Normal	No. 24 RH	121.4	54.5
2	S Ballard	No. 24 LH	108.83	54.5
3	S Pontiac	No. 24 LH	94.98	54.5
4	N Pontiac	No. 24 RH	92.49	54.5

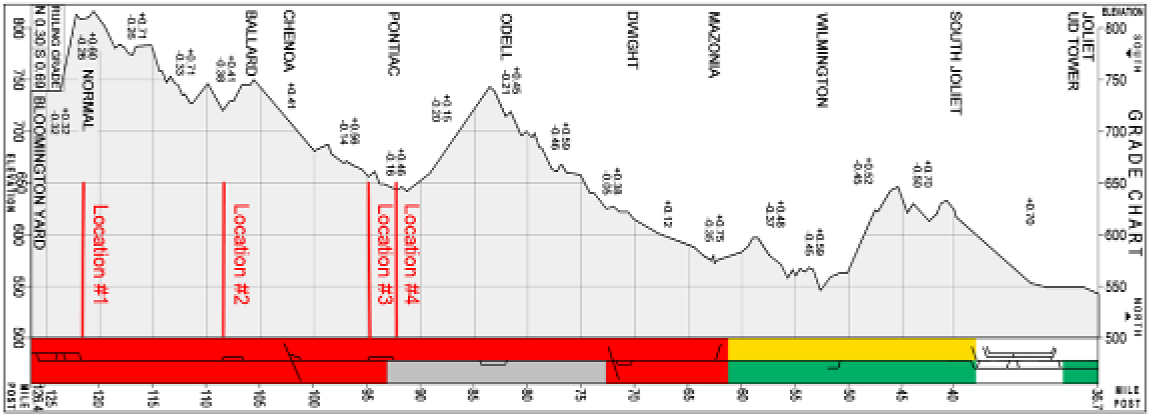

Figure 15. Locations of frogs marked on MP chart

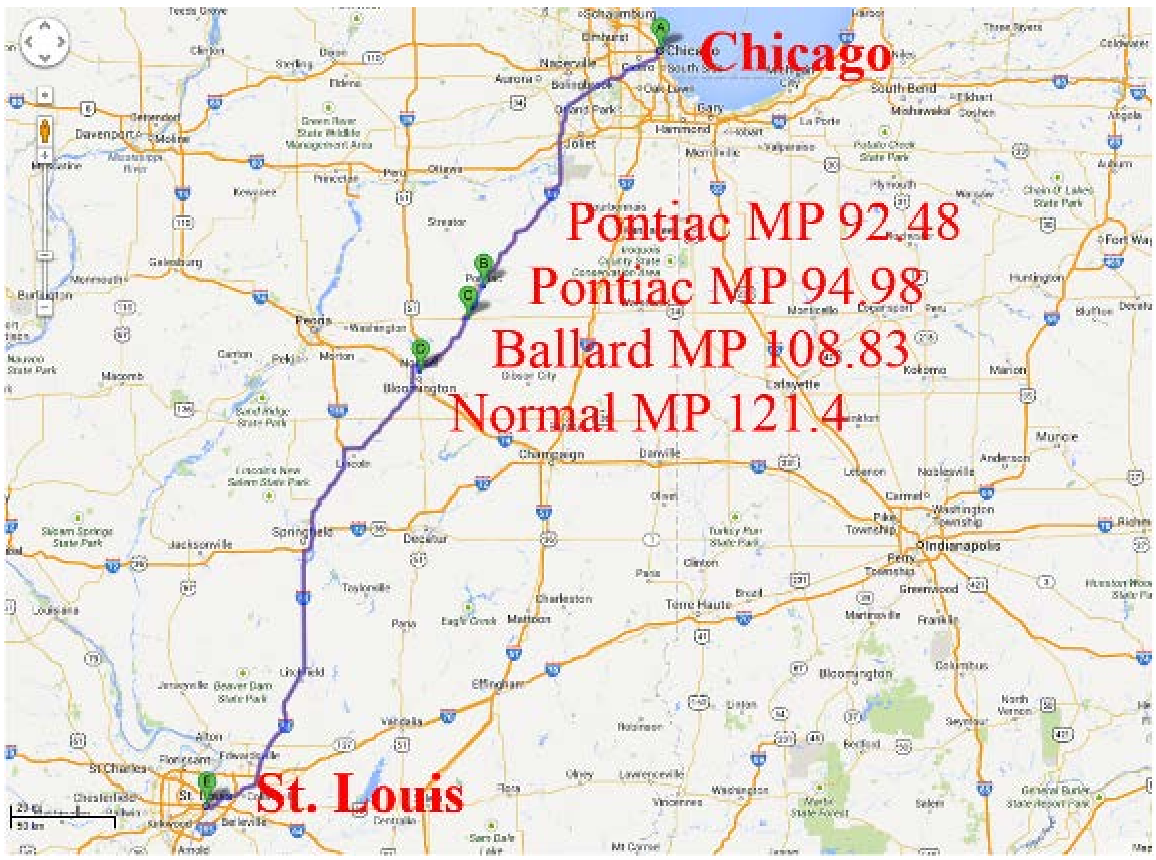

Figure 16. Locations of frogs marked on the map

The frogs were measured on October 23, 2013. The first section measured was 24 inches in front of the 0.5-inch point of frog and the last section was 64 inches behind the 0.5-inch point of frog. The spacing of profiles measured varied from 8 inches (where the running surface shapes did not change significantly) to 2 inches (near the point of frog where the running surface shapes changed significantly). Figure 17 shows a data sheet with some representative sections.

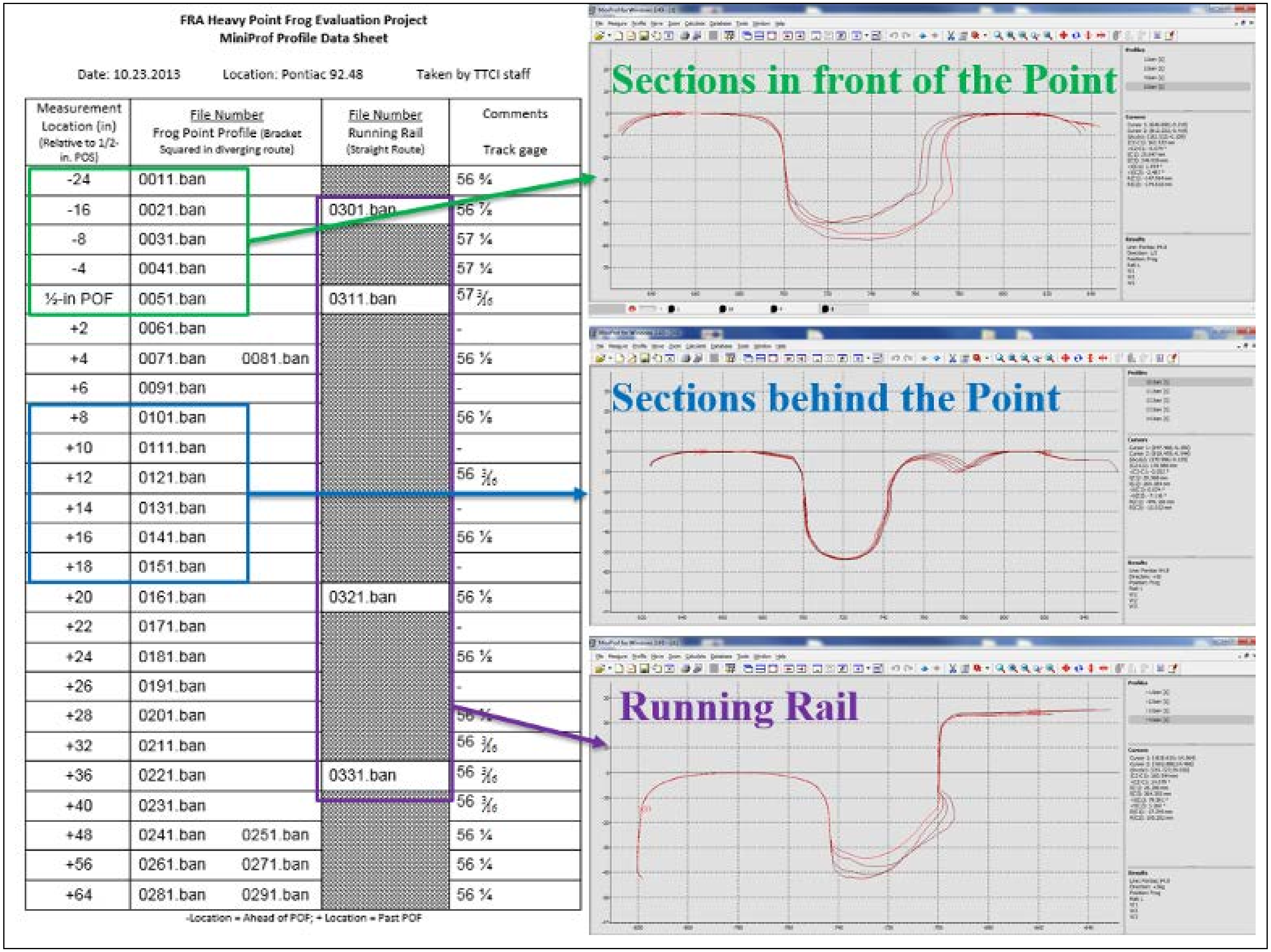

FRA Heavy Point Frog Evaluation Project
MiniProf Profile Data Sheet

Date: 10.23.2013 Location: Pontiac 92.48 Taken by TTCI staff

Measurement Location (in) (Relative to 1/2-in. POS)	File Number Frog Point Profile (Bracket Squared in diverging route)		File Number Running Rail (Straight Route)	Comments Track gage
-24	0011.ban			56 ¾
-16	0021.ban		0301.ban	56 ⅞
-8	0031.ban			57 ¼
-4	0041.ban			57 ¼
½-in POF	0051.ban		0311.ban	57 3/16
+2	0061.ban			-
+4	0071.ban	0081.ban		56 ⅛
+6	0091.ban			-
+8	0101.ban			56 ⅛
+10	0111.ban			-
+12	0121.ban			56 3/16
+14	0131.ban			-
+16	0141.ban			56 ⅛
+18	0151.ban			-
+20	0161.ban		0321.ban	56 ⅛
+22	0171.ban			-
+24	0181.ban			56 ½
+26	0191.ban			-
+28	0201.ban			56 [illegible]
+32	0211.ban			56 3/16
+36	0221.ban		0331.ban	56 3/16
+40	0231.ban			56 3/16
+48	0241.ban	0251.ban		56 ¼
+56	0261.ban	0271.ban		56 ¼
+64	0281.ban	0291.ban		56 ¼

-Location = Ahead of POF; + Location = Past POF

Figure 17. Example of datasheet and HPF section opened in MiniProf software

3.4 Post-processing of Measured Rail Profiles

The data recorded during MiniProf measurements is available in *.BAN format, which can be opened only by MiniProf software. In this case, the recorded data must be post-processed to obtain the file format that can be used as input to NUCARS® simulations.

Post processing procedure:

Step 1. Overlay profiles that were taken in two parts and create single .BAN file.

Step 2. Create *.TXT files from *.BAN files.

Step 3. Use MATLAB® to shift the data points to the appropriate gage line (See Figure 18).

Step 4. Create additional profiles in MATLAB by interpolation between measured locations. Where the measured profiles were taken every 2 inches, the interpolated profiles were every 0.5 inches. This step helped to achieve correct transition during simulations (See Figure 19).

Step 5. Convert the units from millimeters to inches

Step 6. Save the final profiles, modified in MATLAB, as *.WRX files.

Step 7. Generate *.FIT files using the CFIT processor in NUCARS®.

Step 8. Perform a preliminary simulation and check for wheel-rail contact errors, and repeat Step 7 if errors are found.

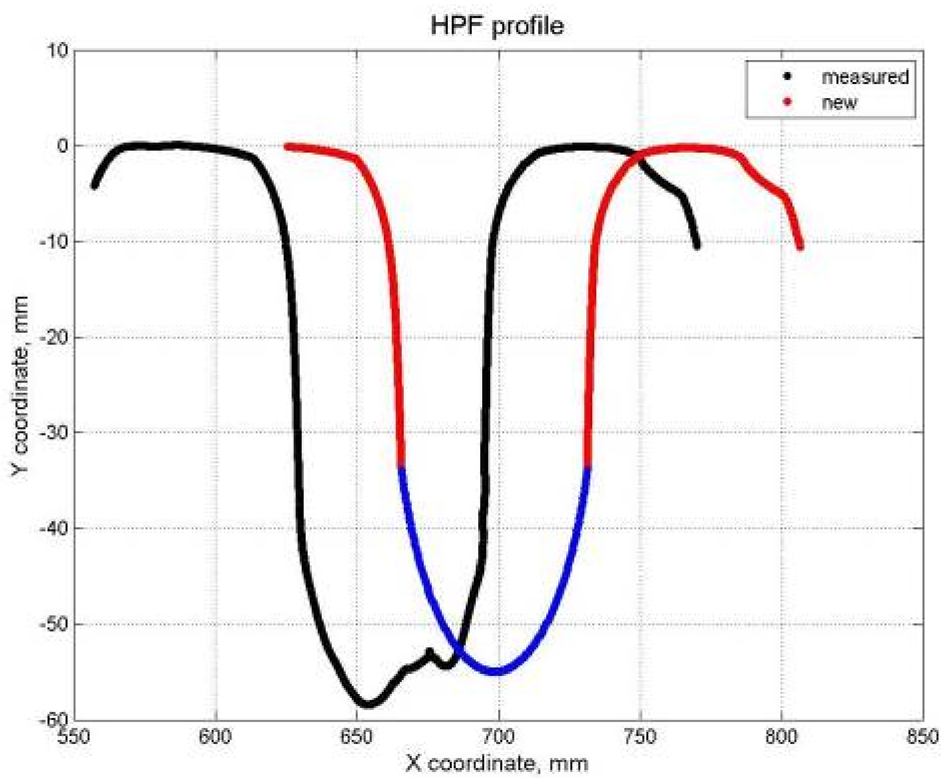

Figure 18. Example of Step 3 - the data points are shifted to the appropriate gage line

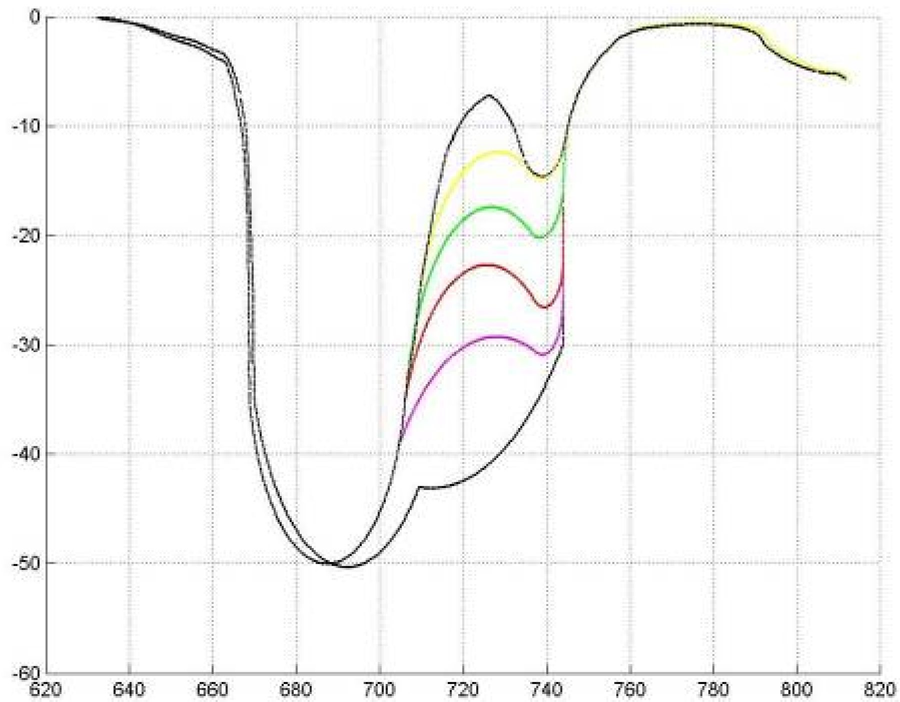

Figure 19. Example of Step 4 - Additional profiles are created by interpolation between measured locations

4. Design HPF

Voestalpine Nortrak, manufacturer and supplier of trackwork and materials in North America, provided drawings of all HPF design profiles, text files with coordinates of characteristic points, and arcs between points. The information was very detailed and some sections of the HPF were at intervals of 0.5 inch.

4.1 Type of Frogs

The frog is a device that allows wheels to cross another rail at the same elevation. This is accomplished by means of a flangeway that allows the wheel flanges to pass through a gap in the crossing rail. There are three types of frogs used by railways today. They differ in their capabilities, purchase costs, and operating costs. Each has viable economic application in the North American railway system. The three types are (listed in order of dynamic performance and initial cost): moveable point frogs, spring frogs, and RBM Frogs. Moveable point frogs are used for high-speed turnouts in multiple track lines. They function like switch points in that the frog point is lined for the selected route through the turnout. They do not use a heavy point on the frog, and thus are outside the scope of this project. For single track lines, spring frogs and RBM frogs (Figure 20) are typically used.

Figure 20. No. 20 RBM Frog

The RBM frog (Figure 20) is a fixed point, fixed wing frog. The name refers to the construction of the frog. It consists of a high alloy (typically 13% Manganese) steel casting that forms the frog flangeways and adjacent running surfaces. The casting is surrounded by rails that are bolted to it to create a “rail bound” frog. The whole unit is joined to the adjacent track with either welds or bolted joints. This design is used extensively in North America, especially on dual use corridors that are being upgraded for HSR service. Due to the flangeway gap in the mainline route, high dynamic loading and subsequent ride quality degradation make these frogs more difficult and expensive to maintain at higher operating speeds.

Figure 21 plots the modeled RBM frog running surfaces.

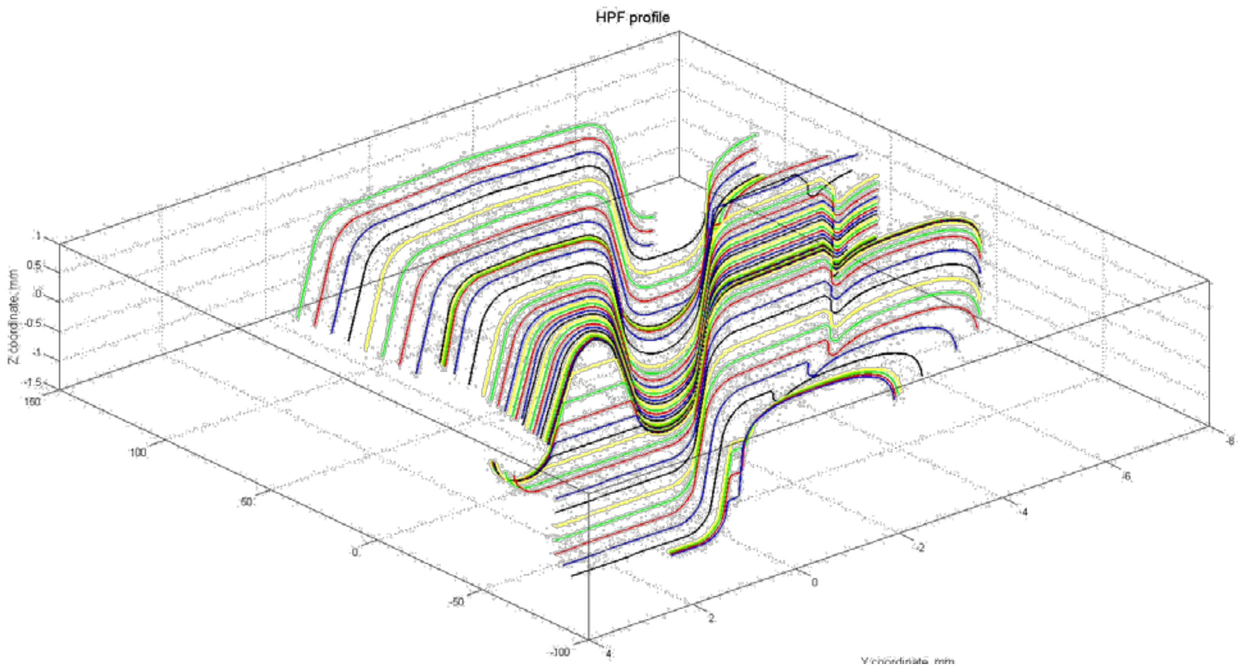

Figure 21. Sections of RBM Frog at the 0.5-inch point of frog presented in 3D

The spring frog (Figure 22) is a fixed point frog with a moveable wing rail. The Figure shows the normal position of the wing rail is closed against the frog point, which eliminates the flangeway gap for the mainline route. Thus, dynamic forces and maintenance demand are reduced while ride quality is improved. This type of frog is often chosen for single track mainlines with heavy traffic and/or higher speed traffic.

Figure 22. Number 24 Spring Frog

Figure 23 plots the modeled spring frog running surfaces.

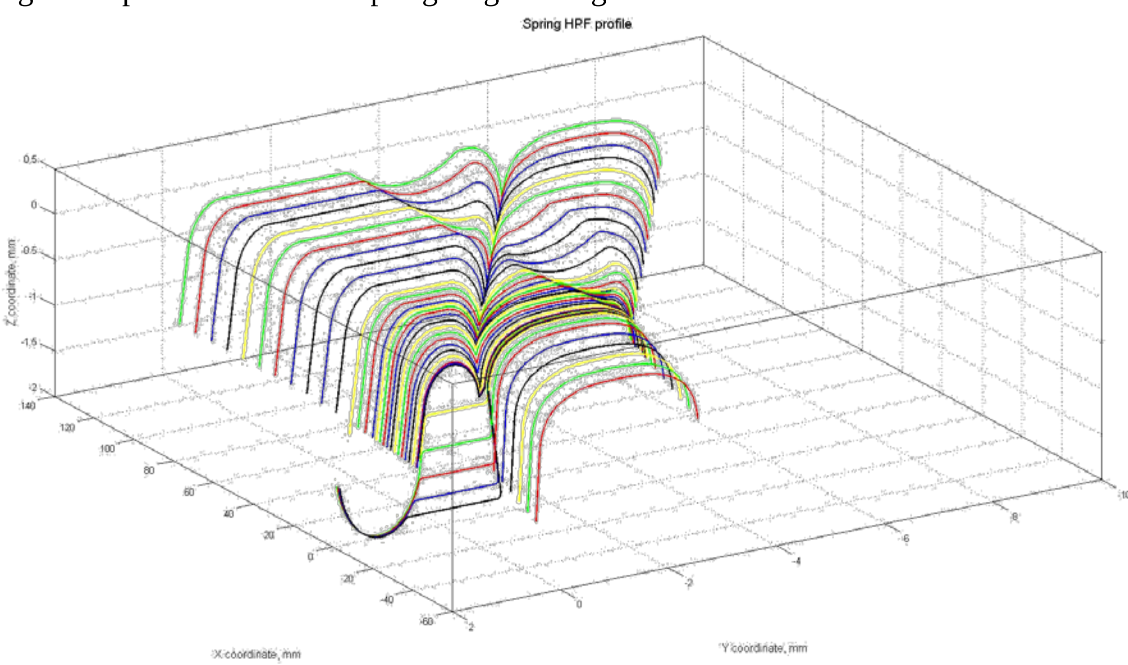

Figure 23. Sections of Spring Frog at the 0.5-inch point of frog presented in 3D

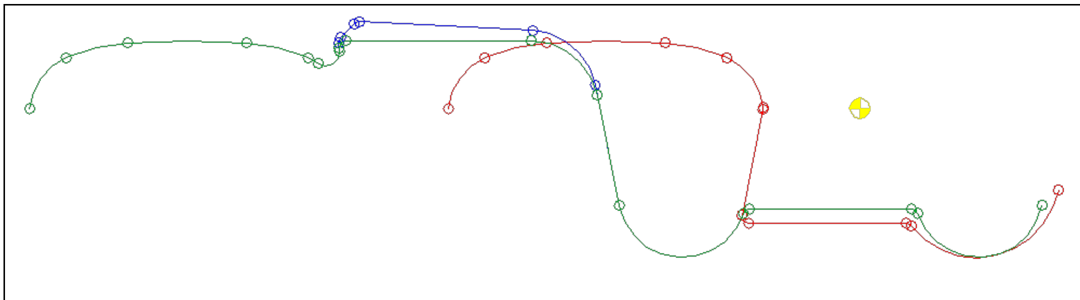	Sections 1in behind the 0.5-inch point of frog
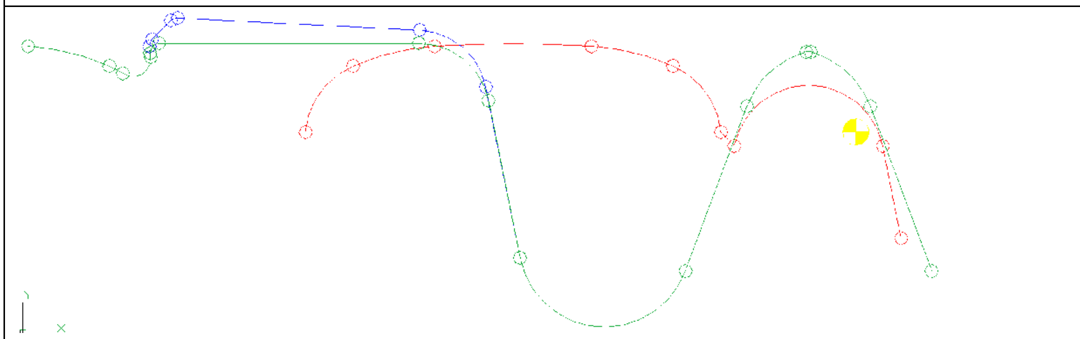	Sections 4 inches behind the 0.5-inch point of frog
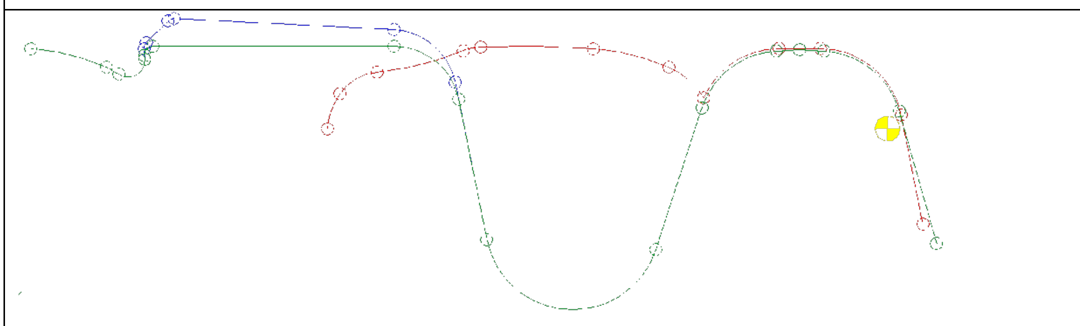	Sections 20 inches behind the 0.5-inch point of frog
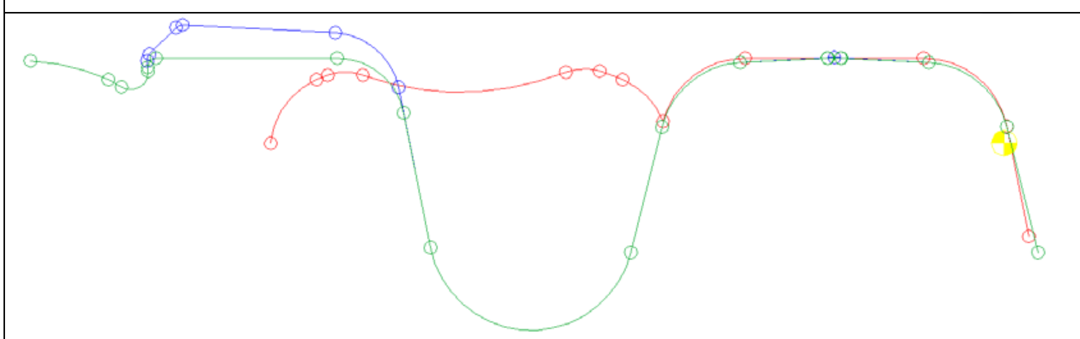	Sections 48 inches behind the 0.5-inch point of frog
No. 24 Spring HPF No. 24 RBM frog with a conformal running surface No. 24 RBM frog with a flat running surface	

Figure 24. Comparison of different types of HPF

In addition to main categories of HPF, the RBM frogs can be manufactured with a conformal (to the wheel shape) running surface or a flat running surface. The conformal running surface frog has been shown to perform better than flat running surface frogs in terms of dynamic loading and service life for heavy haul applications (4). For higher speed traffic, the conformal surface RBM frog is used for No. 24 frogs by major railroads. Therefore for further analysis the RBM frog with conformal surface is considered.

Figure 24 compares all types of HPF used in this project. Appendix A shows more comparisons of HPF sections.

4.2 Post-processing of Design Rail Profiles

The data received from Voestalpine Nortrak was post-processed to obtain the file format that can be used as an input file for NUCARS® simulations. A MATLAB algorithm was developed to post-process the .TXT files, and then the CFIT processor in NUCARS® was used to create .FIT files.

Post-processing procedure:

Step 1. Use the MATLAB algorithm to modify the received files to the appropriate format.

Step 2. Generate *.FIT files using the CFIT processor in NUCARS®. This step is demanding, because all sections are complex and contain a large number of characteristic points. In addition, some part of the section has sharp transitions and tangency check is hard to achieve.

Step 3. Perform a preliminary simulation and check for wheel-rail contact errors. If errors are found, follow Steps 4 and 5 to improve the *.FIT file.

Step 4. Develop some interpolated profiles in MATLAB to create the correct transition during simulation process.

Step 5. Modify some sections of the as-designed HPF by cutting off the parts where wheel-rail contact does not occur.

Step 6. Repeat the preliminary simulation and check for wheel-rail contact. If errors are still found, repeat Steps 4 and 5 until the improved *.FIT file produces valid wheel-rail contact.

5. Simulation Results and Evaluation

FRA VTI safety standards were used to examine the performance of the passenger equipment over HPF. The results of the simulation were compared with FRA requirements to identify wheel-rail forces and accelerations of vehicles that were outside the limiting conditions for a particular class of track. Tables 5 and 6 summarize the requirements for carbody accelerations and rail forces. Sections 5.1 through 5.5 include plots of results for the different simulation cases.

Carbody Accelerations Requirements:

- The peak-to-peak lateral accelerations, measured as the algebraic difference between the two extreme values of measured acceleration in any 1-second time period, excluding any peak lasting less than 50 milliseconds, shall not exceed 0.65g for passenger cars and 0.75g for other vehicles.
- The peak-to-peak vertical accelerations, measured as the algebraic difference between the two extreme values of measured acceleration in any 1-second time period, excluding any peak lasting less than 50 milliseconds, shall not exceed 1.0g for passenger cars and 1.25g for other vehicles.

Table 5. Summary of carbody accelerations requirements

	T16	**GP40**
Lateral (Transient) Carbody Acceleration (g)	≤0.65	≤0.75
Vertical (Transient) Carbody Acceleration (g)	≤1.0	≤1.25

Wheel-rail Force Requirements:

- No wheel of the vehicle shall be permitted to unload to less than 15 percent of the static vertical wheel load for 5 or more continuous feet. The static vertical wheel load is defined as the load that the wheel would carry when stationary on level track.
- The ratio of the lateral force that any wheel exerts on an individual rail to the vertical force exerted by the same wheel on the rail shall not be greater than the safety limit calculated for the wheel's flange angle (δ) for 5 or more continuous feet. The safety limit uses Equation 1

$$\leq \frac{\tan(\delta) - 0.5}{1 + 0.5\tan(\delta)} \qquad (1)$$

- The net axle lateral force, in kips, exerted by any axle on the track shall not exceed a total of 5 kips plus 40 percent of the static vertical load that the axle exerts on the track for 5 or more continuous feet using Equation 2

$$(V_a = \text{static vertical load in kips}) \qquad (2)$$

- The ratio of the lateral forces that the wheels on one side of any truck exert on an individual rail to the wheels on the rail shall not be greater than 0.6 for 5 or more continuous feet.

Table 6. Summary of Rail Forces Requirements

	T16	GP40
Single Wheel Vertical Load Ratio	≥ 0.15	≥ 0.15
Single Wheel L/V Ratio, $\delta = 75$ degree	≤ 1.13	≤ 1.13
Net Axle Lateral L/V Ratio	≤ 0.55	≤ 0.47
Truck Side L/V Ratio	≤ 0.6	≤ 0.6

The lateral and vertical wheel forces shall be measured and processed through a low pass filter with a minimum cut-off frequency of 25 Hz. The sample rate for wheel force data shall be at least 250 samples per second.

Although the maximum speed for Class 6 track is 110 mph, 120 mph is included for simulation purposes, but it is not considered for evaluating the performance for Class 6 track.

5.1 Lateral (Transient) Carbody Acceleration

5.1.1 As-designed HPF with T16

Figures 25–29 show results of carbody maximum lateral acceleration on the T16 passenger car for as-designed HPF with different scenarios from the parametric study.

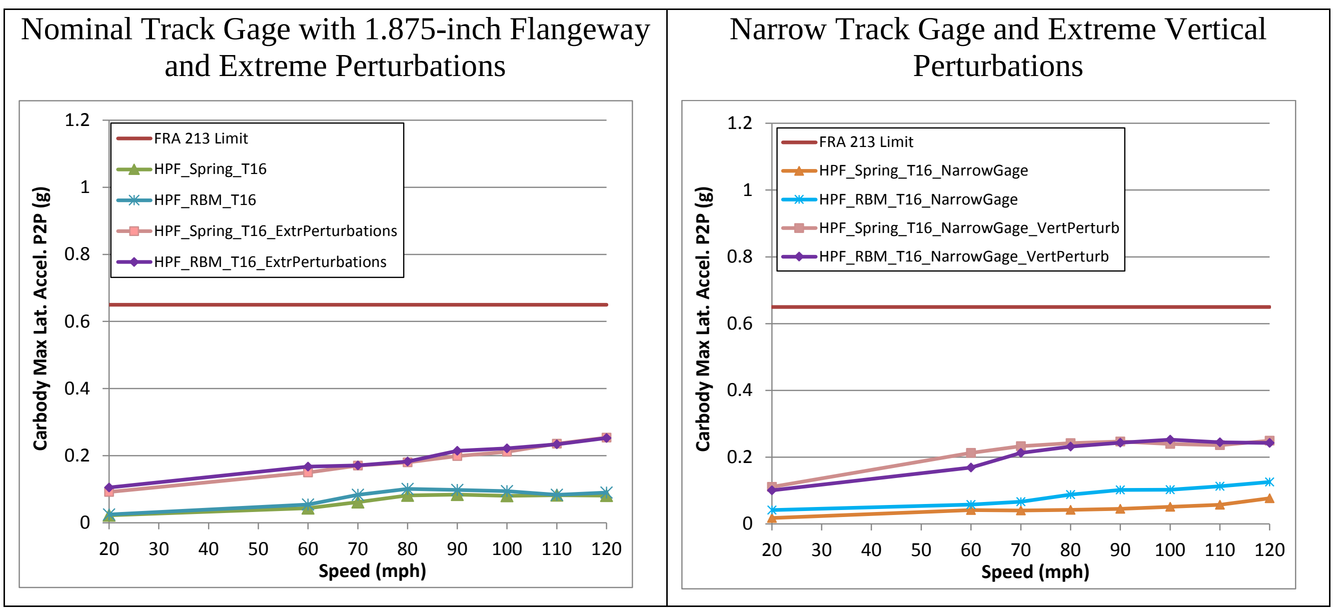

Figure 25. Carbody maximum lateral acceleration on the T16 passenger car - nominal track gage (left) and narrow track gage (right)

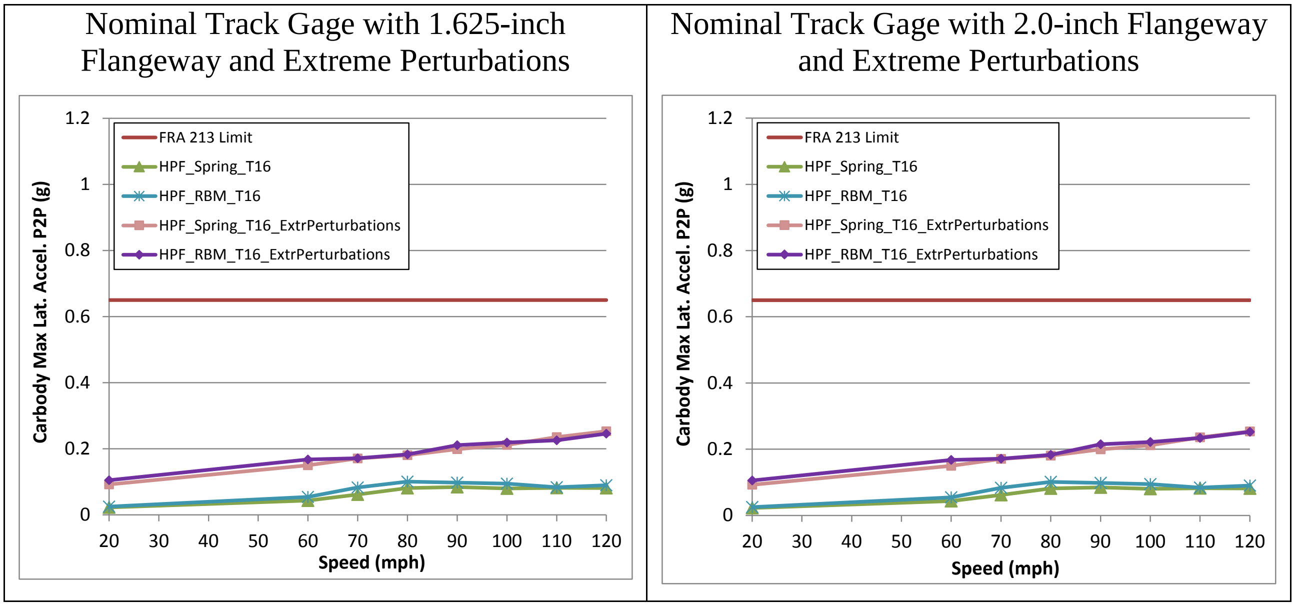

Figure 26. Carbody maximum lateral acceleration on the T16 passenger car - nominal track gage with 1.625-inch flangeway (left) and 2.0-inch flangeway (right)

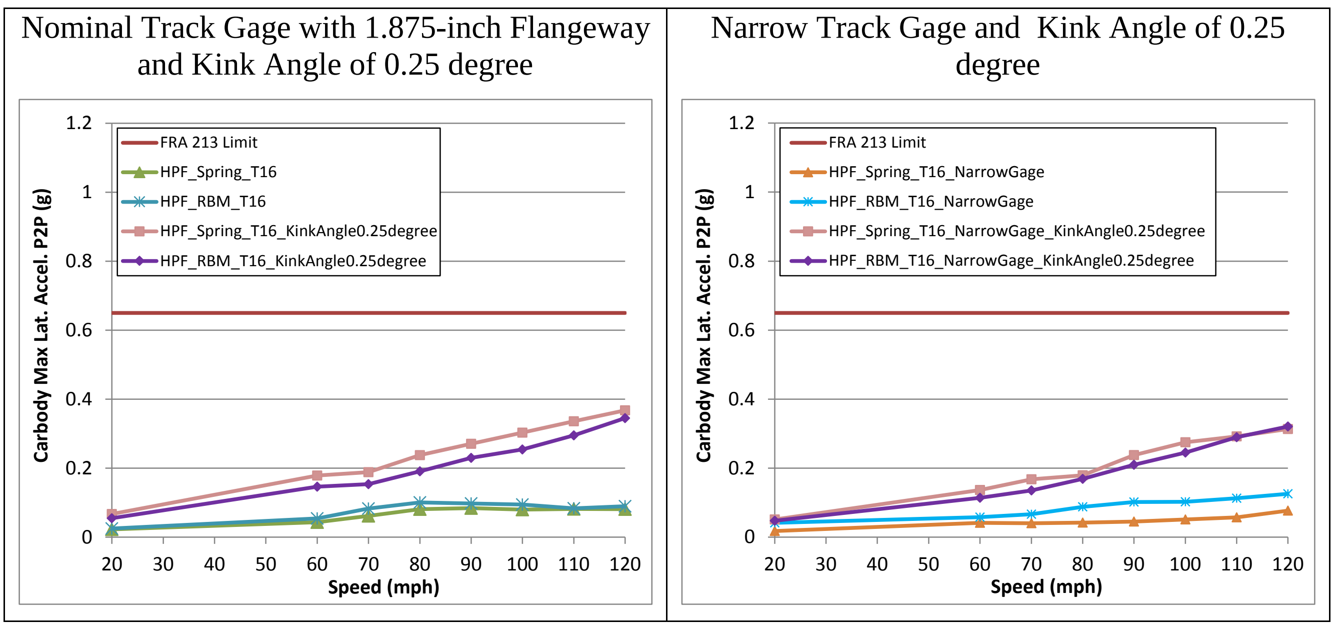

Figure 27. Carbody maximum lateral acceleration on the T16 passenger car - kink angle of 0.25 degree with nominal track gage (left) and narrow track gage (right)

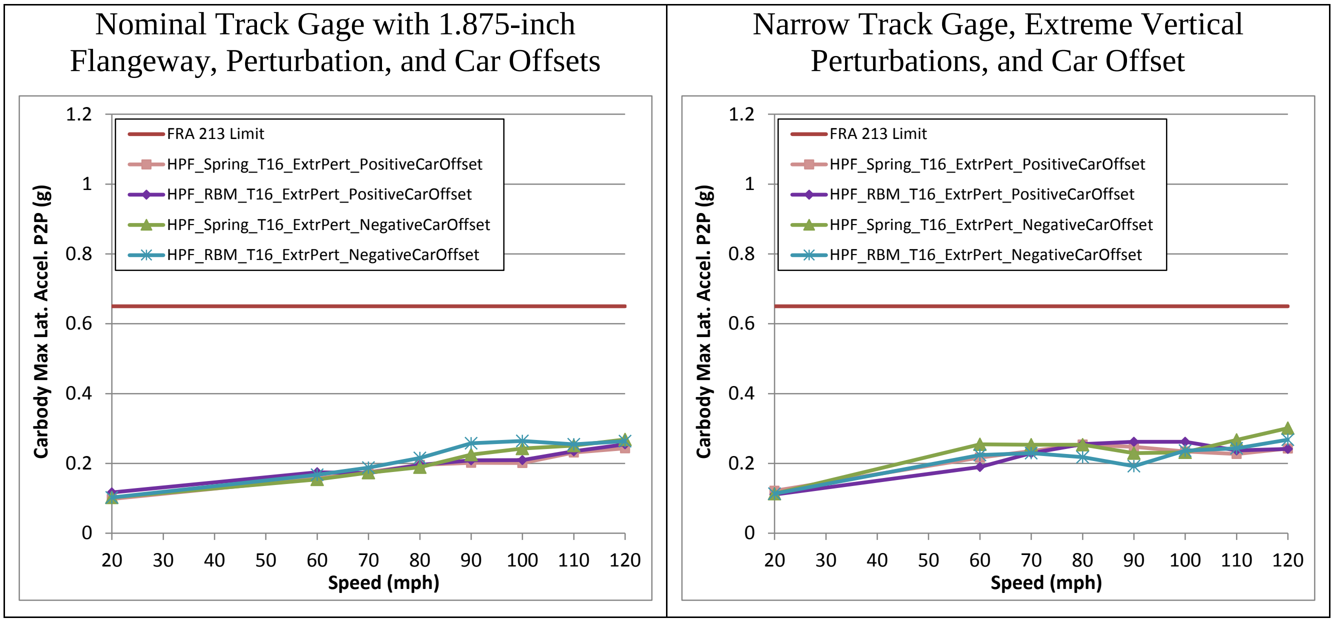

Figure 28. Carbody maximum lateral acceleration on the T16 passenger car - car offsets with nominal track gage (left) and narrow track gage (right)

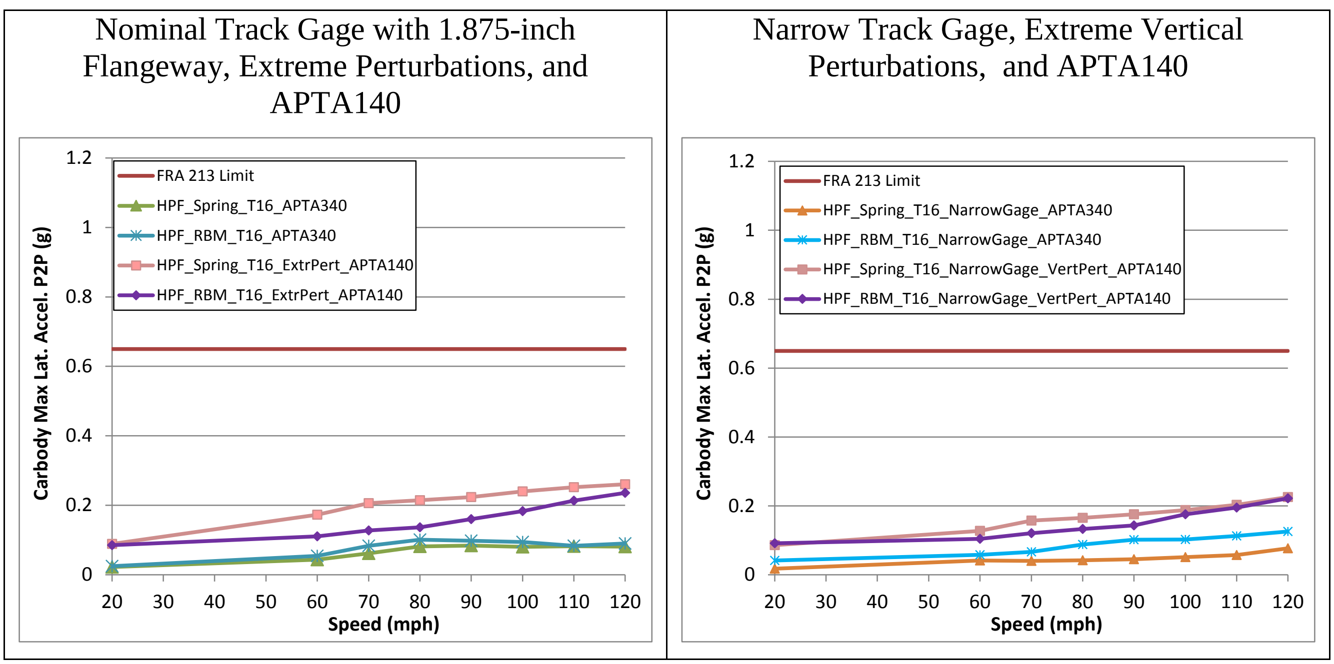

Figure 29. Carbody maximum lateral acceleration on the T16 passenger car - APTA140 with nominal track gage (left) and narrow track gage (right)

5.1.2 AS-designed HPF with GP40

Figures 30–34 show results of carbody maximum lateral acceleration on the GP40 passenger locomotive for as-designed HPF with different scenarios from the parametric study.

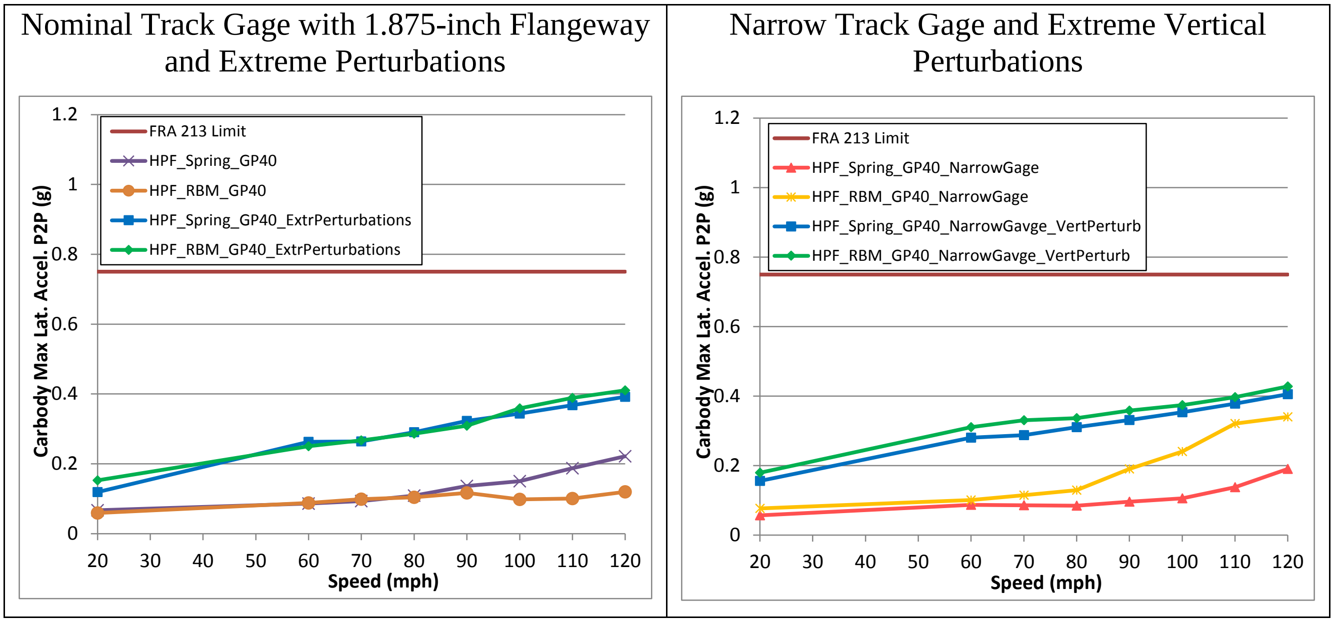

Figure 30. Carbody maximum lateral acceleration on the GP40 passenger locomotive - nominal track gage (left) and narrow track gage (right)

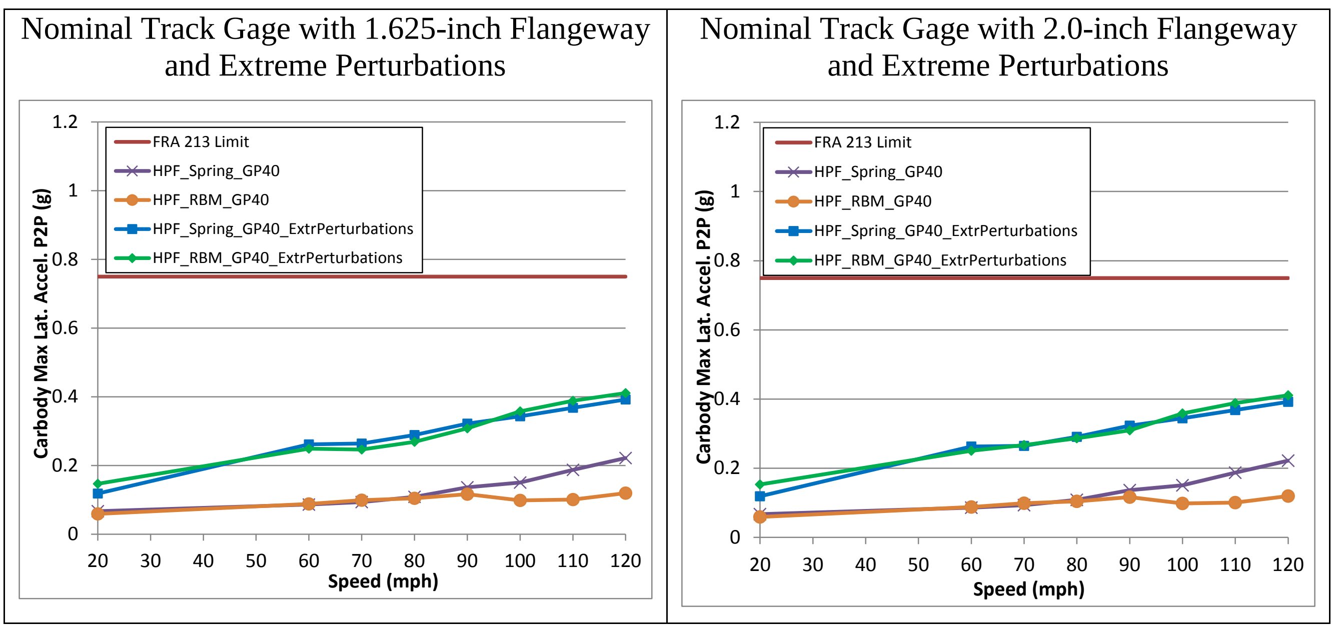

Figure 31. Carbody maximum lateral acceleration on the GP40 passenger locomotive - nominal track gage with 1.625-inch flangeway (left) and 2.0-inch flangeway (right)

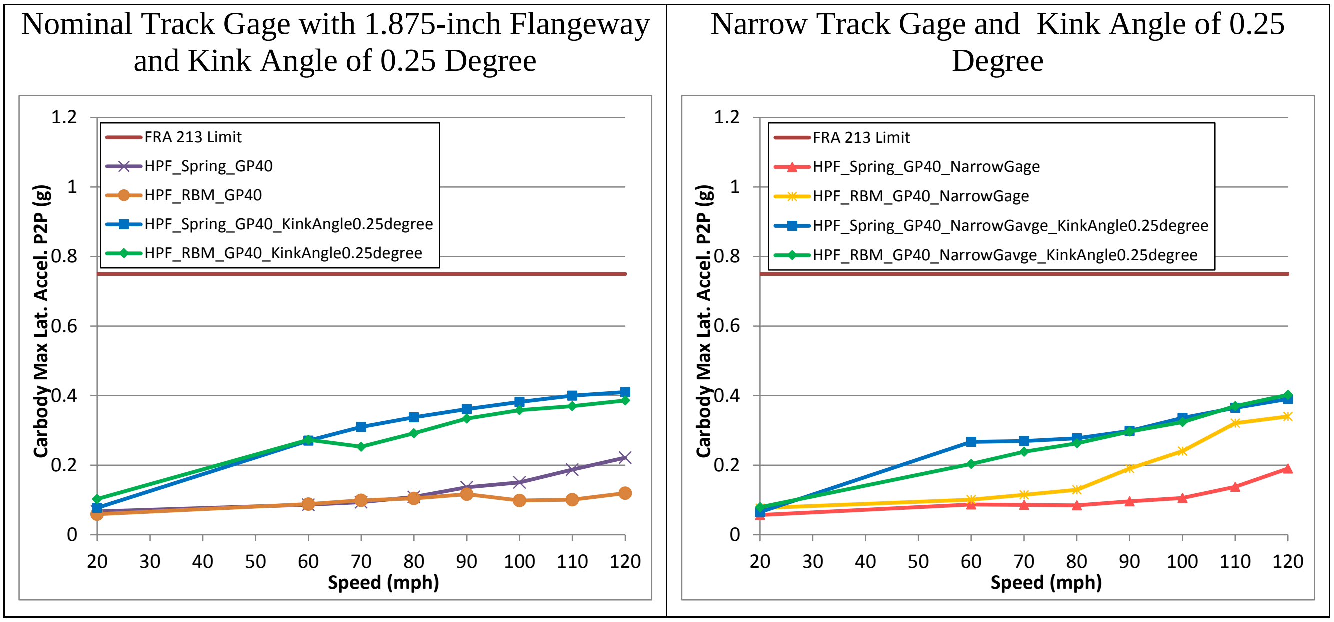

Figure 32. Carbody maximum lateral acceleration on the GP40 passenger locomotive - kink Angle of 0.25 degree with nominal track gage (left) and narrow track gage (right)

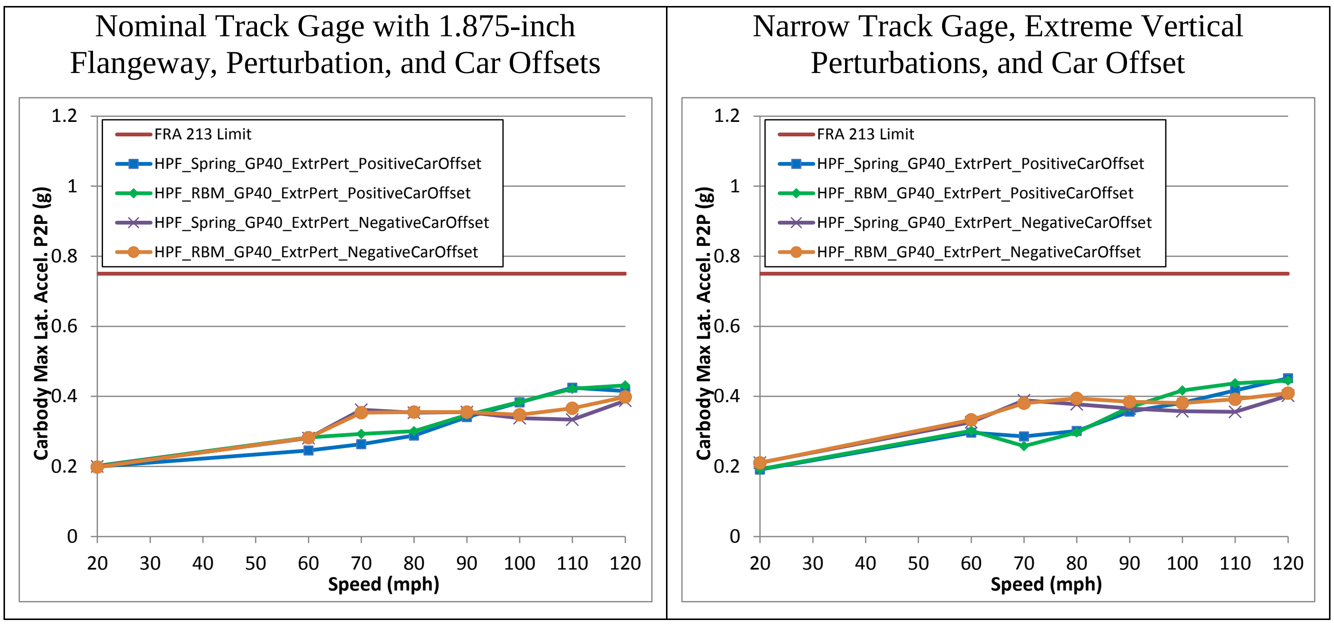

Figure 33. Carbody maximum lateral acceleration on the GP40 passenger locomotive - car offsets with nominal track gage (left) and narrow track gage (right)

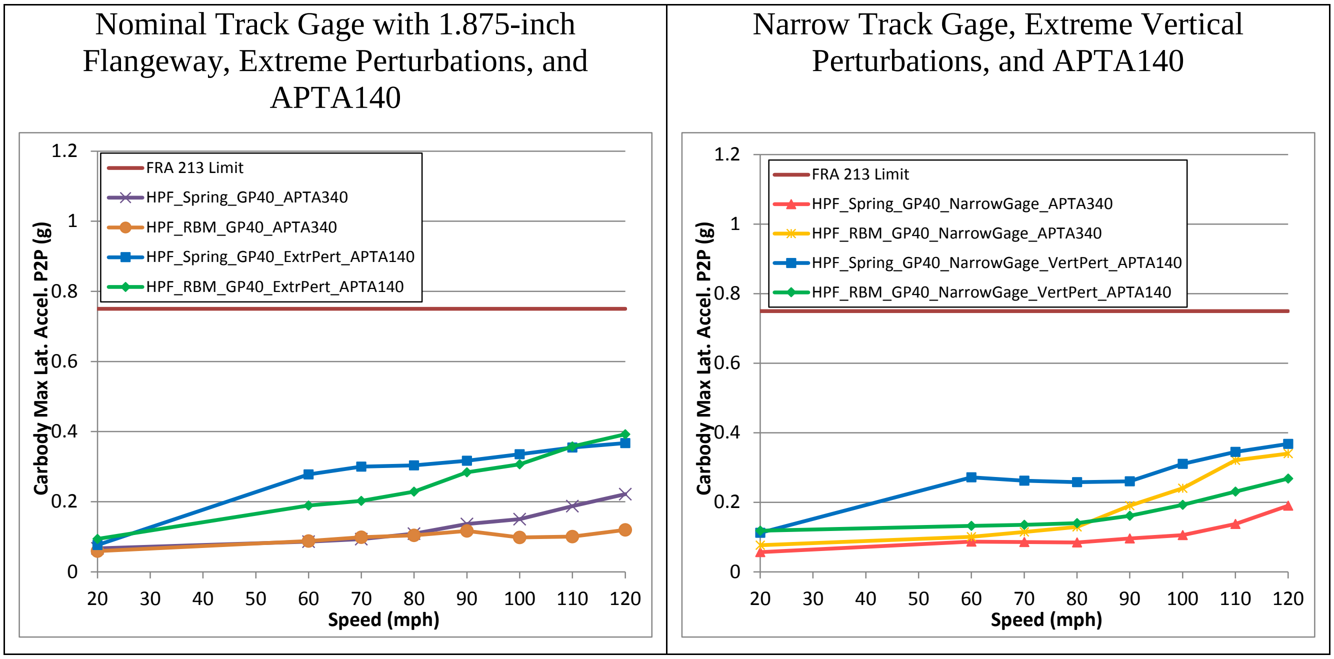

Figure 34. Carbody maximum lateral acceleration on the GP40 passenger locomotive - APTA140 with nominal track gage (left) and narrow track gage (right)

5.1.3 Measured HPF with T16

Figures 35–36 show results of carbody maximum lateral acceleration on the T16 passenger car for measured HPF with different scenarios from the parametric study.

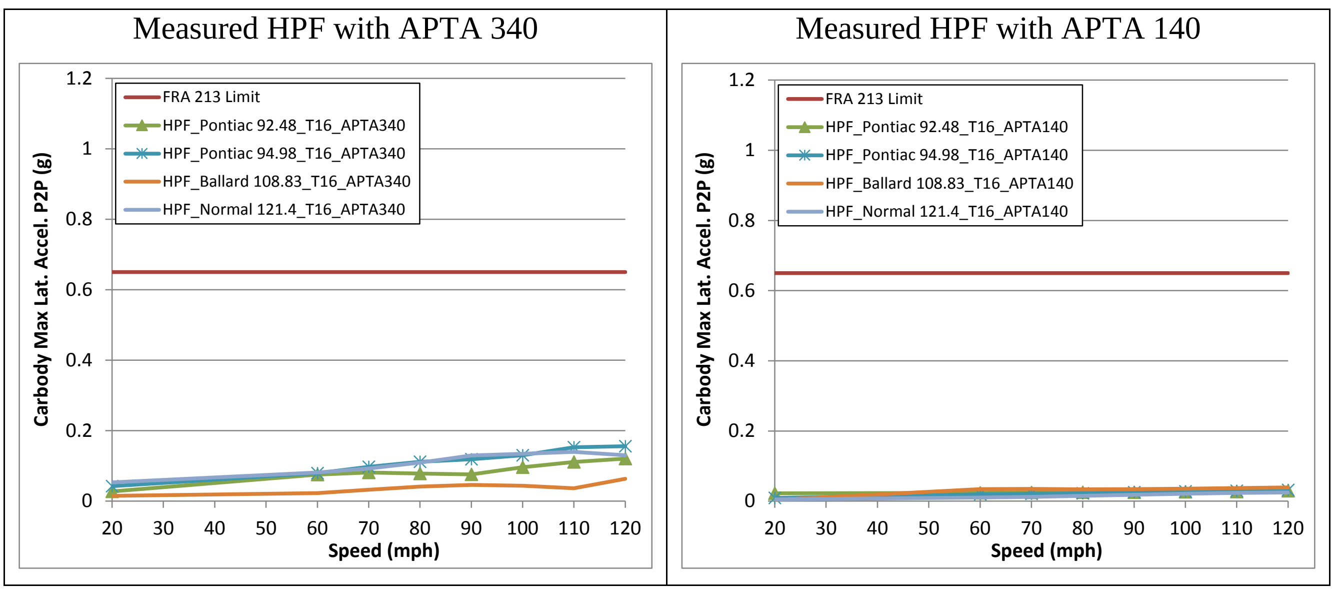

Figure 35. Carbody maximum lateral acceleration on the T16 passenger car - measured HPFs with wheelsets APTA 340 (left) and APTA140 (right)

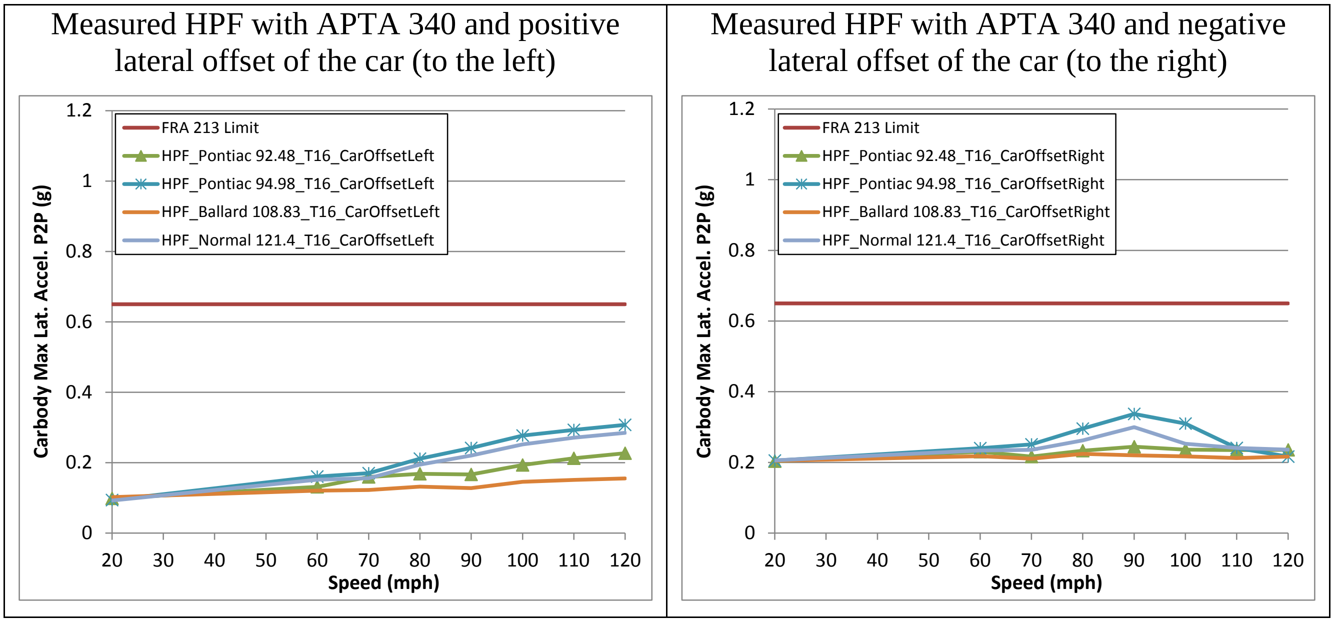

Figure 36. Carbody maximum lateral acceleration on the T16 passenger car - measured HPFs with positive car offset (left) and negative car offset (right)

5.1.4 Measured HPF with GP40

Figures 37–38 show results of carbody maximum lateral acceleration on the GP40 passenger locomotive for measured HPF with different scenarios from the parametric study.

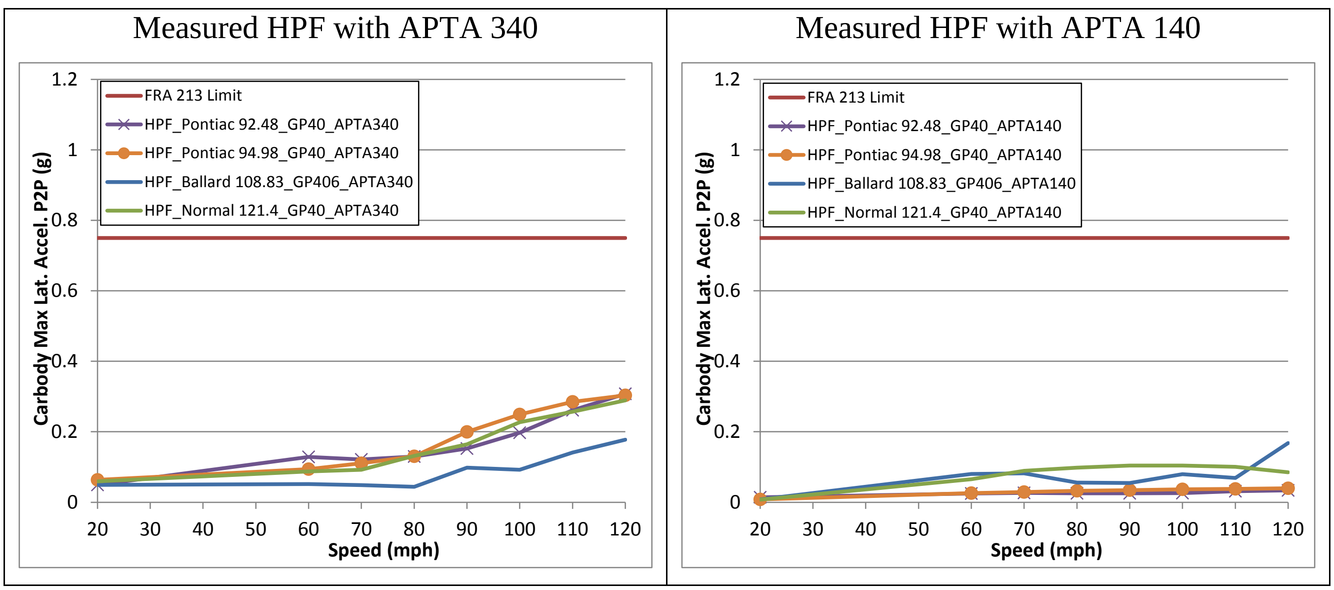

Figure 37. Carbody maximum lateral acceleration on the GP40 passenger locomotive - measured HPFs with wheelsets APTA 340 (left) and APTA140 (right)

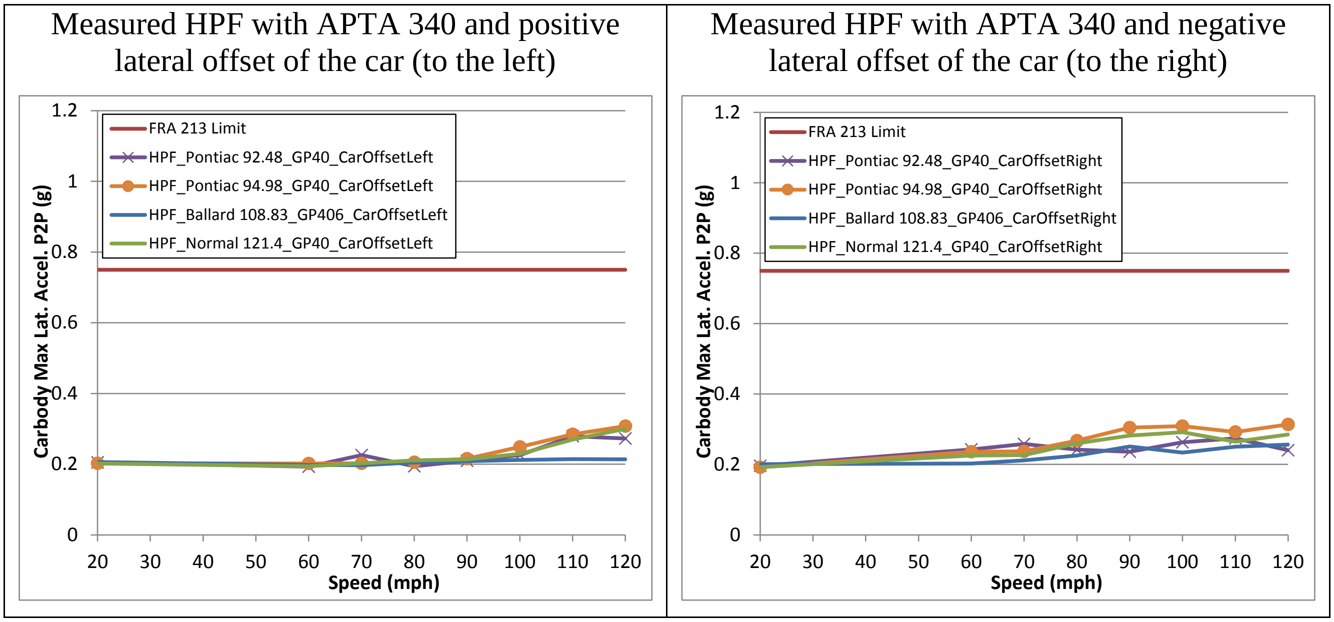

Figure 38. Carbody maximum lateral acceleration on the GP40 passenger locomotive - measured HPFs with positive car offset (left) and negative car offset (right)

5.2 Vertical (Transient) Carbody Acceleration

5.2.1 AS-designed HPF with T16

Figures 39–43 show results of carbody maximum vertical acceleration on the T16 passenger car for as-designed HPF with different scenarios from the parametric study.

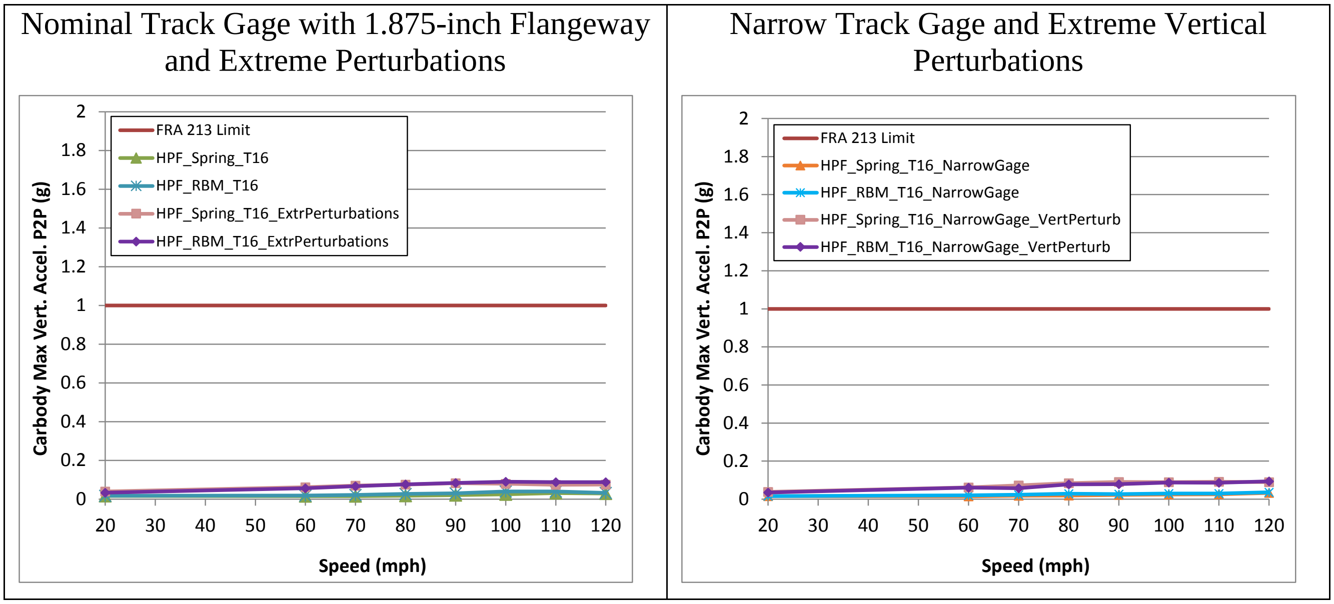

Figure 39. Carbody maximum vertical acceleration on the T16 passenger car - nominal track gage (left) and narrow track gage (right)

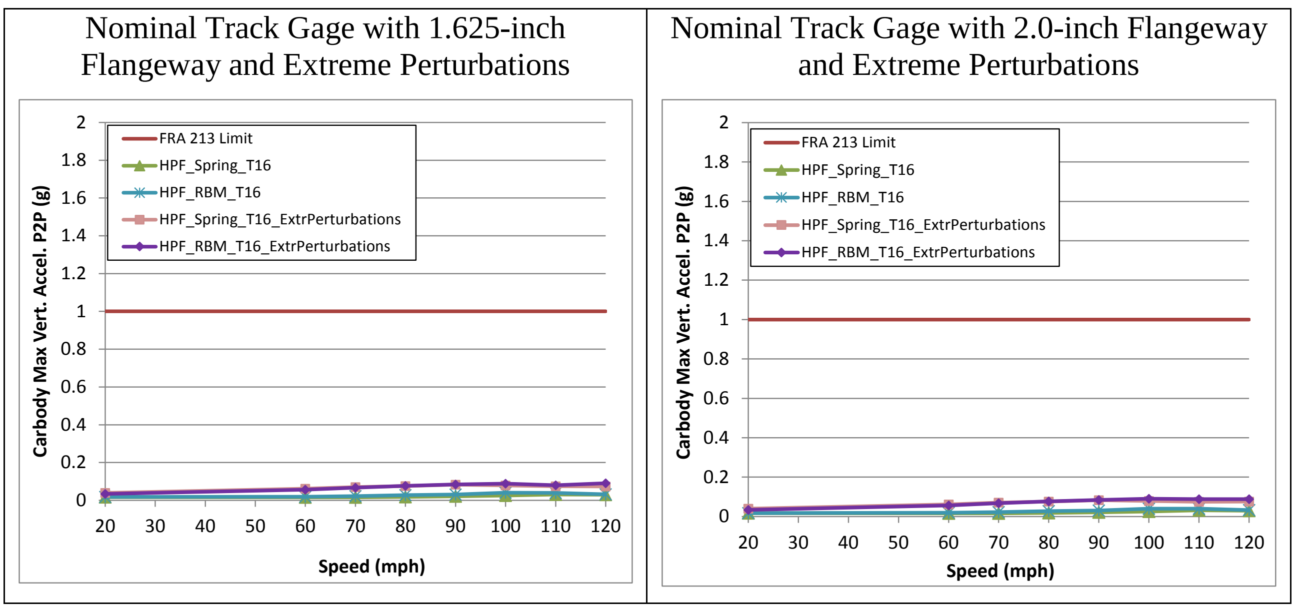

Figure 40. Carbody maximum vertical acceleration on the T16 passenger car - nominal track gage with 1.625-inch flangeway (left) and 2.0-inch flangeway (right)

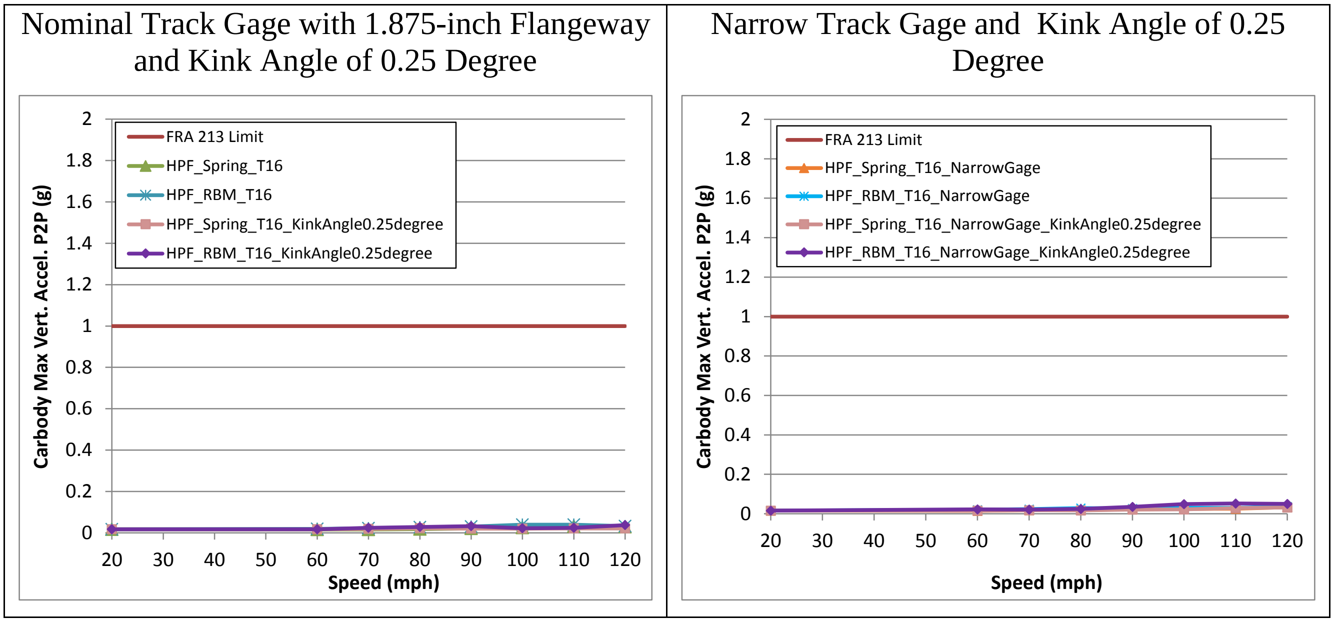

Figure 41. Carbody maximum vertical acceleration on the T16 passenger car - kink angle of 0.25 degree with nominal track gage (left) and narrow track gage (right)

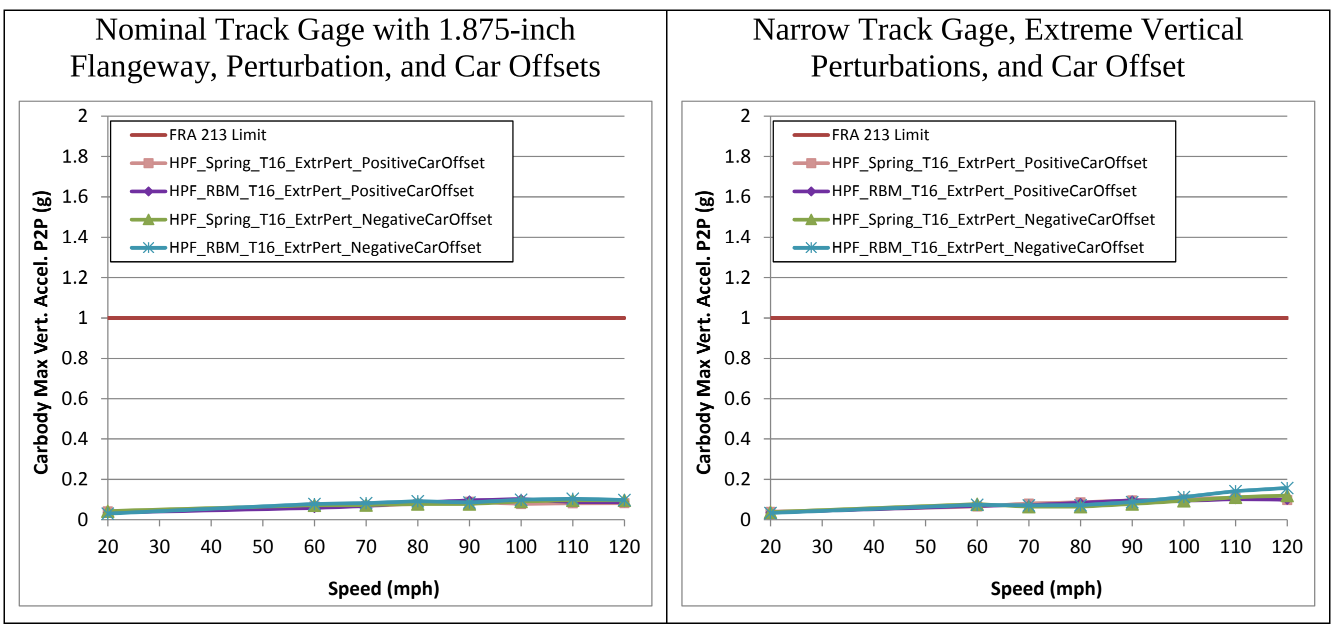

Figure 42. Carbody maximum vertical acceleration on the T16 passenger car - car offsets with nominal track gage (left) and narrow track gage (right)

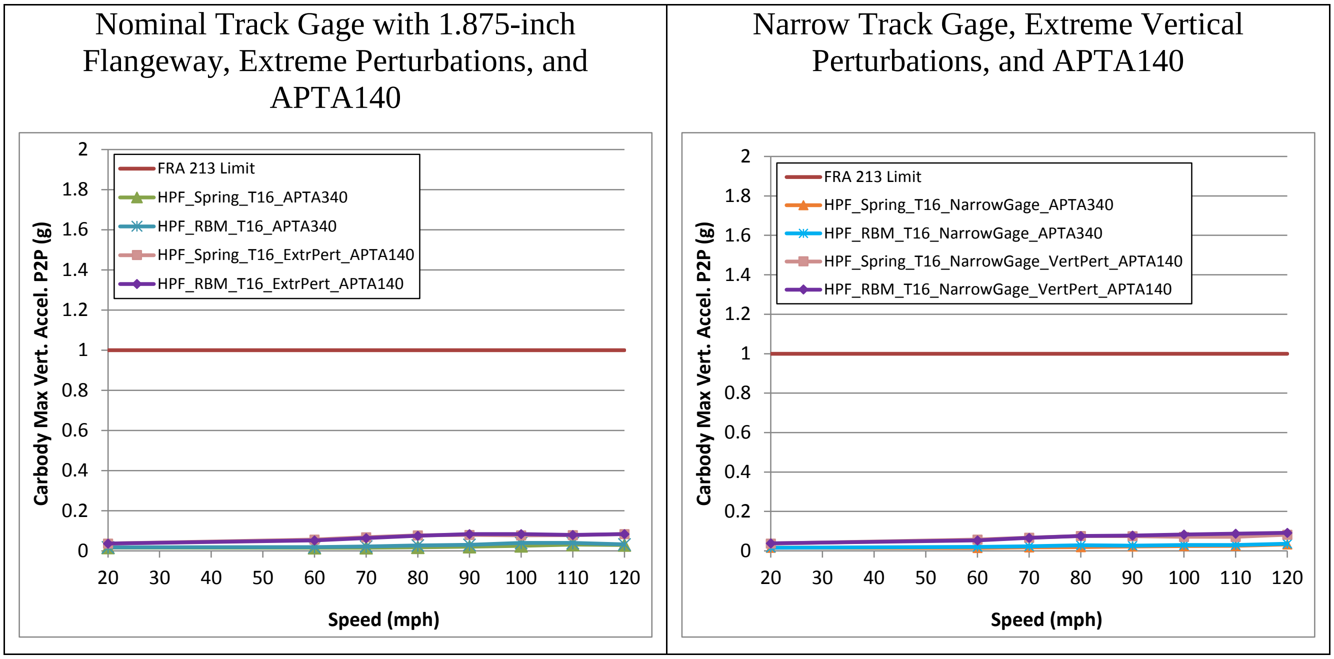

Figure 43. Carbody maximum vertical acceleration on the T16 passenger car - APTA140 with nominal track gage (left) and narrow track gage (right)

5.2.2 As-designed HPF with GP40

Figures 44–48 show results of carbody maximum vertical acceleration on the GP40 passenger locomotive for as-designed HPF with different scenarios from the parametric study.

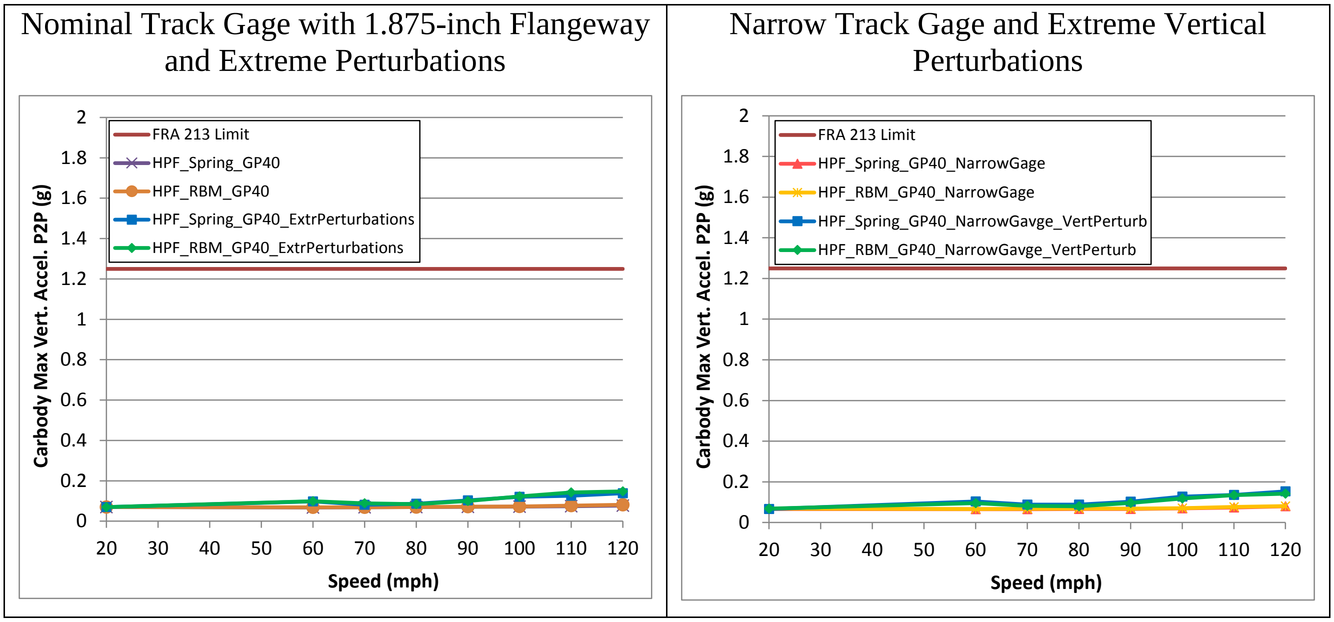

Figure 44. Carbody maximum vertical acceleration on the GP40 passenger locomotive - nominal track gage (left) and narrow track gage (right)

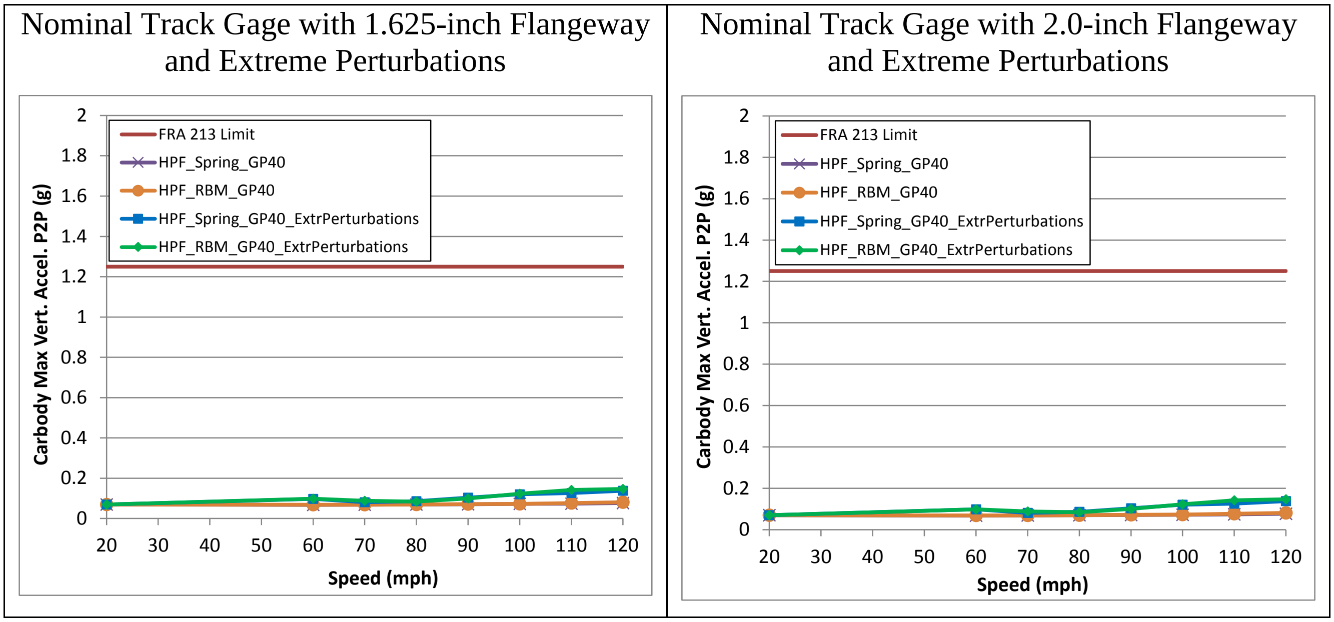

Figure 45. Carbody maximum vertical acceleration on the GP40 passenger locomotive - nominal track gage with 1.625-inch flangeway (left) and 2.0-inch flangeway (right)

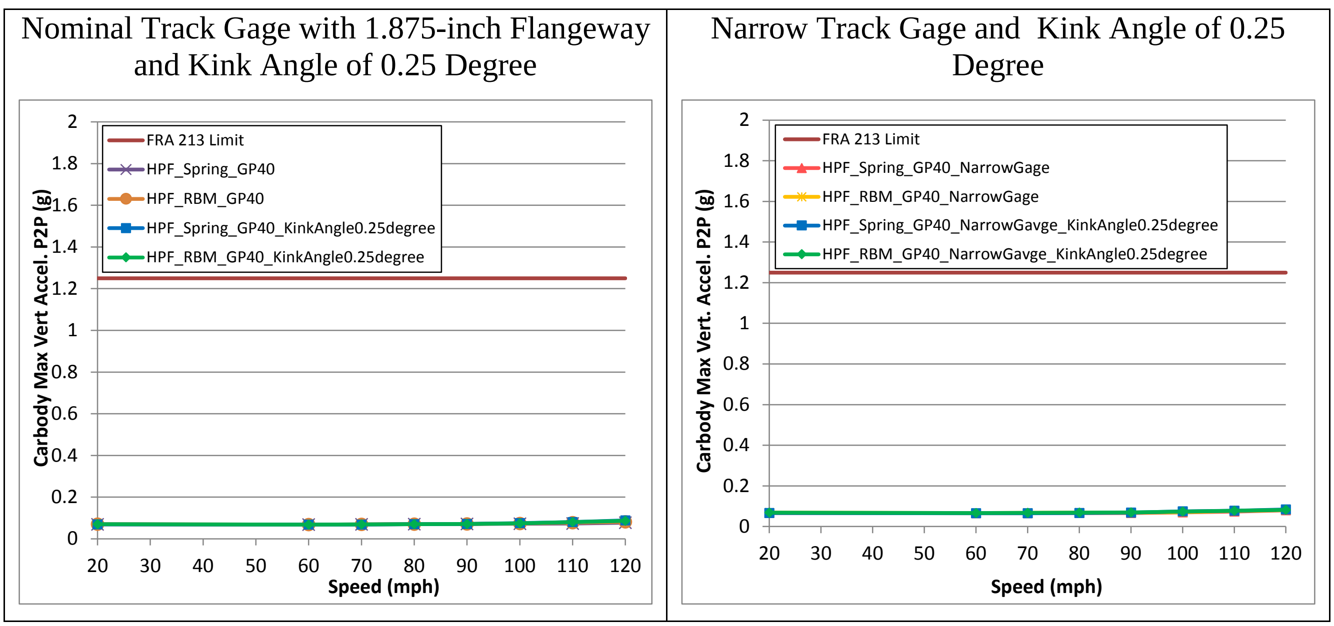

Figure 46. Carbody maximum vertical acceleration on the GP40 passenger locomotive - kink angle of 0.25 degree with nominal track gage (left) and narrow track gage (right)

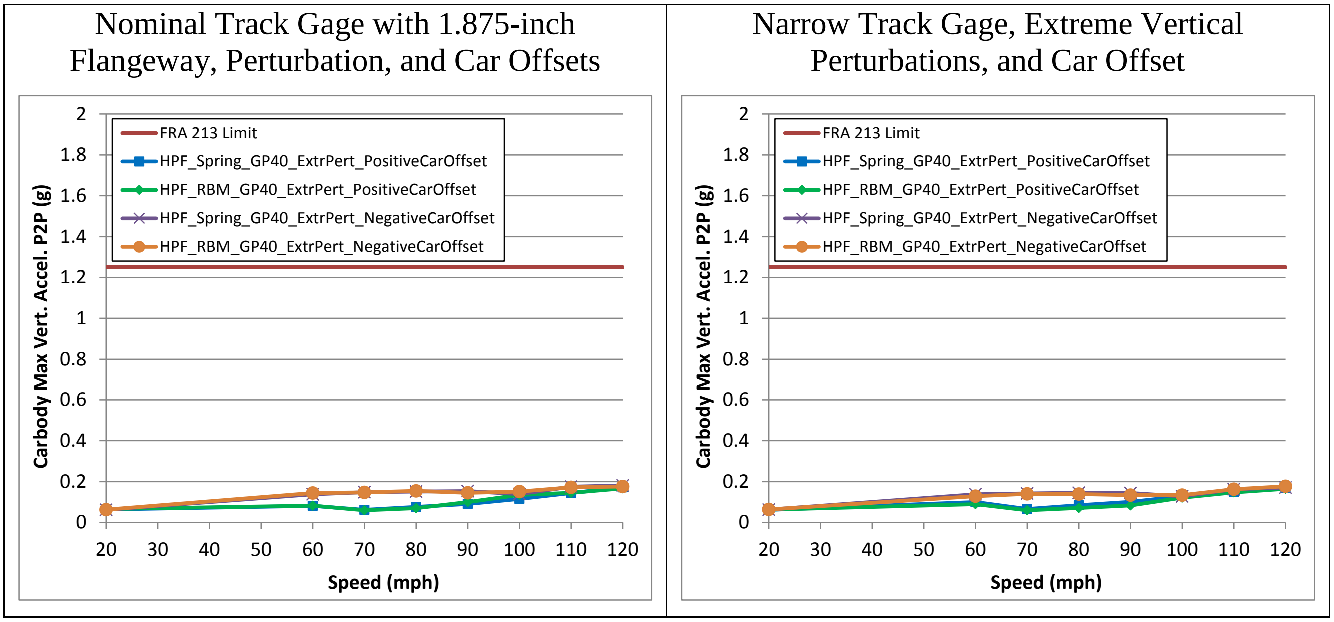

Figure 47. Carbody maximum vertical acceleration on the GP40 passenger locomotive - car offsets with nominal track gage (left) and narrow track gage (right)

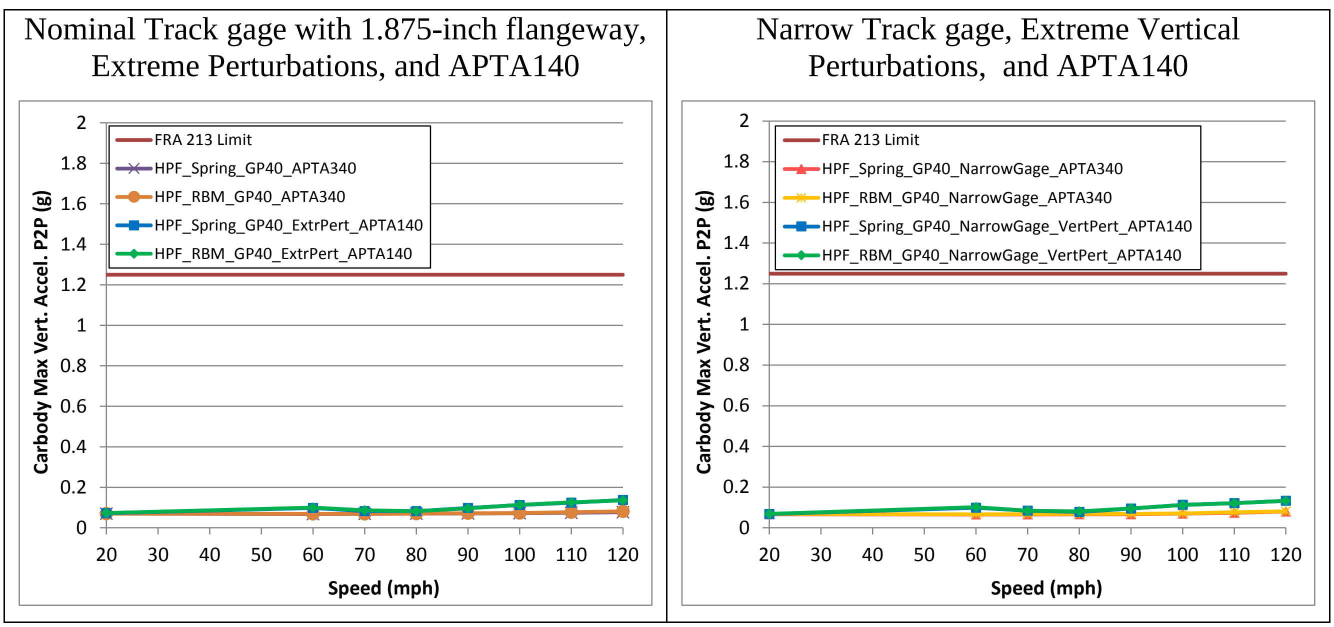

Figure 48. Carbody maximum vertical acceleration on the GP40 passenger locomotive - APTA140 with nominal track gage (left) and narrow track gage (right)

5.2.3 *Measured HPF with T16*

Figures 49–50 show results of carbody maximum vertical acceleration on the T16 passenger car for measured HPF with different scenarios from the parametric study.

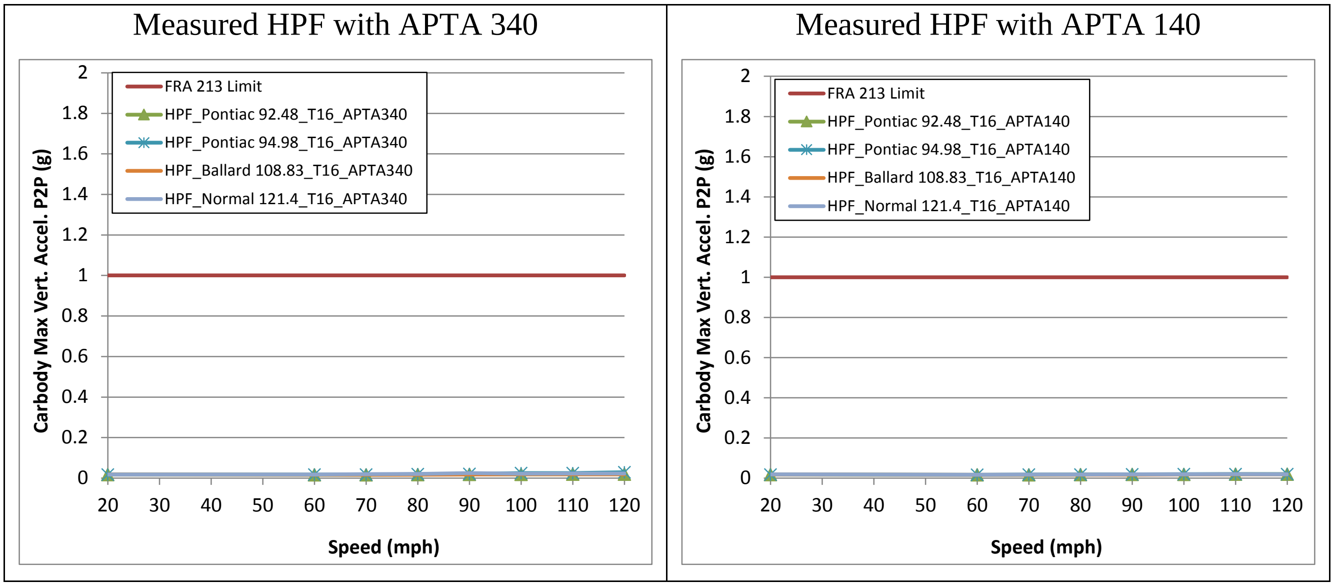

Figure 49. Carbody maximum vertical acceleration on the T16 passenger car - measured HPFs with wheelsets APTA 340 (left) and APTA140 (right)

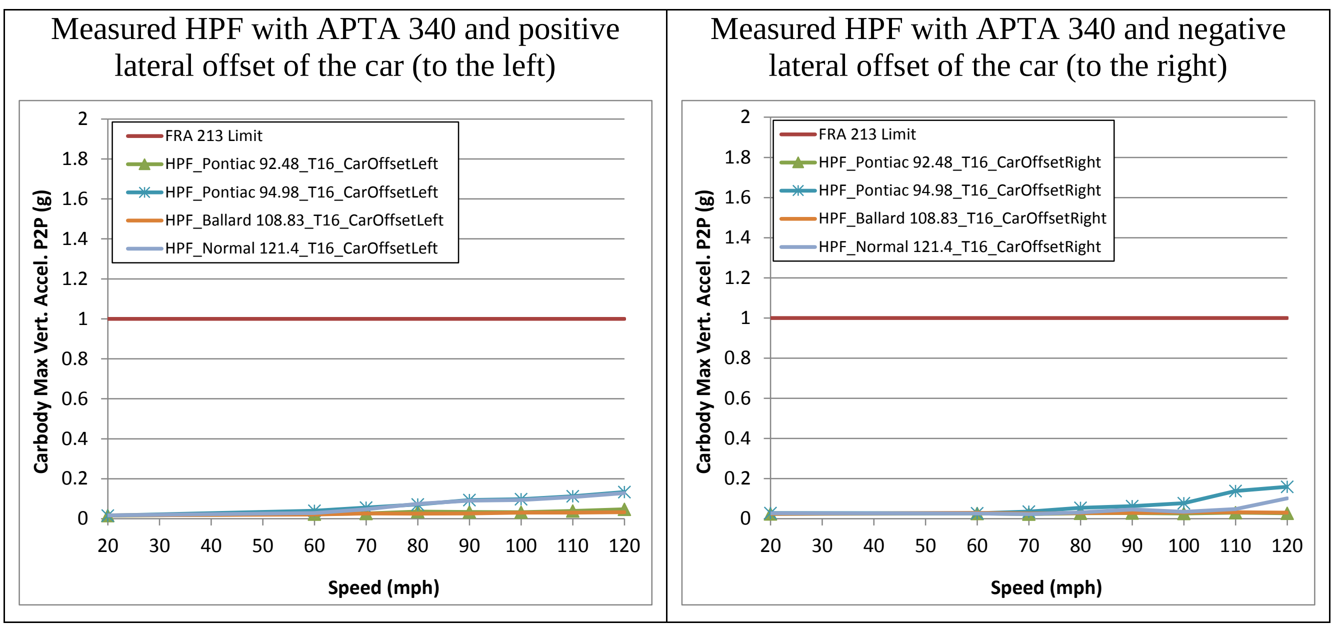

Figure 50. Carbody maximum vertical acceleration on the T16 passenger car - measured HPFs with positive car offset (left) and negative car offset (right)

5.2.4 Measured HPF with GP40

Figures 51–52 show results of carbody maximum vertical acceleration on the GP40 passenger locomotive for measured HPF with different scenarios from the parametric study.

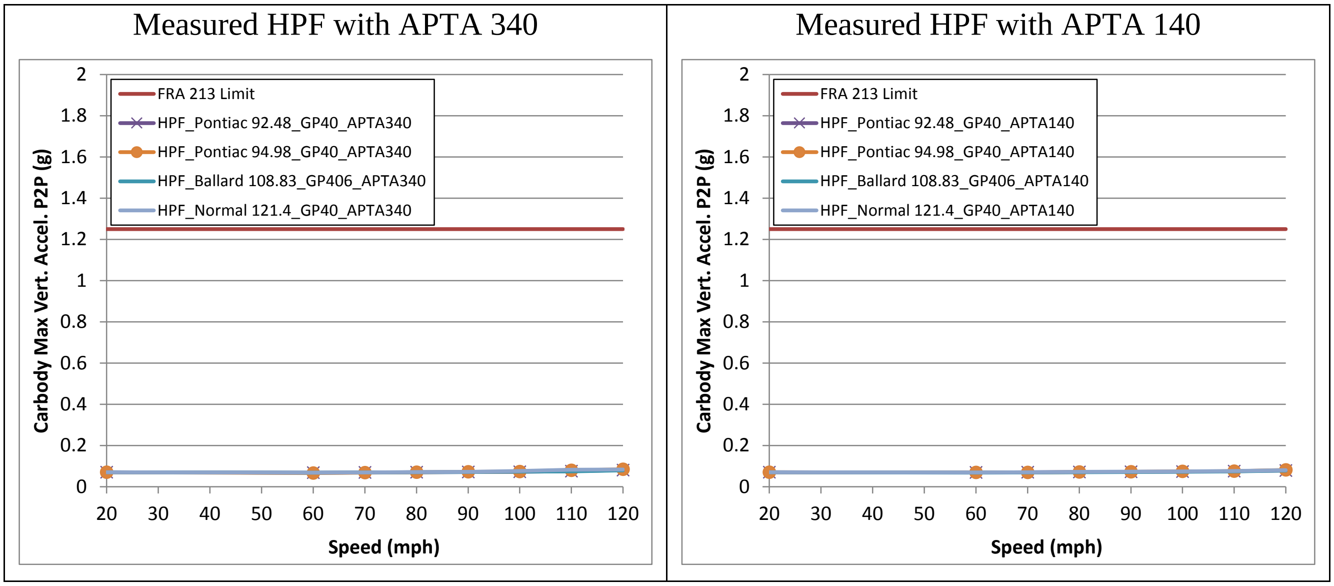

Figure 51. Carbody maximum vertical acceleration on the GP40 passenger locomotive - measured HPFs with wheelsets APTA 340 (left) and APTA140 (right)

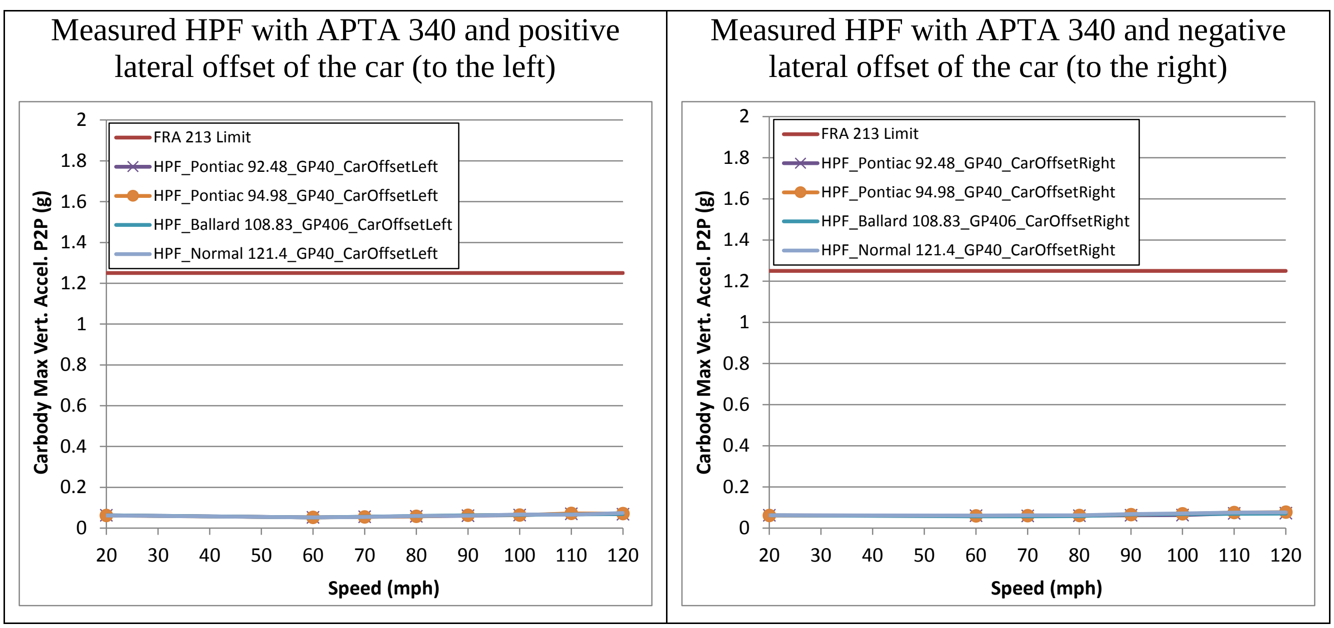

Figure 52. Carbody maximum vertical acceleration on the GP40 passenger locomotive - measured HPFs with positive car offset (left) and negative car offset (right) Single Wheel Vertical Load Ratio

5.3 Single Wheel Vertical Load Ratio

5.3.1 As-designed HPF with T16

Figures 53–57 show results of minimum wheel unload ratio under the T16 passenger car for the as-designed HPF with different scenarios from the parametric study.

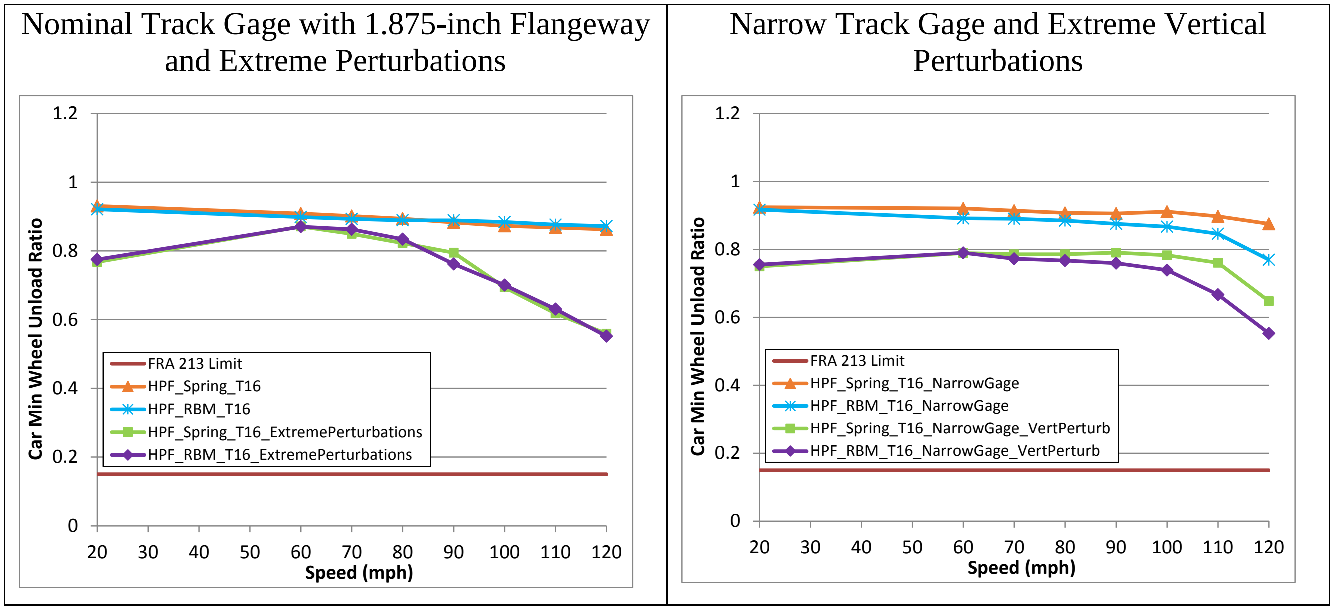

Figure 53. Minimum wheel unload ratio under the T16 passenger car - nominal track gage (left) and narrow track gage (right)

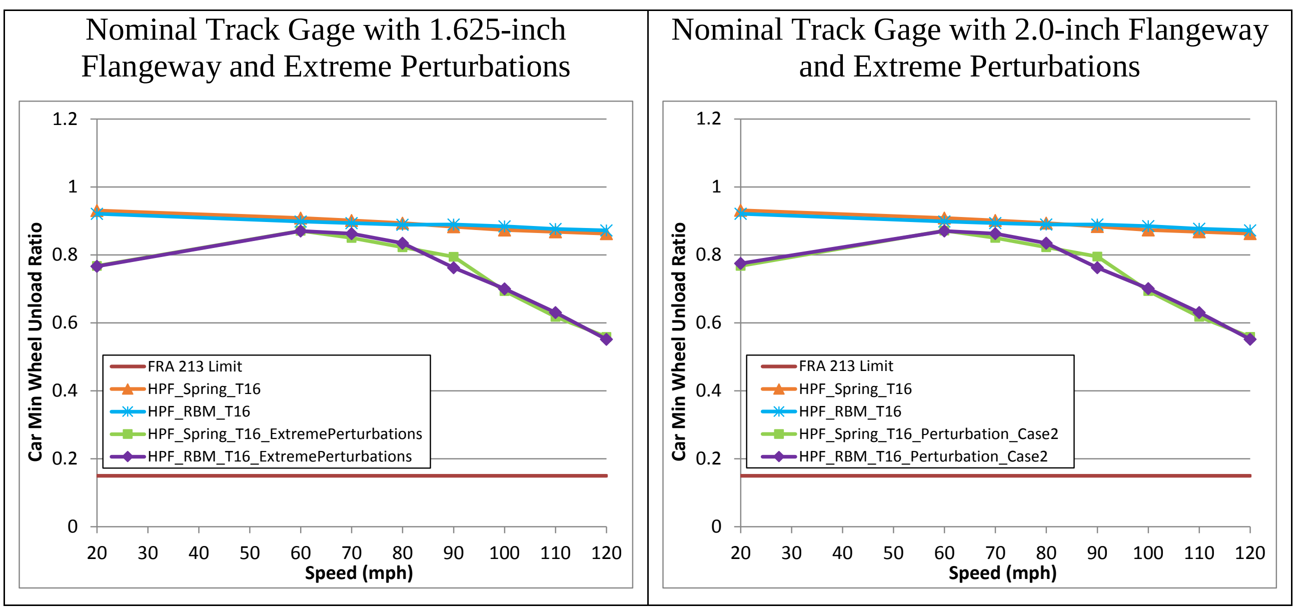

Figure 54. Minimum wheel unload ratio under the T16 passenger car - nominal track gage with 1.625-inch flangeway (left) and 2.0-inch flangeway (right)

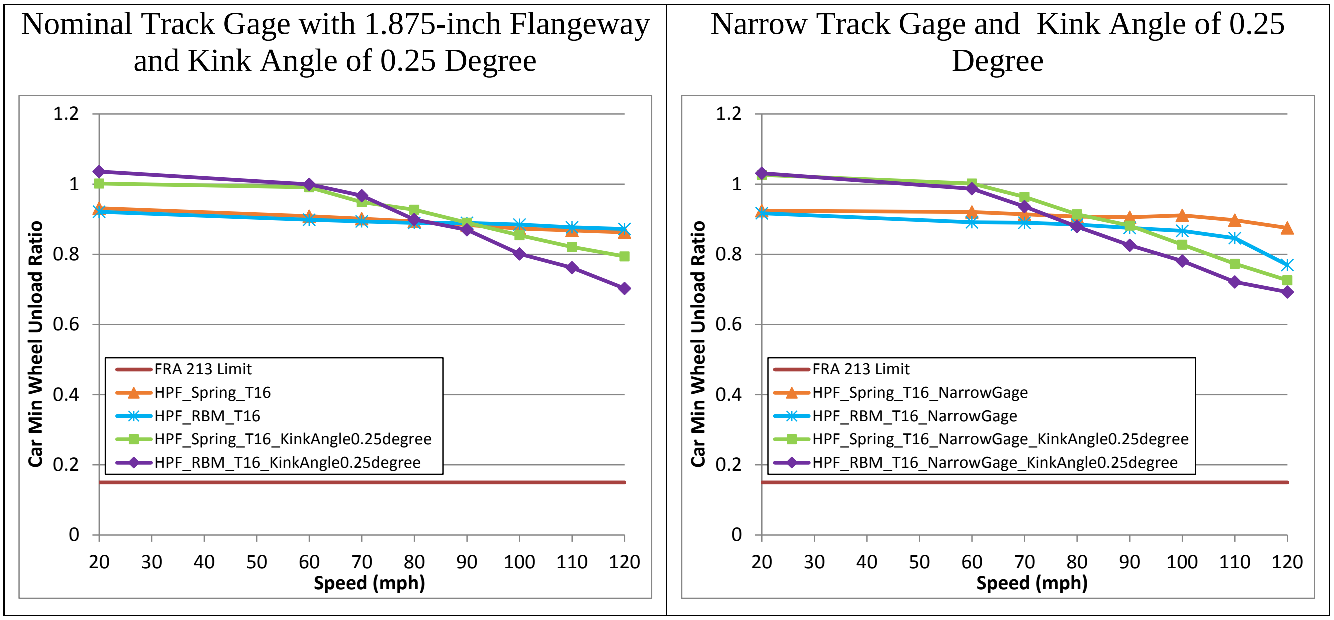

Figure 55. Minimum wheel unload ratio under the T16 passenger car - kink angle of 0.25 degree with nominal track gage (left) and narrow track gage (right)

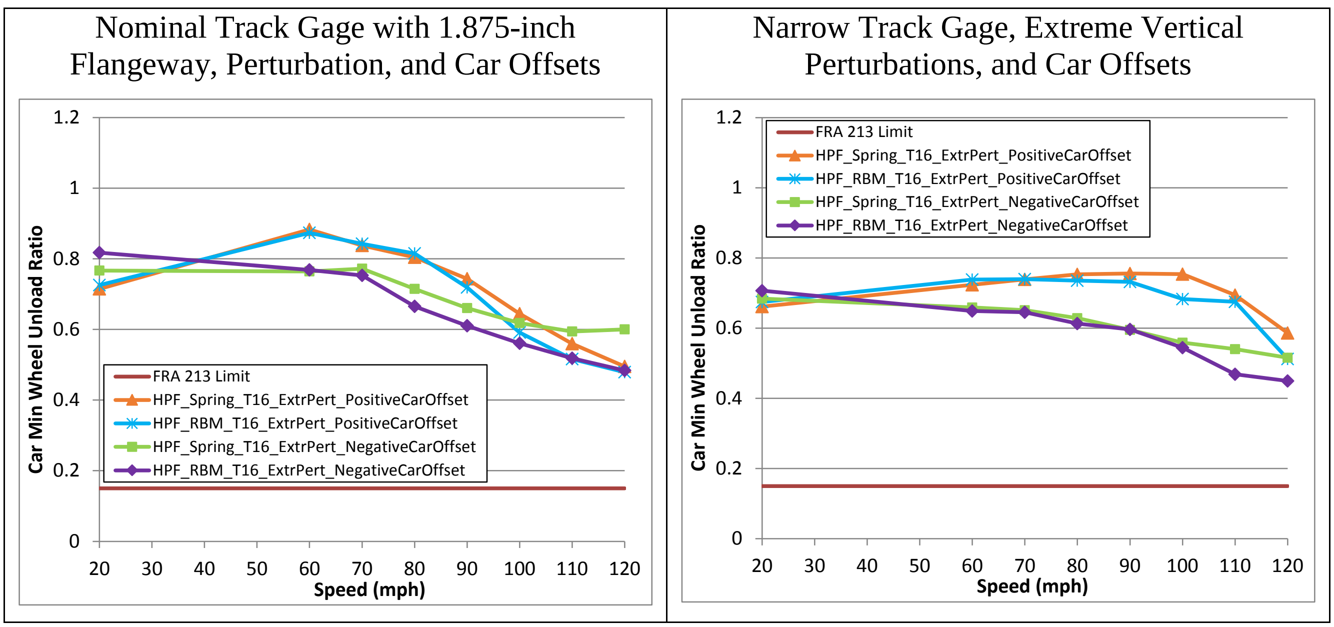

Figure 56. Minimum wheel unload ratio under the T16 passenger car - car offsets with nominal track gage (left) and narrow track gage (right)

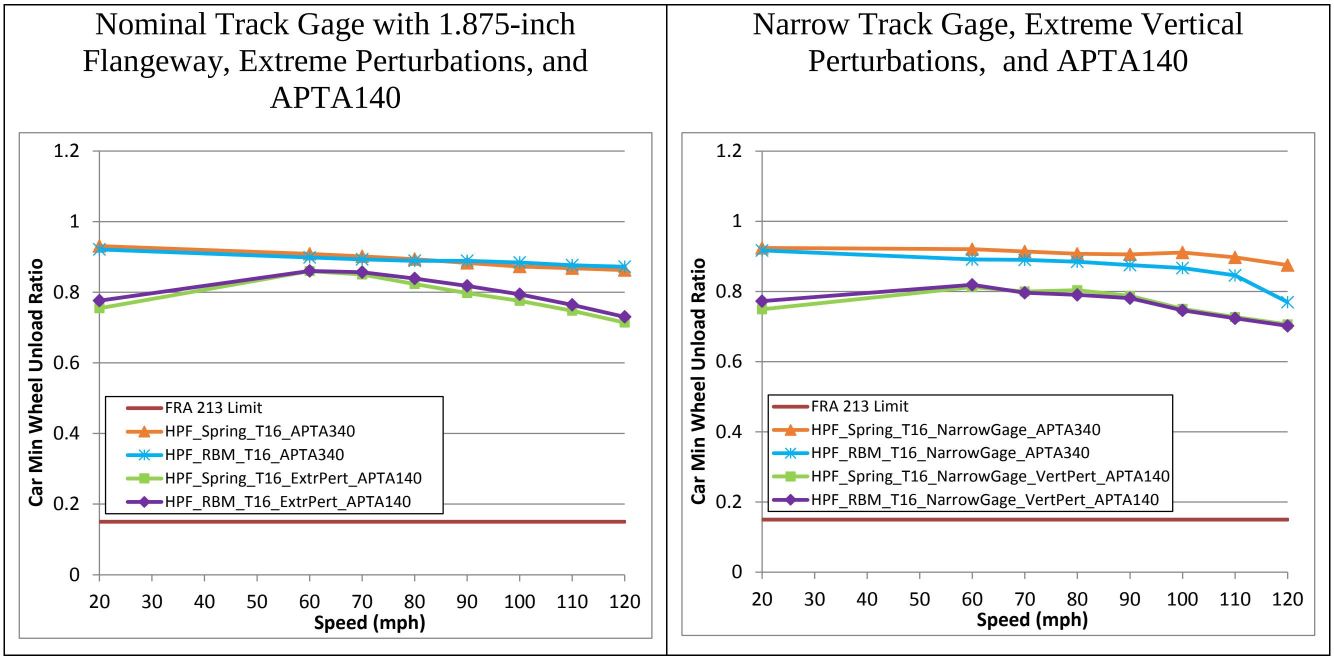

Figure 57. Minimum wheel unload ratio under the T16 passenger car - APTA140 with nominal track gage (left) and narrow track gage (right)

5.3.2 As-designed HPF with GP40

Figures 58–62 show results of minimum wheel unload ratio under the GP40 passenger locomotive for as-designed HPF with different scenarios from the parametric study.

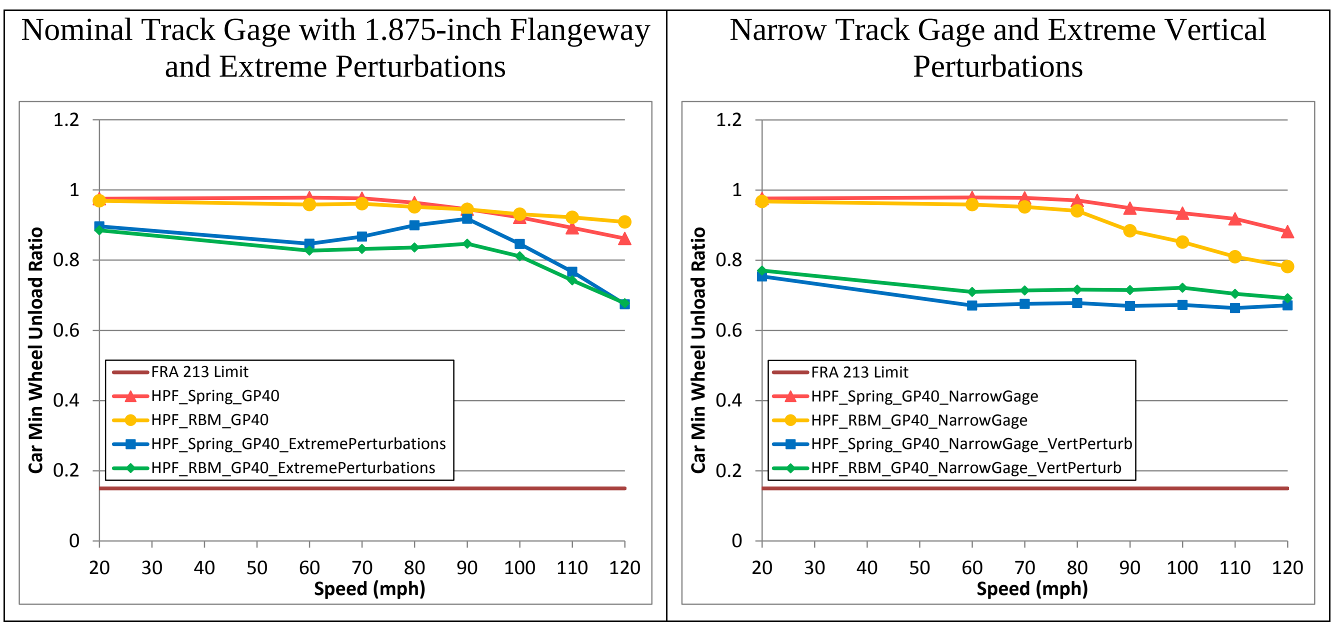

Figure 58. Minimum wheel unload ratio under the GP40 passenger locomotive - nominal track gage (left) and narrow track gage (right)

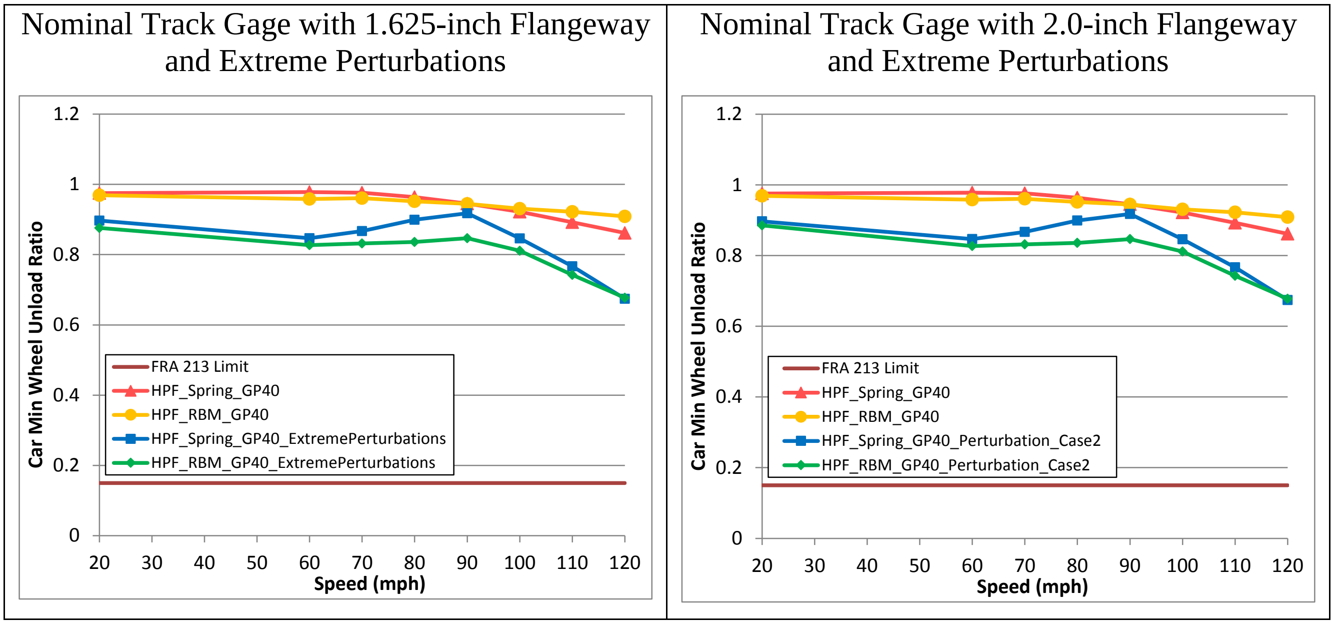

Figure 59. Minimum wheel unload ratio under the GP40 passenger locomotive - nominal track gage with 1.625-inch flangeway (left) and 2.0-inch flangeway (right)

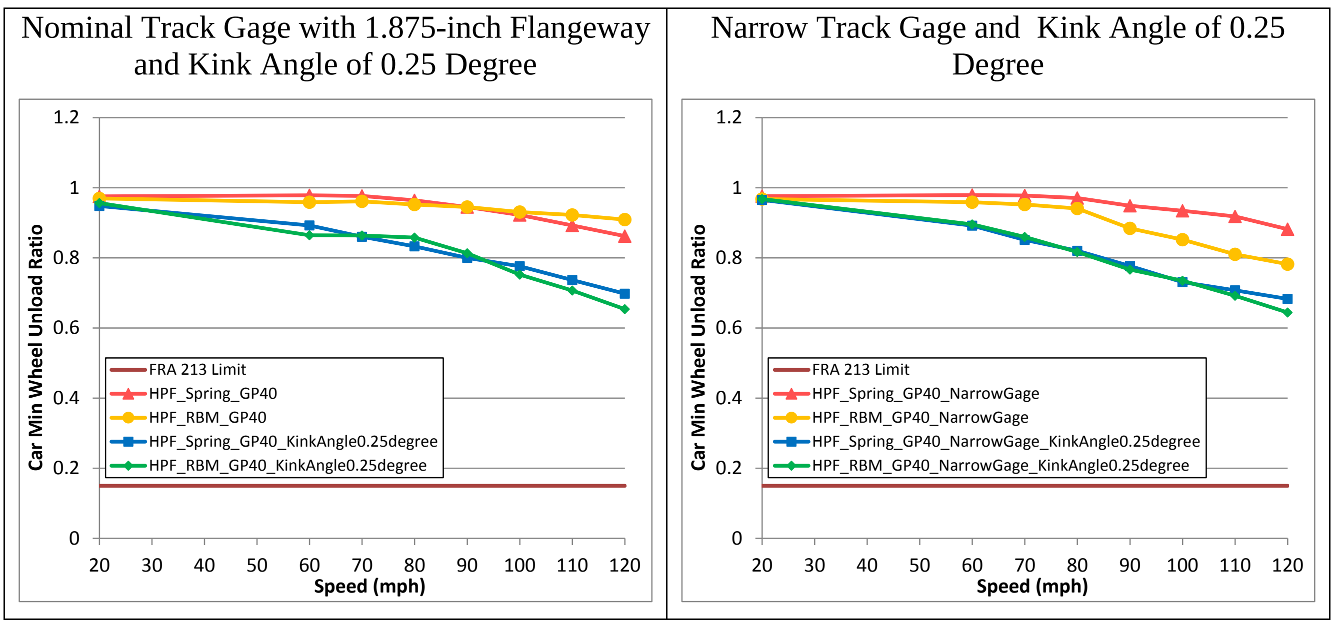

Figure 60. Minimum wheel unload ratio under the GP40 passenger locomotive - kink angle of 0.25 degree with nominal track gage (left) and narrow track gage (right)

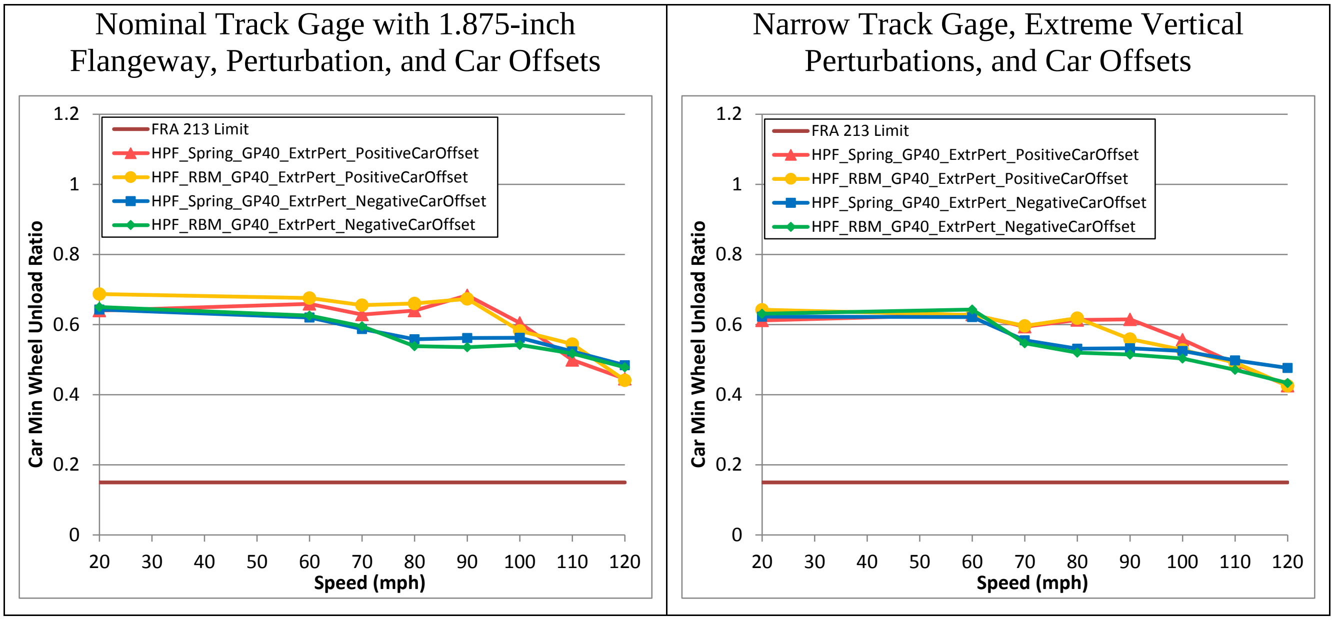

Figure 61. Minimum wheel unload ratio under the GP40 passenger locomotive - car offsets with nominal track gage (left) and narrow track gage (right)

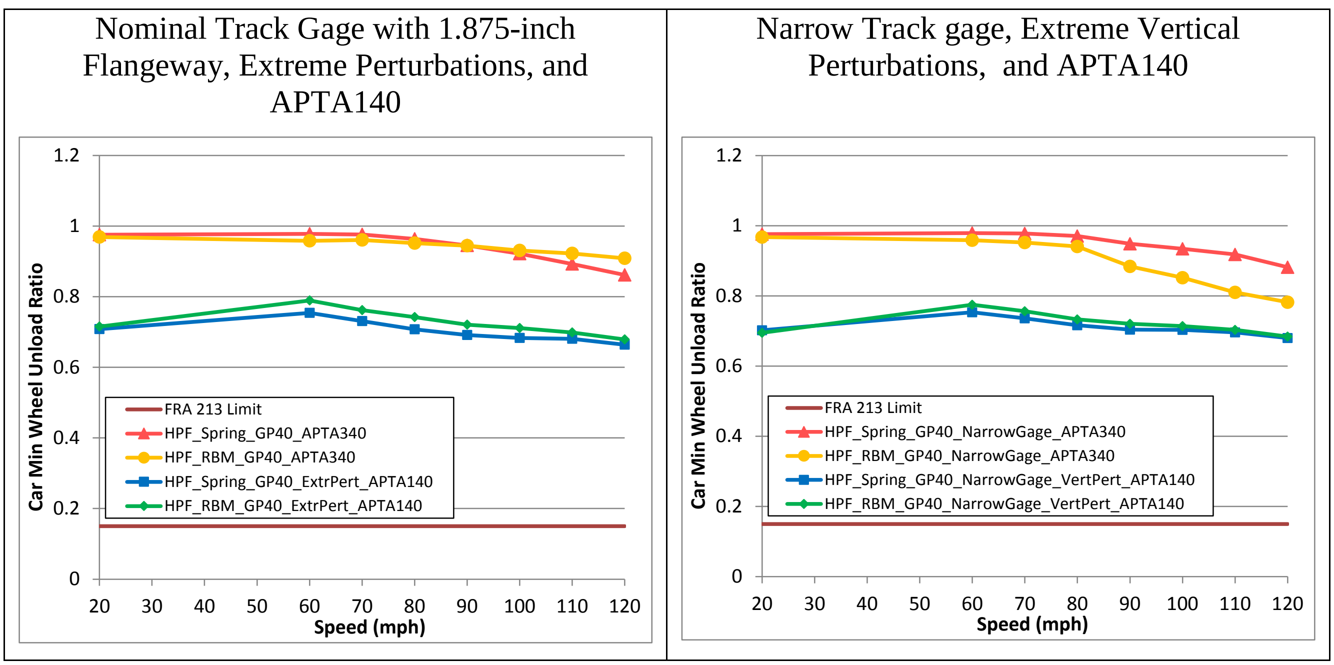

Figure 62. Minimum wheel unload ratio under the GP40 passenger locomotive - APTA140 with nominal track gage (left) and narrow track gage (right)

5.3.3 Measured HPF with T16

Figures 63–64 show results of minimum wheel unload ratio under the T16 passenger car for measured HPF with different scenarios from the parametric study.

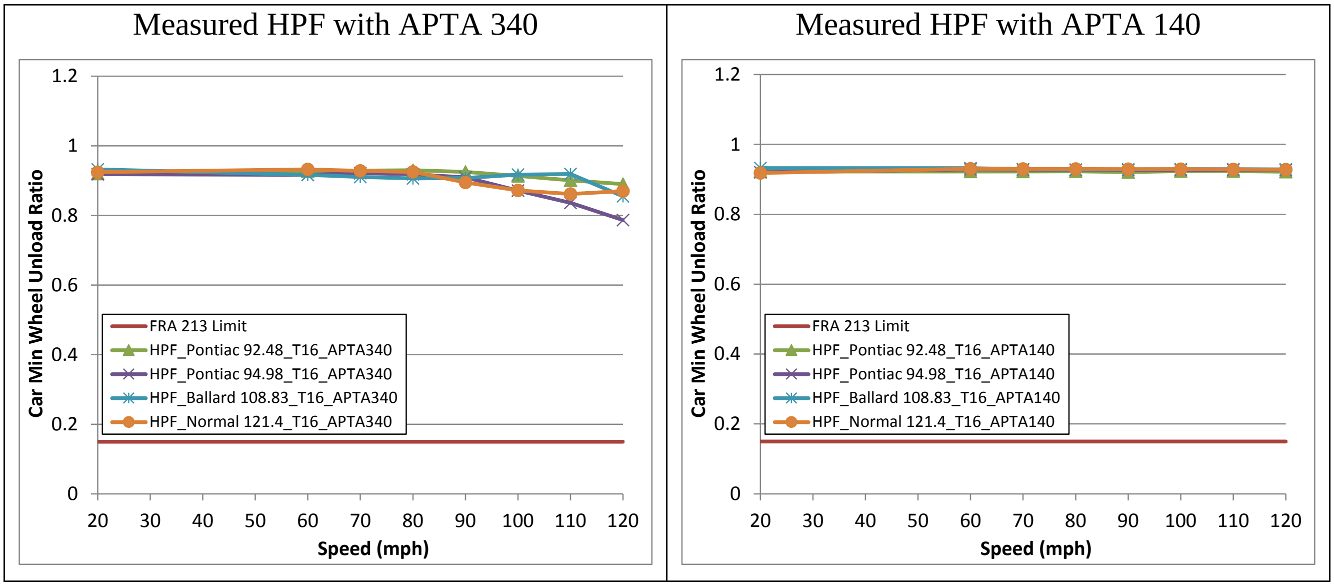

Figure 63. Minimum wheel unload ratio under the T16 passenger car - measured HPFs with wheelsets APTA 340 (left) and APTA140 (right)

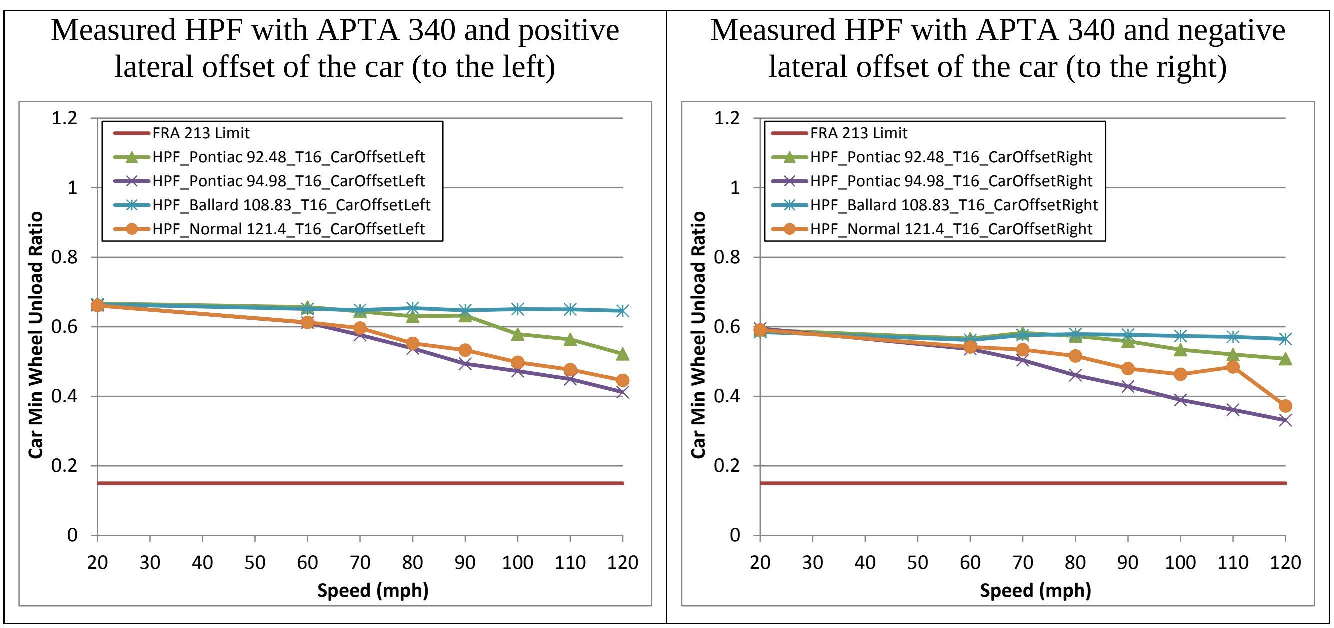

Figure 64. Minimum wheel unload ratio under the T16 passenger car - measured HPFs with positive car offset (left) and negative car offset (right)

5.3.4 Measured HPF with GP40

Figures 65–66 show results of minimum wheel unload ratio under the GP40 passenger locomotive for measured HPF with different scenarios from the parametric study.

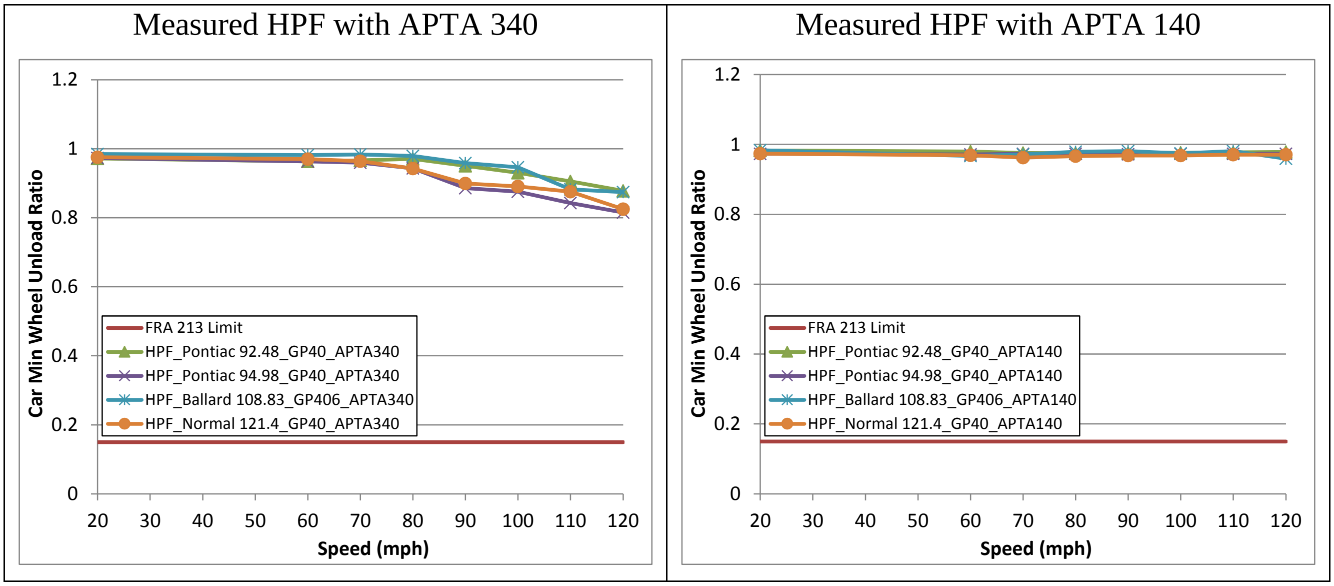

Figure 65. Minimum wheel unload ratio under the GP40 passenger locomotive - measured HPFs with wheelsets APTA 340(left) and APTA140 (right)

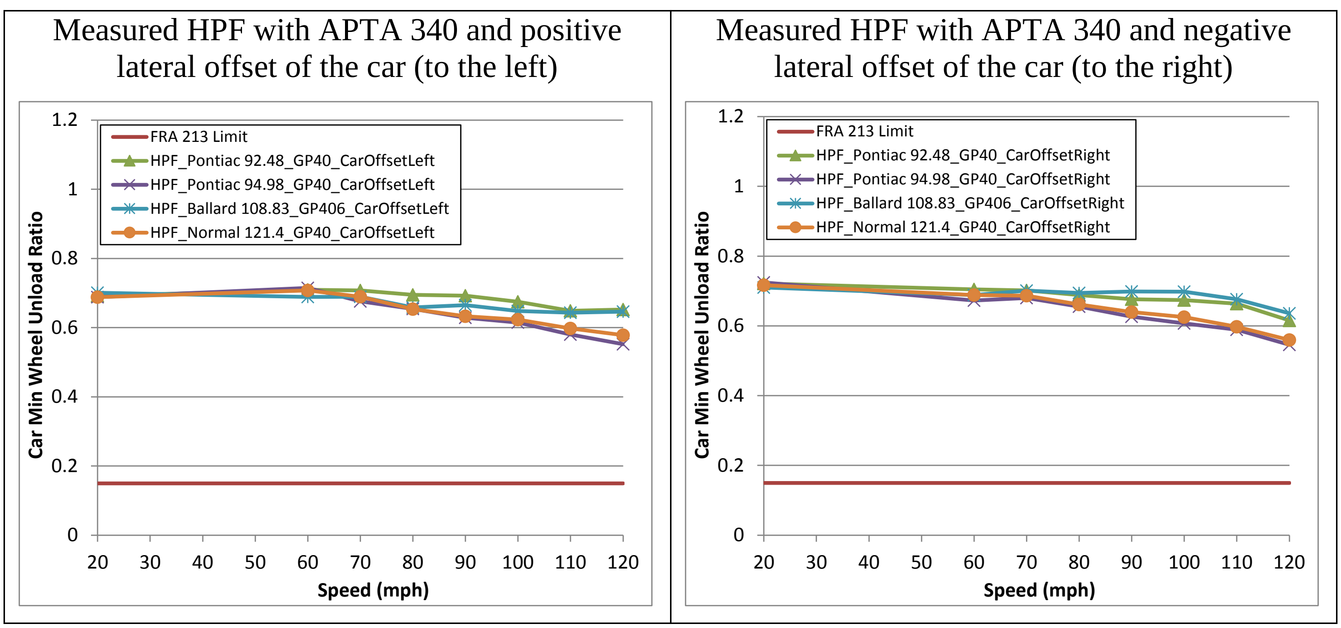

Figure 66. Minimum wheel unload ratio under the GP40 passenger locomotive - measured HPFs with positive car offset (left) and negative car offset (right)

5.4 Single Wheel L/V Ratio

5.4.1 As-designed HPF with T16

Figures 67–71 show results of single-wheel maximum L/V ratio under the T16 passenger car for the as-designed HPF with different scenarios from the parametric study.

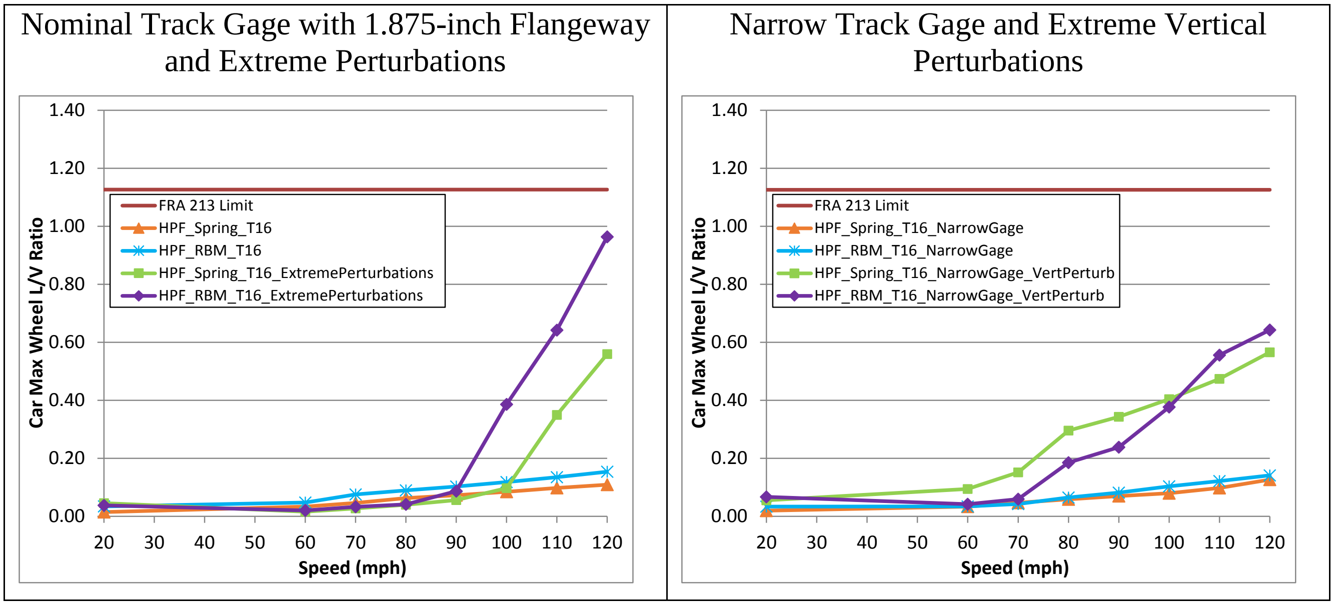

Figure 67. Single-wheel maximum L/V ratio under the T16 passenger car - nominal track gage (left) and narrow track gage (right)

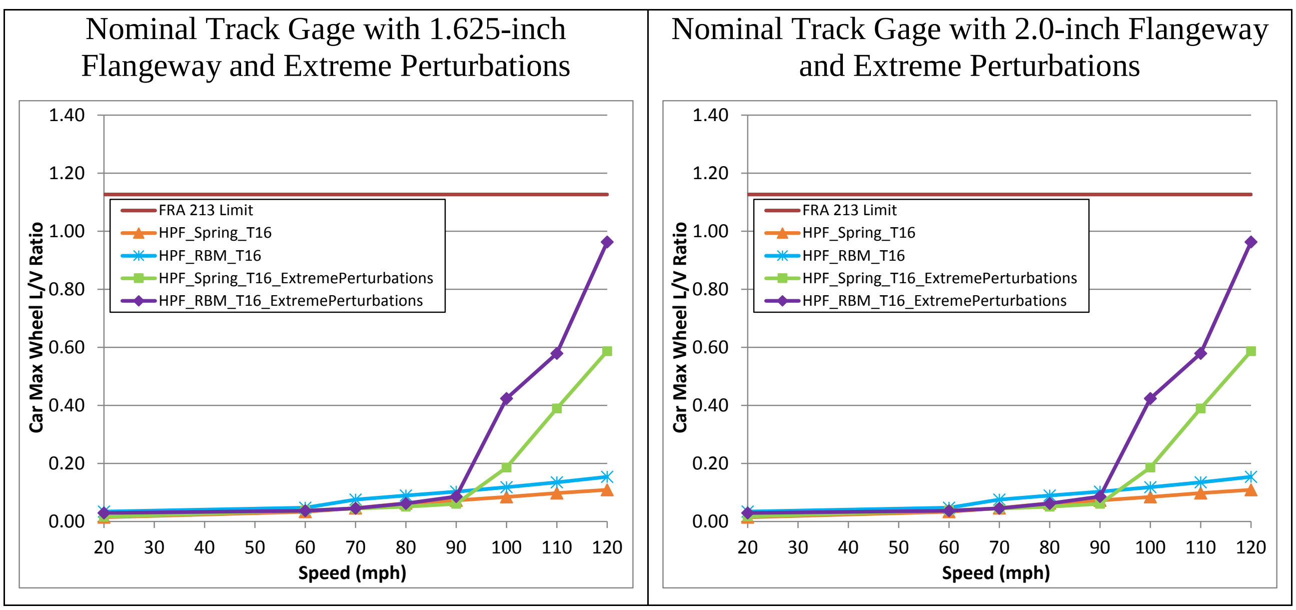

Figure 68. Single-wheel maximum L/V ratio under the T16 passenger car - nominal track gage with 1.625-inch flangeway (left) and 2.0-inch flangeway (right)

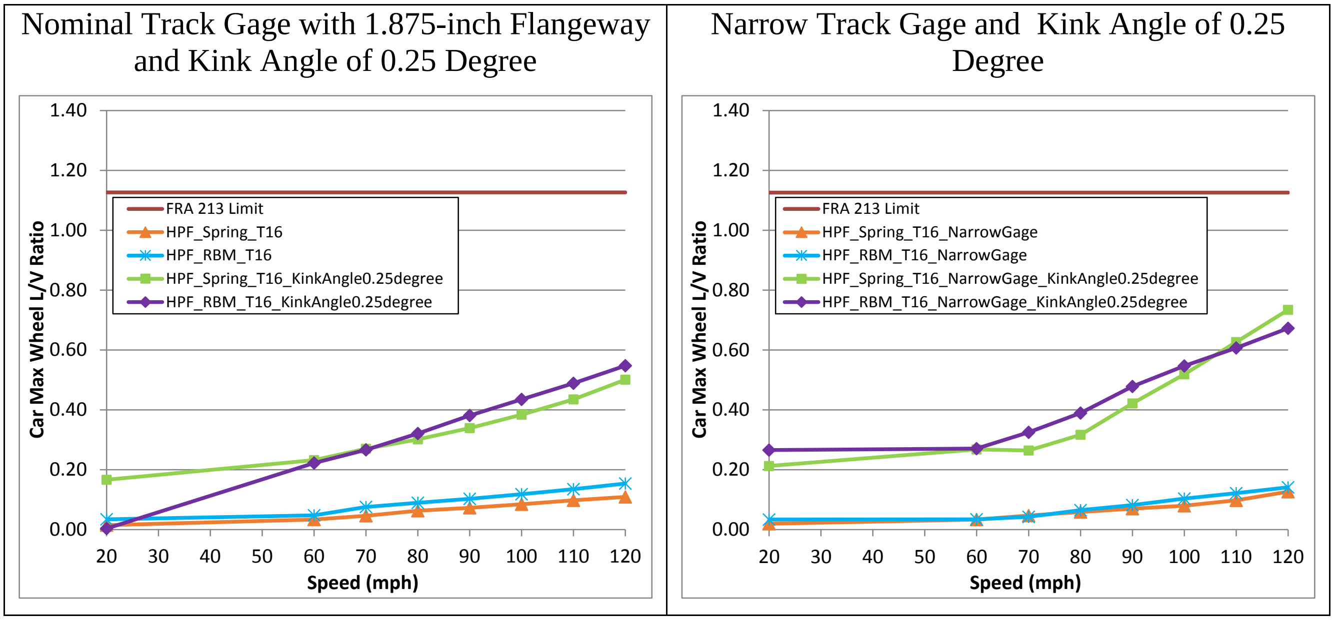

Figure 69. Single-wheel maximum L/V ratio under the T16 passenger car - kink angle of 0.25 degree with nominal track gage (left) and narrow track gage (right)

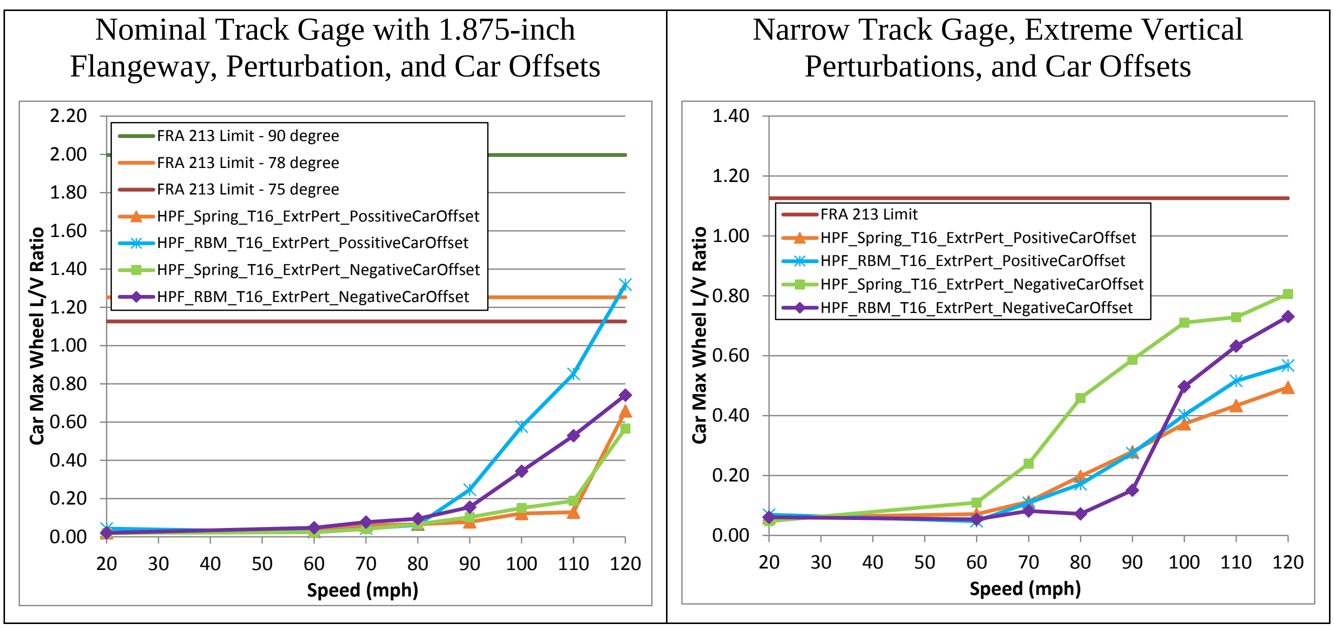

Figure 70. Single-wheel maximum L/V ratio under the T16 passenger car - car offsets with nominal track gage (left) and narrow track gage (right)

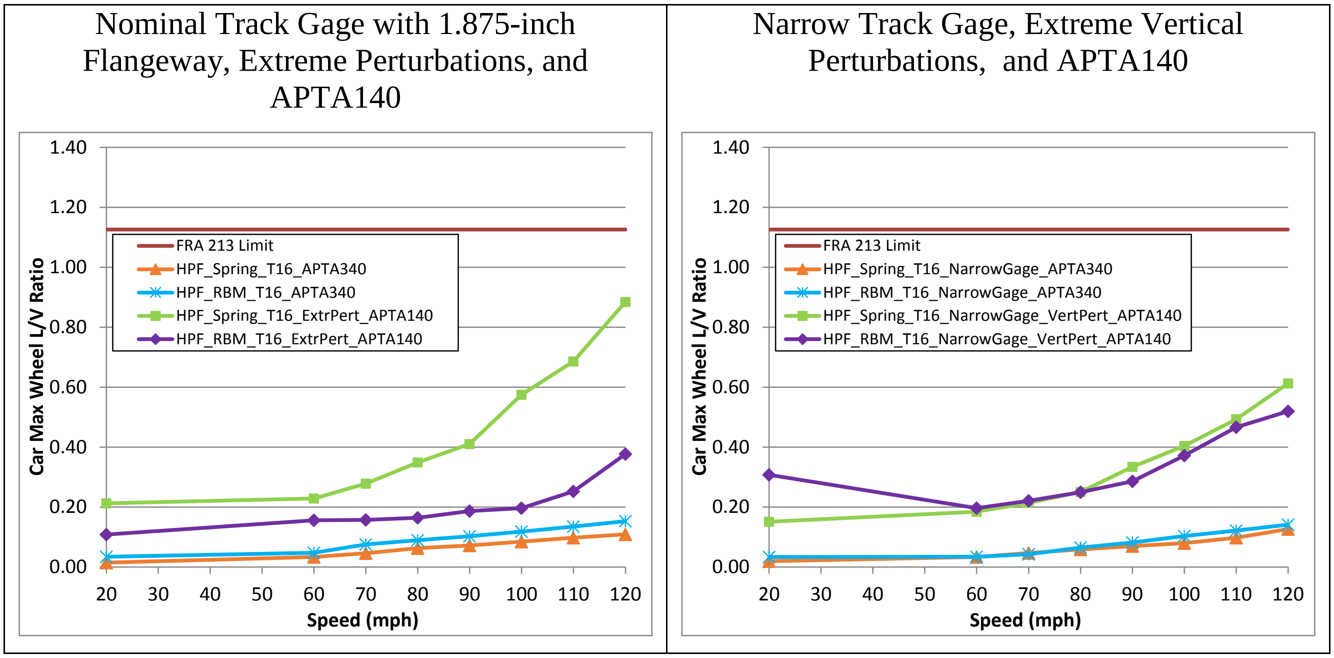

Figure 71. Single-wheel maximum L/V ratio under the T16 passenger car - APTA140 with nominal track gage (left) and narrow track gage (right)

5.4.2 As-designed HPF with GP40

Figures 72–76 show results of single-wheel maximum L/V ratio under the GP40 passenger locomotive for the as-designed HPF with different scenarios from the parametric study.

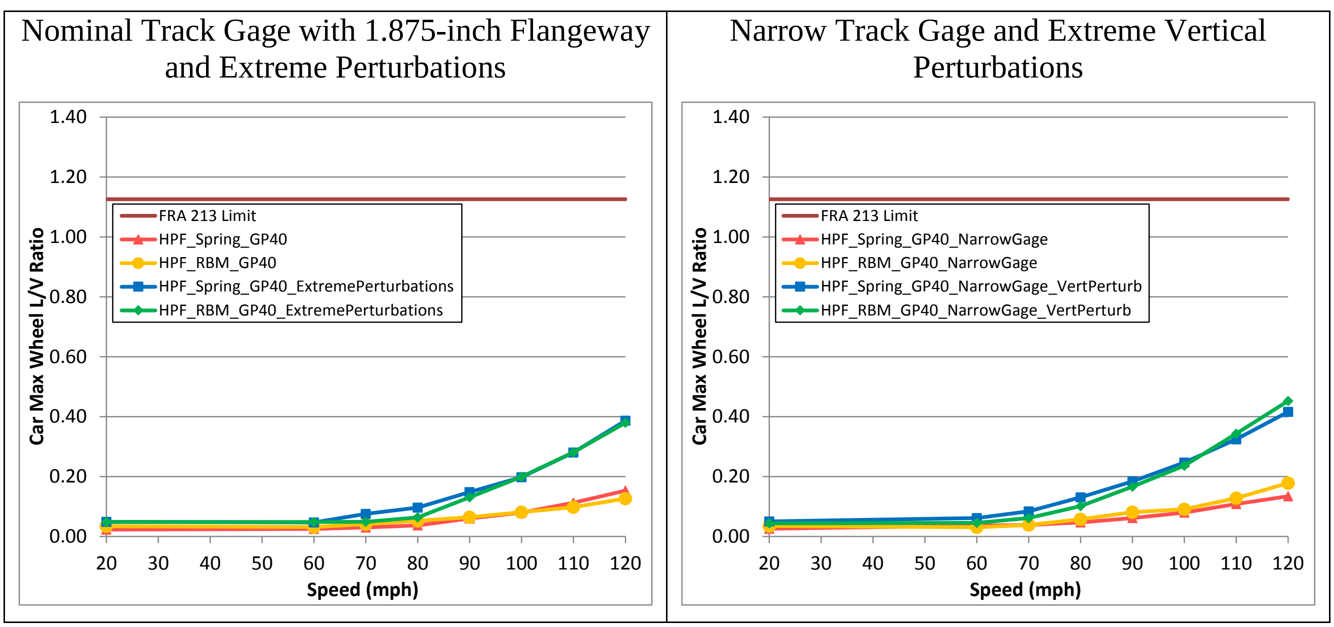

Figure 72. Single-wheel maximum L/V ratio under the GP40 passenger locomotive - nominal track gage (left) and narrow track gage (right)

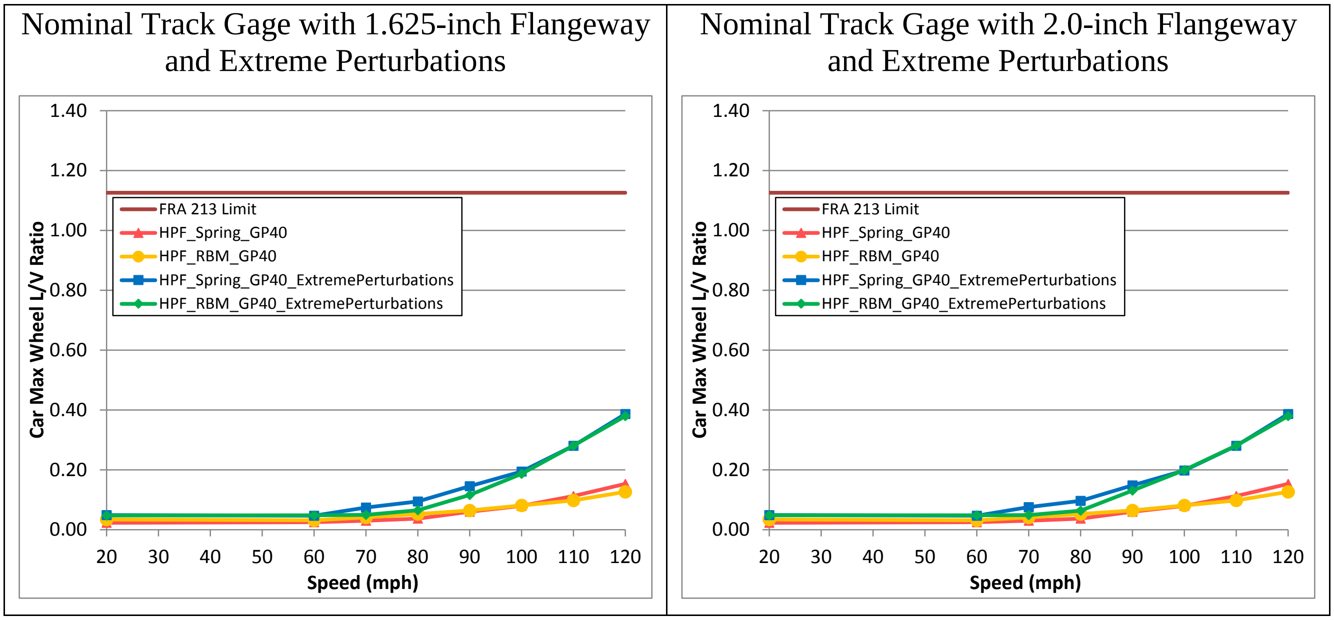

Figure 73. Single-wheel maximum L/V ratio under the GP40 passenger locomotive - nominal track gage with 1.625-inch flangeway (left) and 2.0-inch flangeway (right)

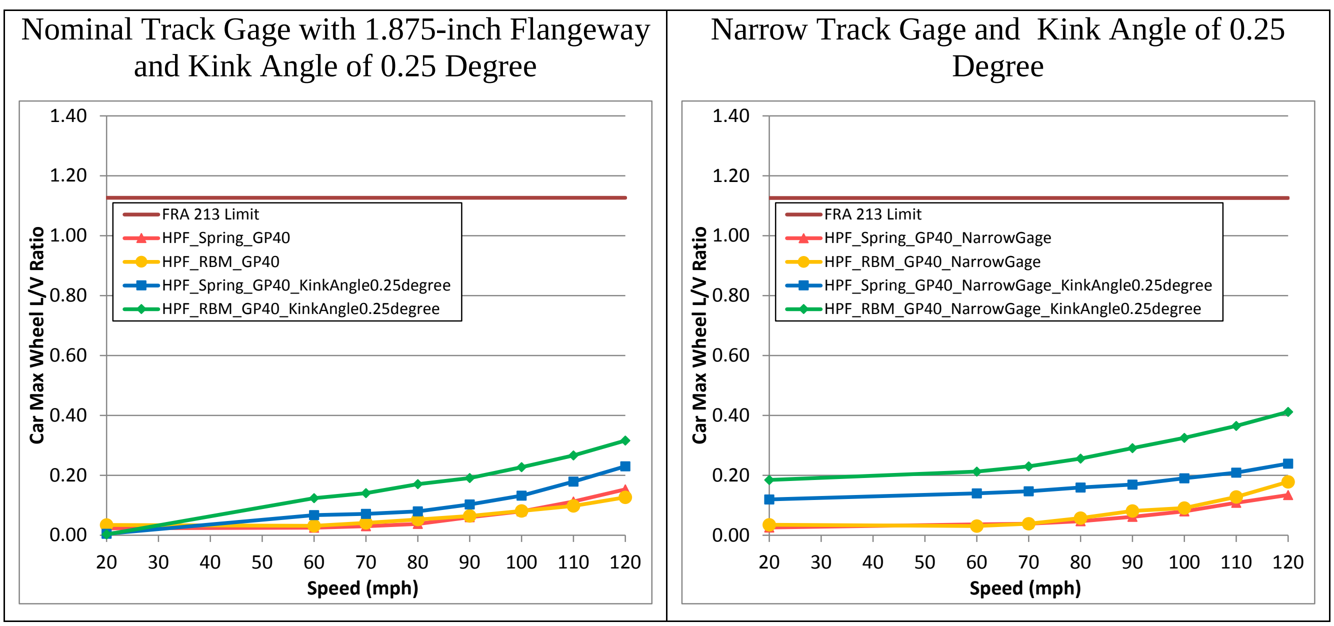

Figure 74. Single-wheel maximum L/V ratio under the GP40 passenger locomotive - kink angle of 0.25 degree with nominal track gage (left) and narrow track gage (right)

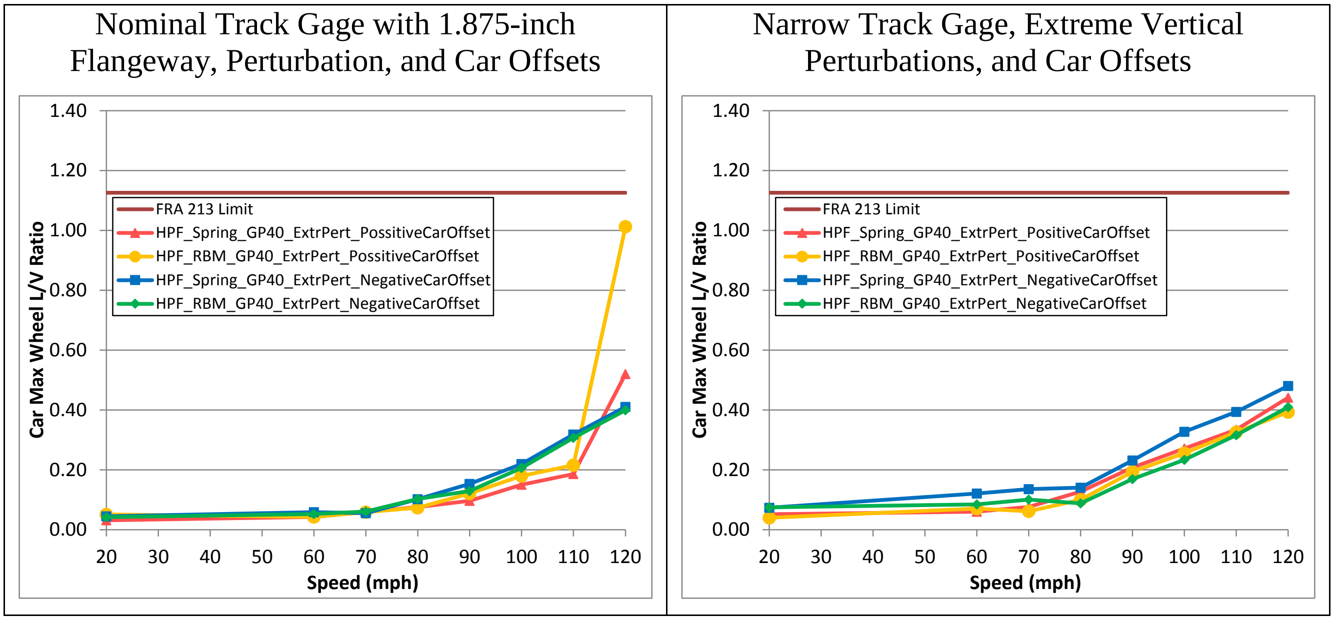

Figure 75. Single-wheel maximum L/V ratio under the GP40 passenger locomotive - car offsets with nominal track gage (left) and narrow track gage (right)

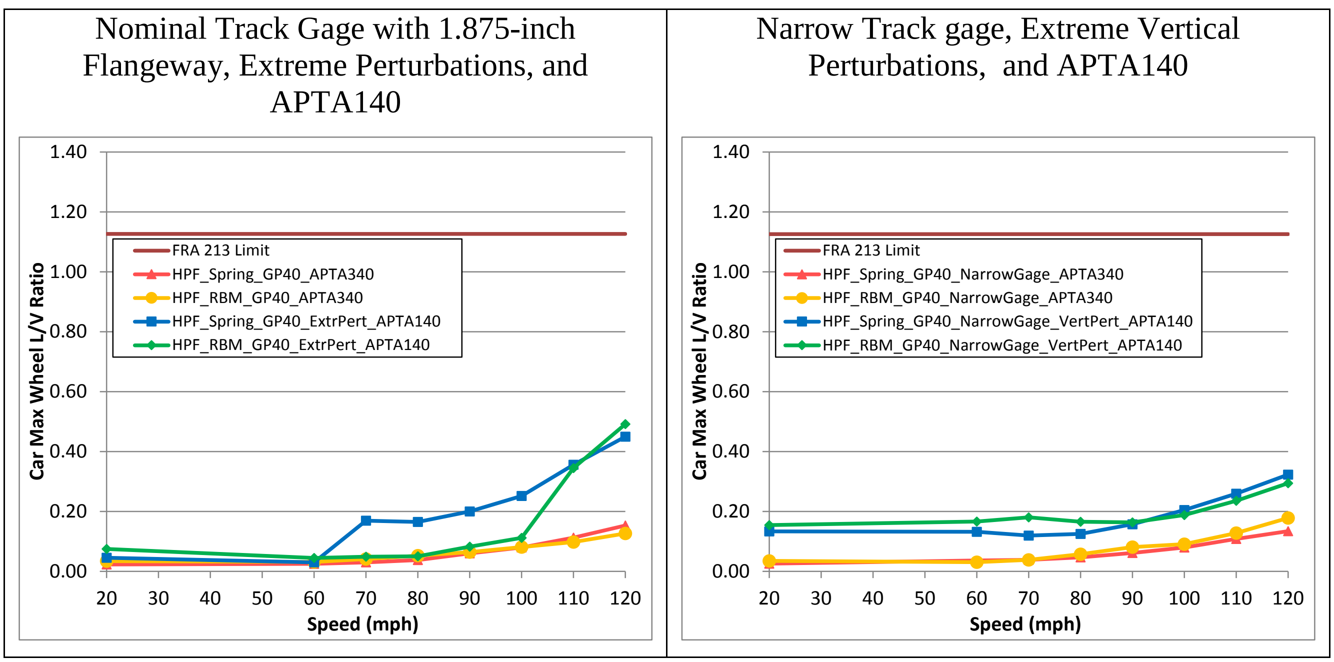

Figure 76. Single-wheel maximum L/V ratio under the GP40 passenger locomotive - APTA140 with nominal track gage (left) and narrow track gage (right)

5.4.3 Measured HPF with T16

Figures 77–78 show results of single-wheel maximum L/V ratio under the T16 passenger car for measured HPF with different scenarios from the parametric study.

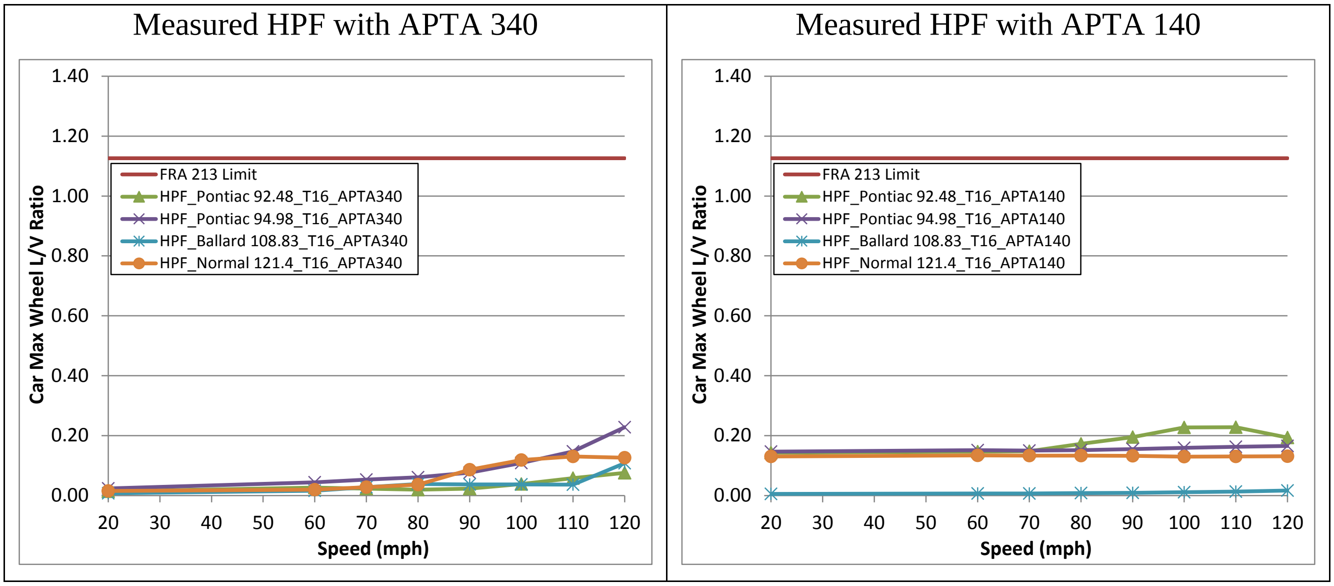

Figure 77. Single-wheel maximum L/V ratio under the T16 passenger car - measured HPFs with wheelsets APTA 340 (left) and APTA140 (right)

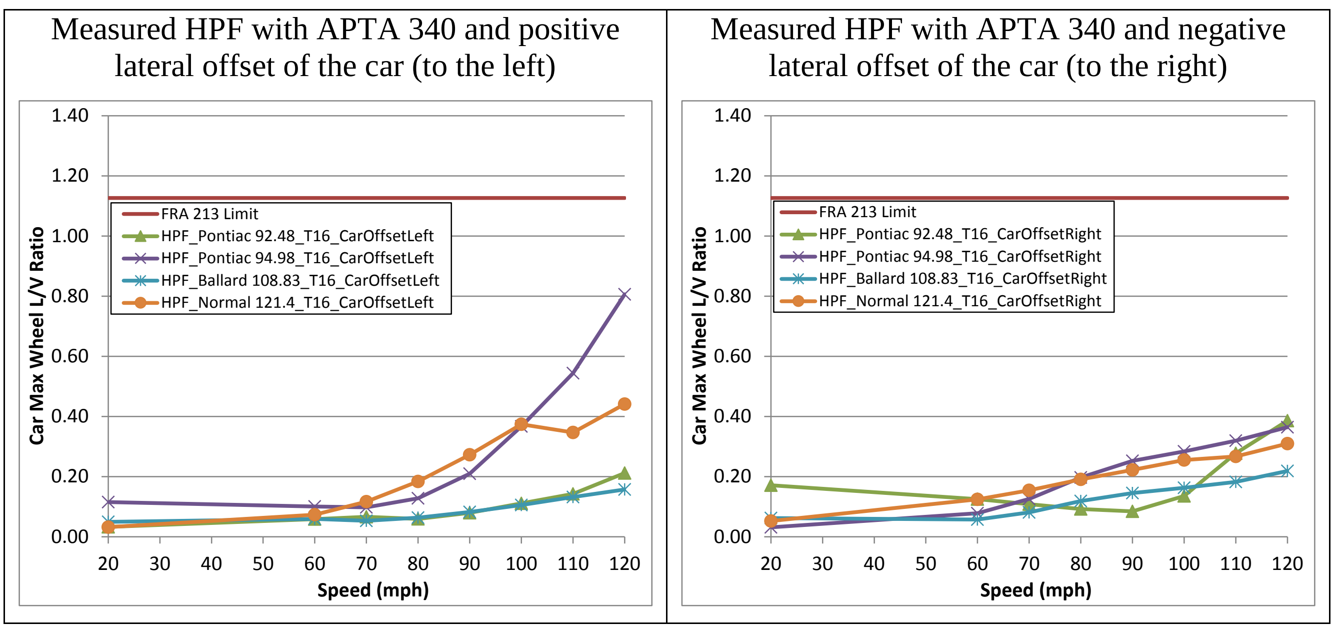

Figure 78. Single-wheel maximum L/V ratio under the T16 passenger car - measured HPFs with positive car offset (left) and negative car offset (right)

5.4.4 Measured HPF with GP40

Figures 79–80 show results of single-wheel maximum L/V ratio under the GP40 passenger locomotive for measured HPF with different scenarios from the parametric study.

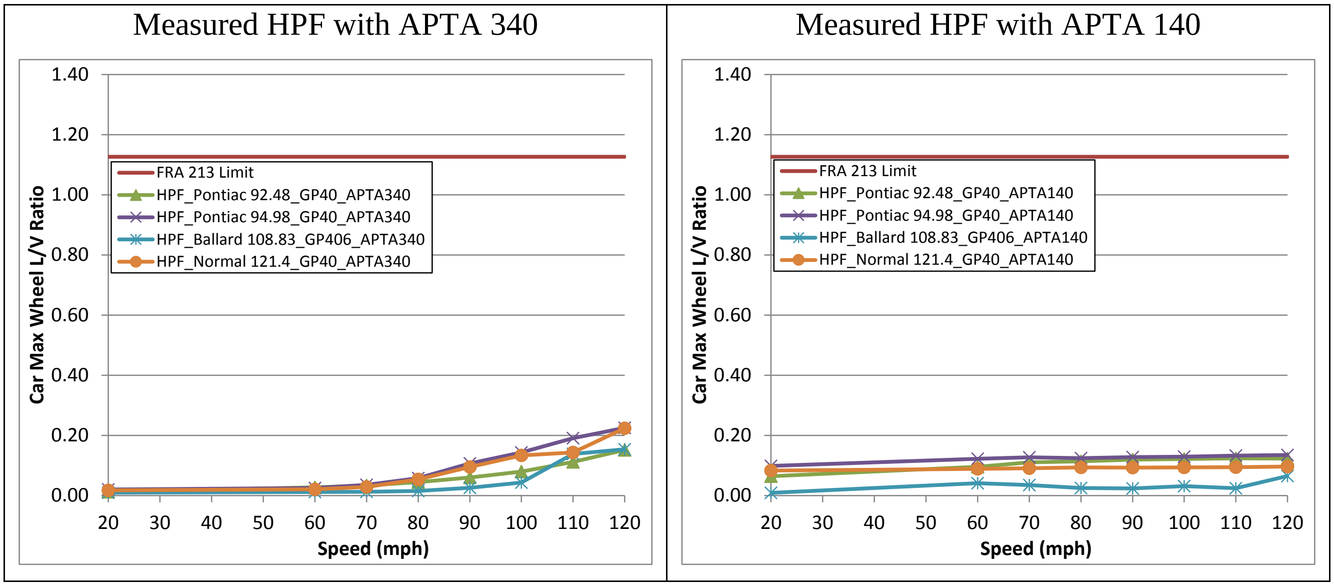

Figure 79. Single-wheel maximum L/V ratio under the GP40 passenger locomotive - measured HPFs with wheelsets APTA 340 (left) and APTA140 (right)

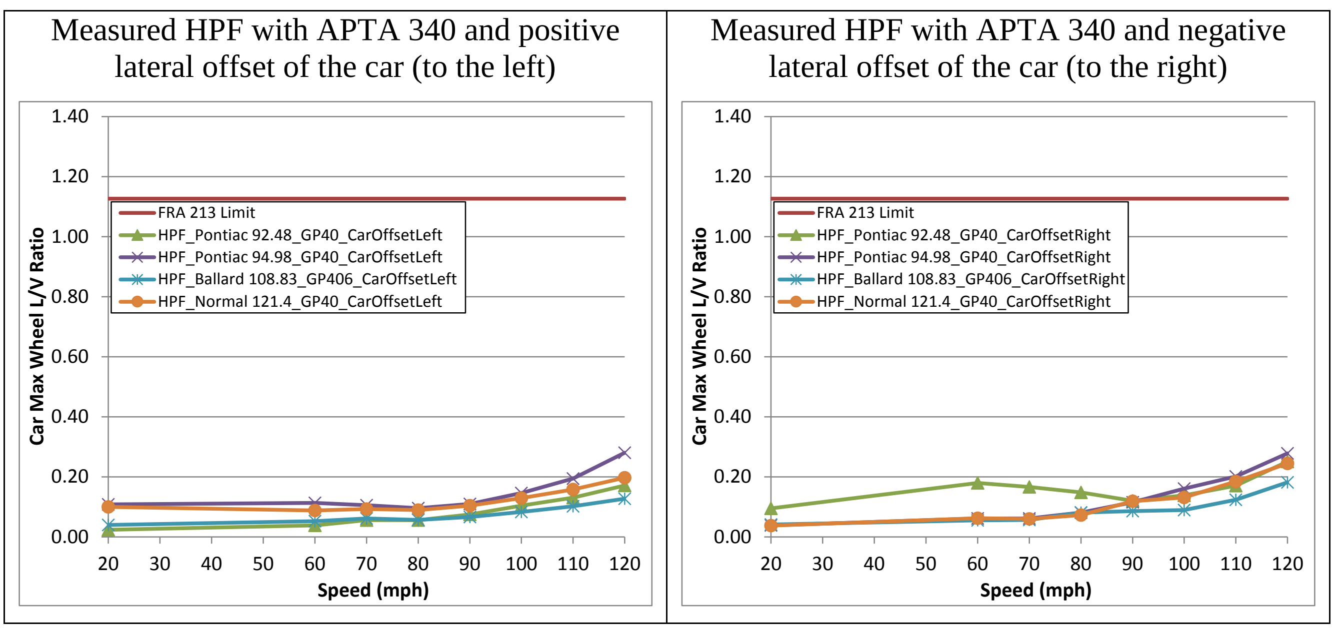

Figure 80. Single-wheel maximum L/V ratio under the GP40 passenger locomotive - measured HPFs with positive car offset (left) and negative car offset (right)

5.5 Net Axle Lateral L/V Ratio

5.5.1 As-designed HPF with T16

Figures 81–85 show results of maximum net axle lateral L/V ratio under the T16 passenger car for as-designed HPF with different scenarios from the parametric study.

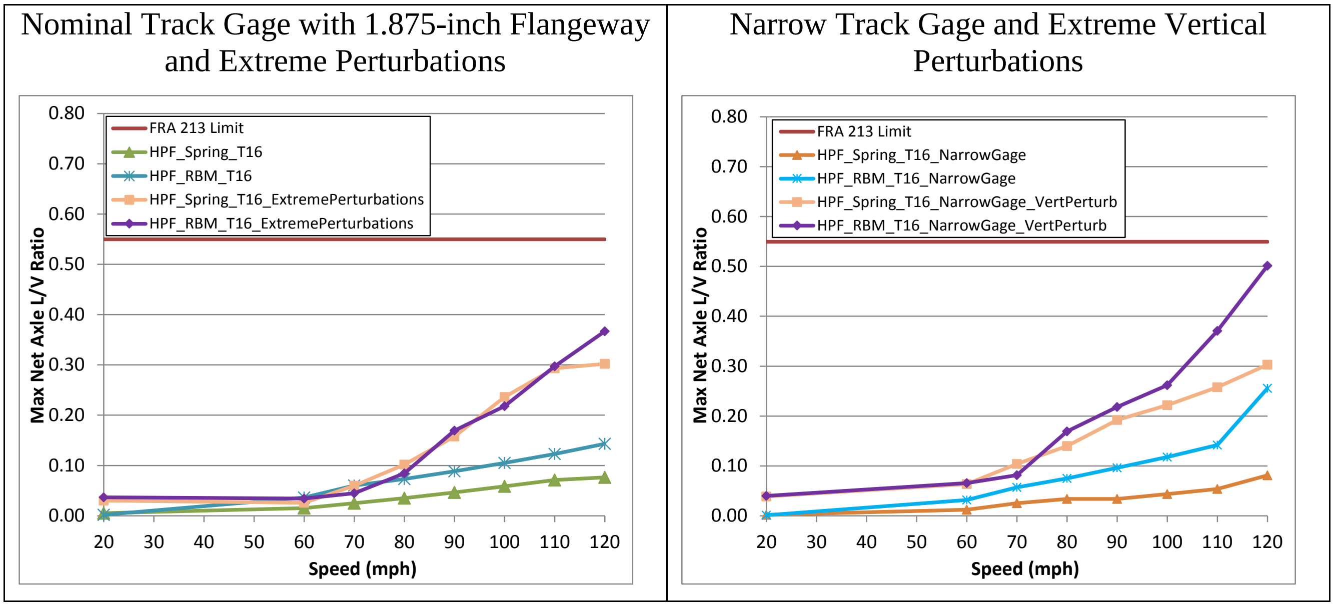

Figure 81. Maximum net axle lateral L/V ratio under the T16 passenger car - nominal track gage (left) and narrow track gage (right)

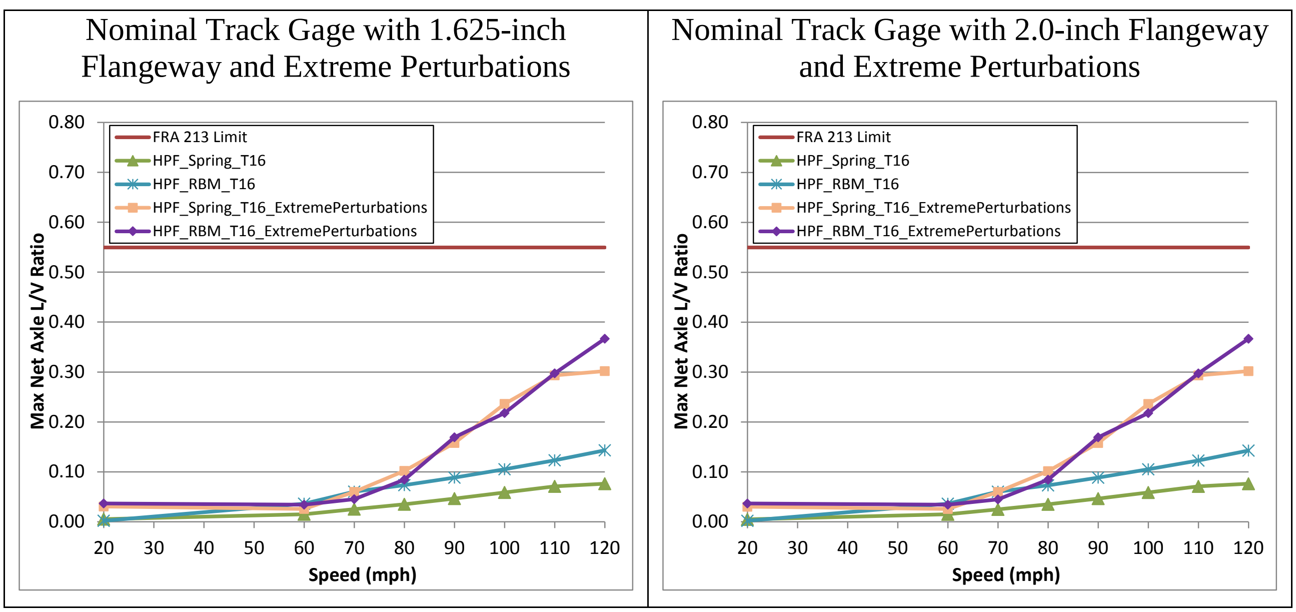

Figure 82. Maximum net axle lateral L/V ratio under the T16 passenger car - nominal track gage with 1.625-inch flangeway (left) and 2.0-inch flangeway (right)

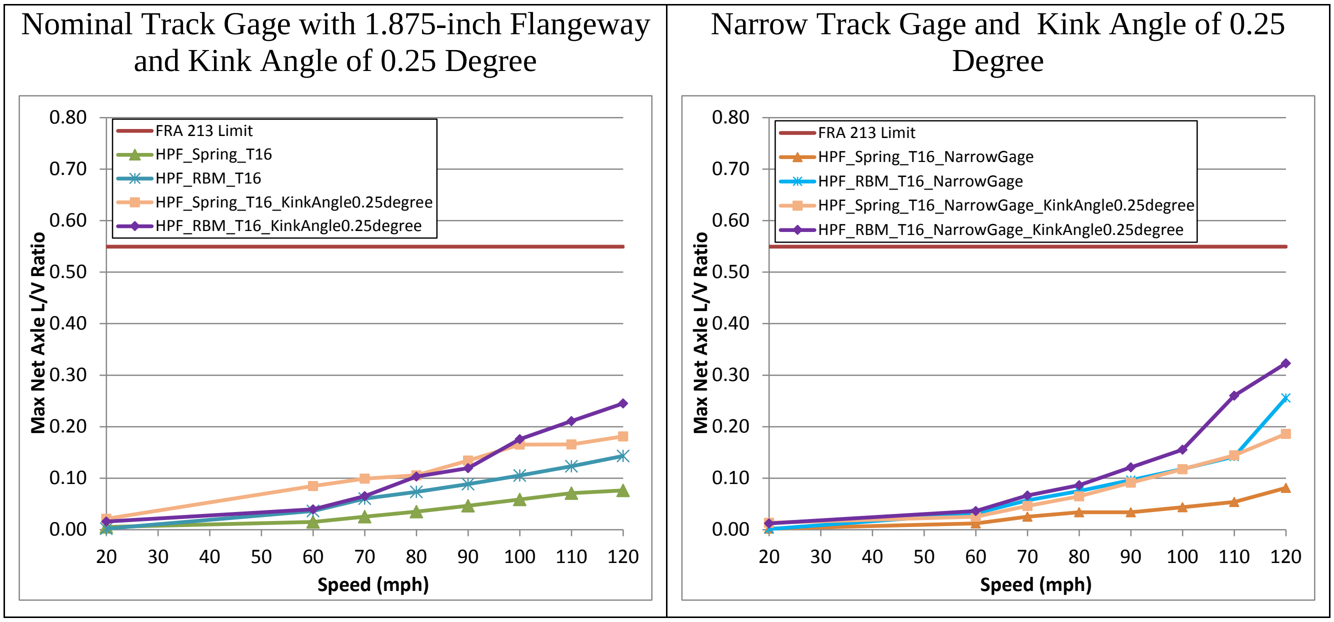

Figure 83. Maximum net axle lateral L/V ratio under the T16 passenger car - kink angle of 0.25 degree with nominal track gage (left) and narrow track gage (right)

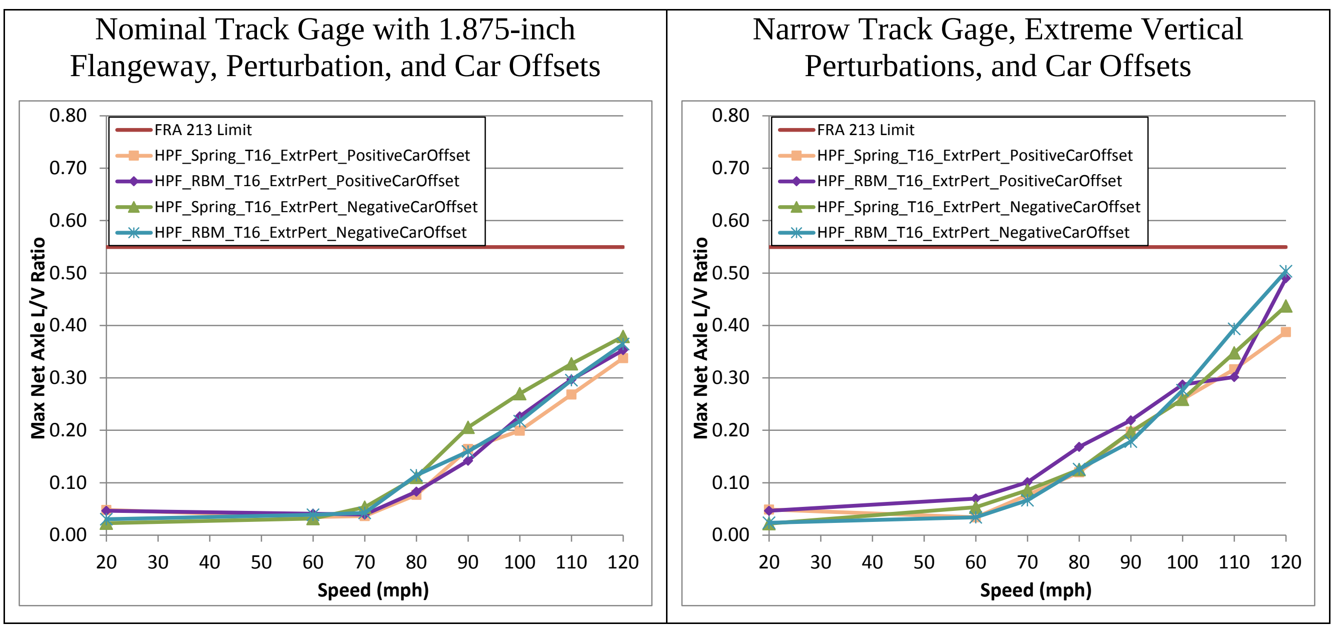

Figure 84. Maximum net axle lateral L/V ratio under the T16 passenger car - car offsets with nominal track gage (left) and narrow track gage (right)

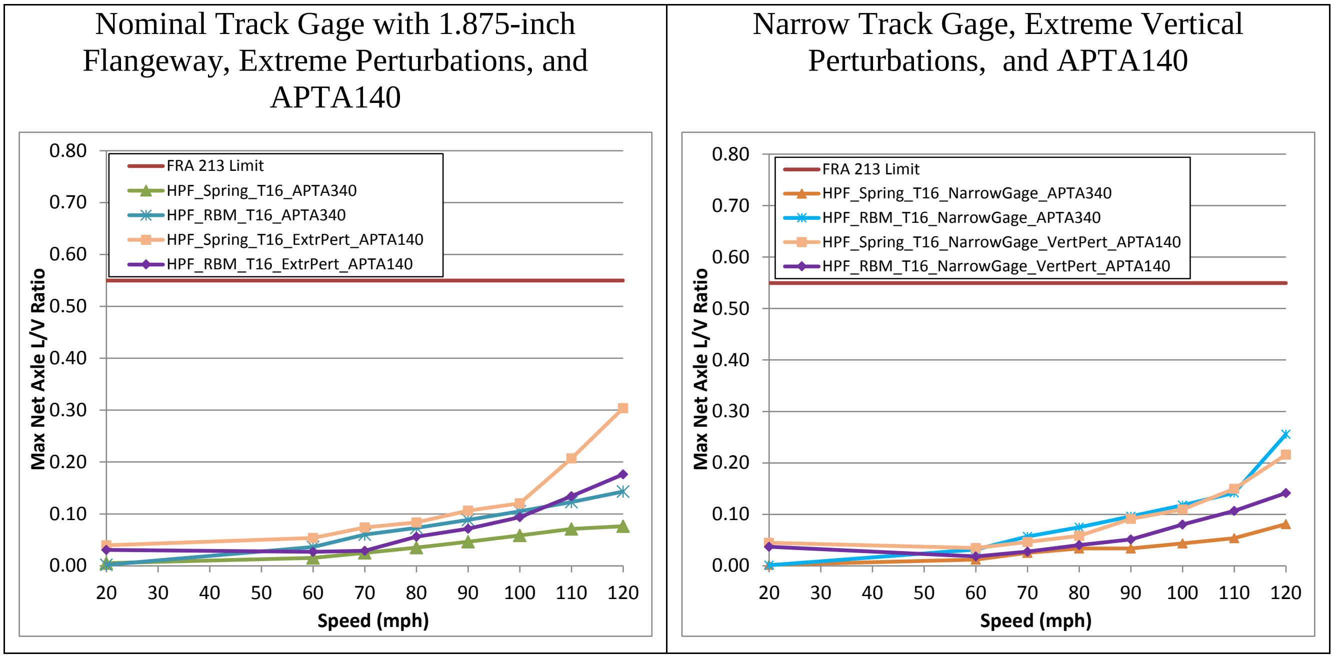

Figure 85. Maximum net axle lateral L/V ratio under the T16 passenger car - APTA140 with nominal track gage (left) and narrow track gage (right)

5.5.2 As-designed HPF with GP40

Figures 86–90 show results of car maximum net axle lateral L/V ratio under the GP40 passenger locomotive for the as-designed HPF with different scenarios from the parametric study.

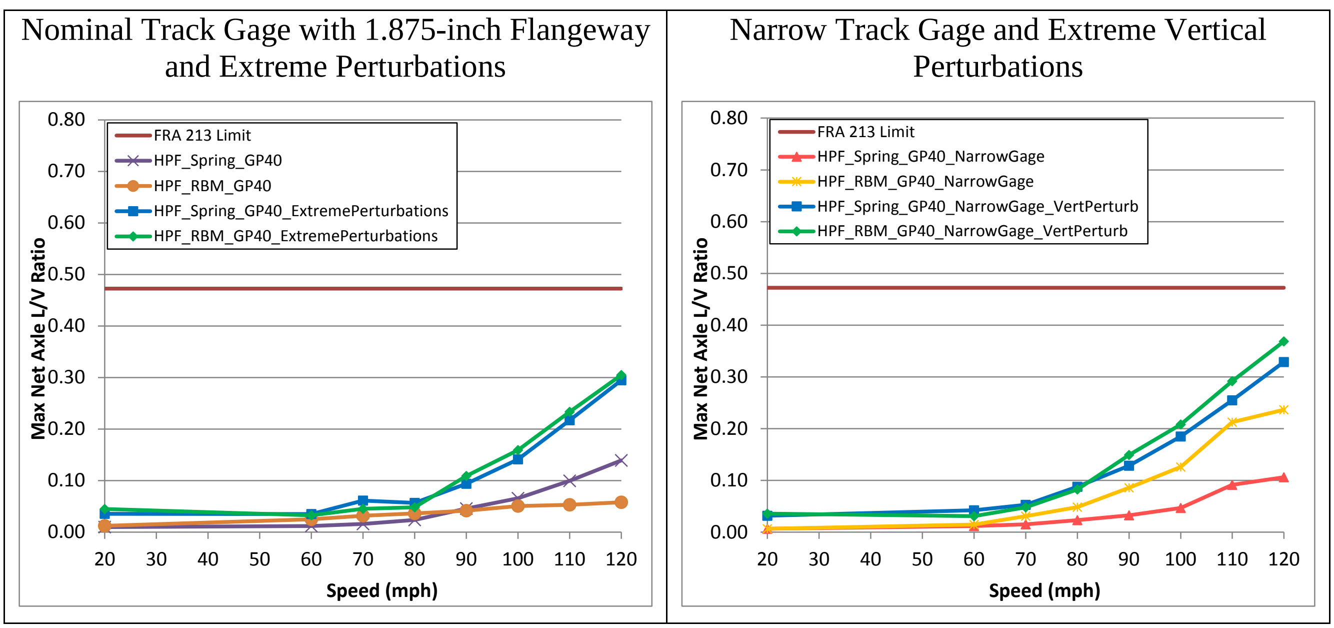

Figure 86. Maximum net axle lateral L/V ratio under the GP40 passenger locomotive - nominal track gage (left) and narrow track gage (right)

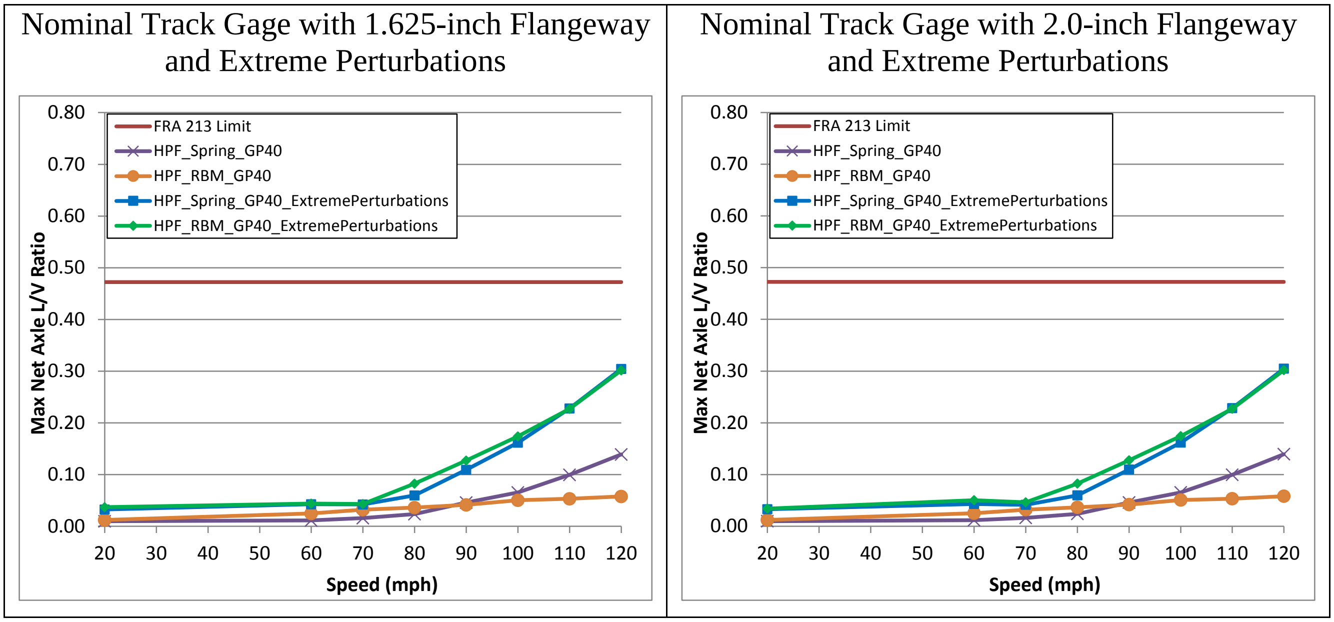

Figure 87. Maximum net axle lateral L/V ratio under the GP40 passenger locomotive - nominal track gage with 1.625-inch flangeway (left) and 2.0-inch flangeway (right)

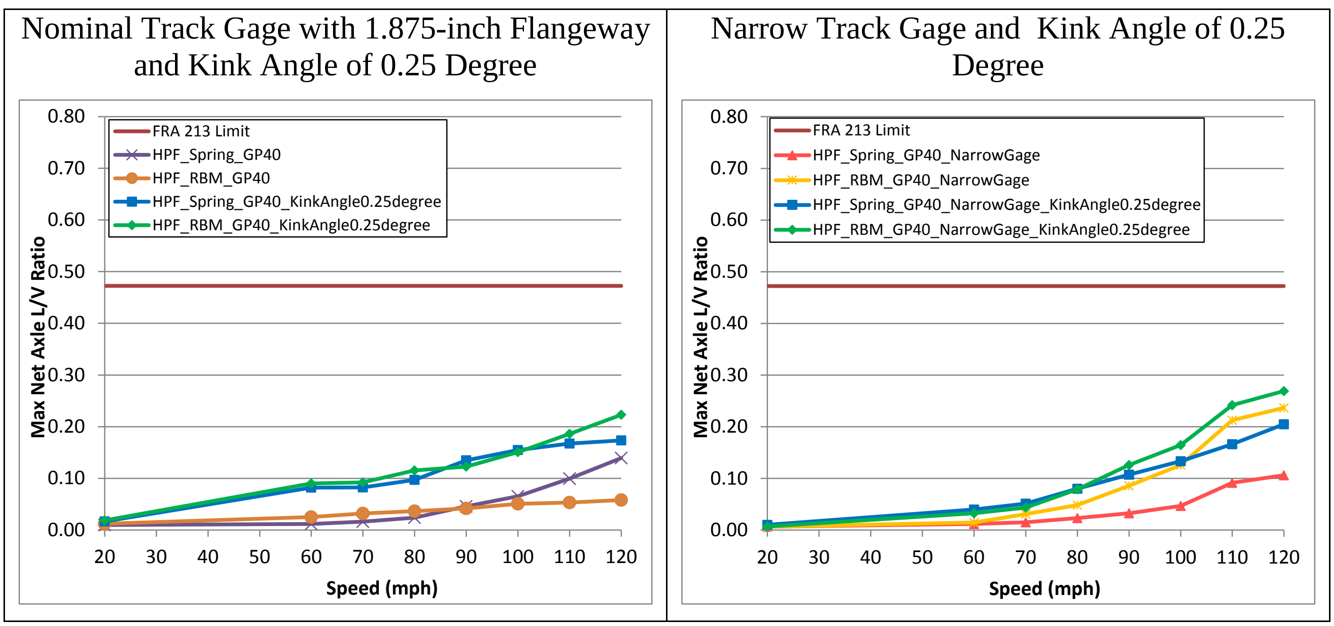

Figure 88. Maximum net axle lateral L/V ratio under the GP40 passenger locomotive - kink angle of 0.25 degree with nominal track gage (left) and narrow track gage (right)

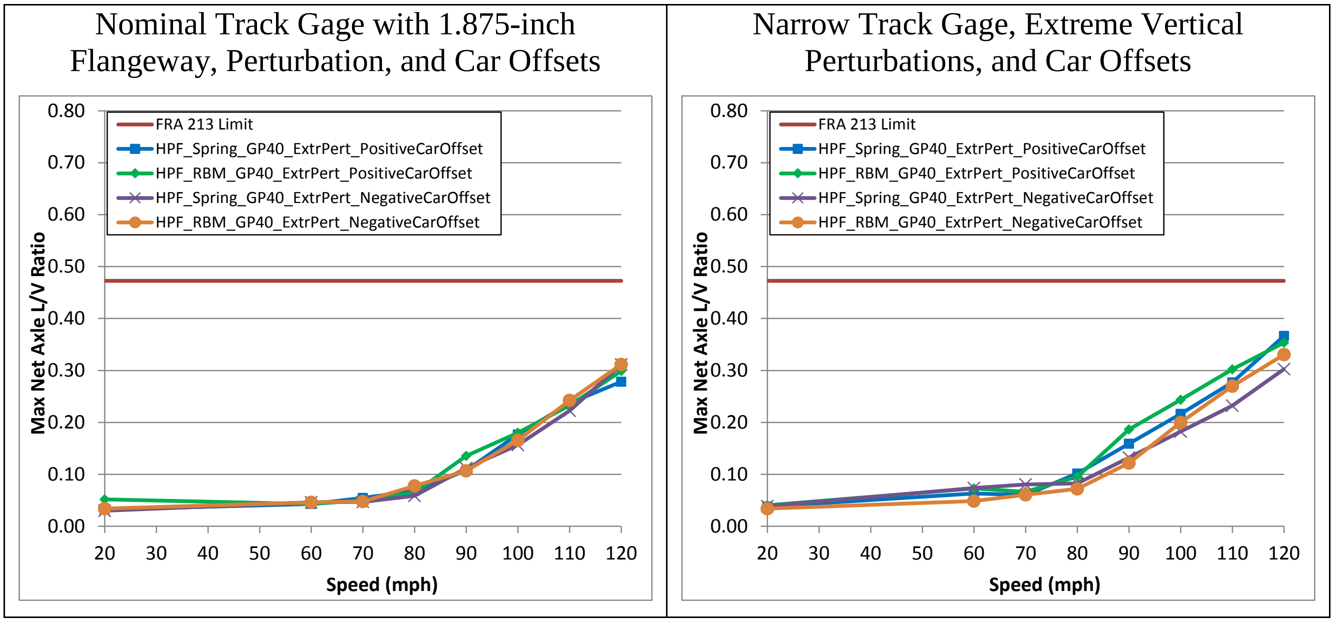

Figure 89. Maximum net axle lateral L/V ratio under the GP40 passenger locomotive - car offsets with nominal track gage (left) and narrow track gage (right)

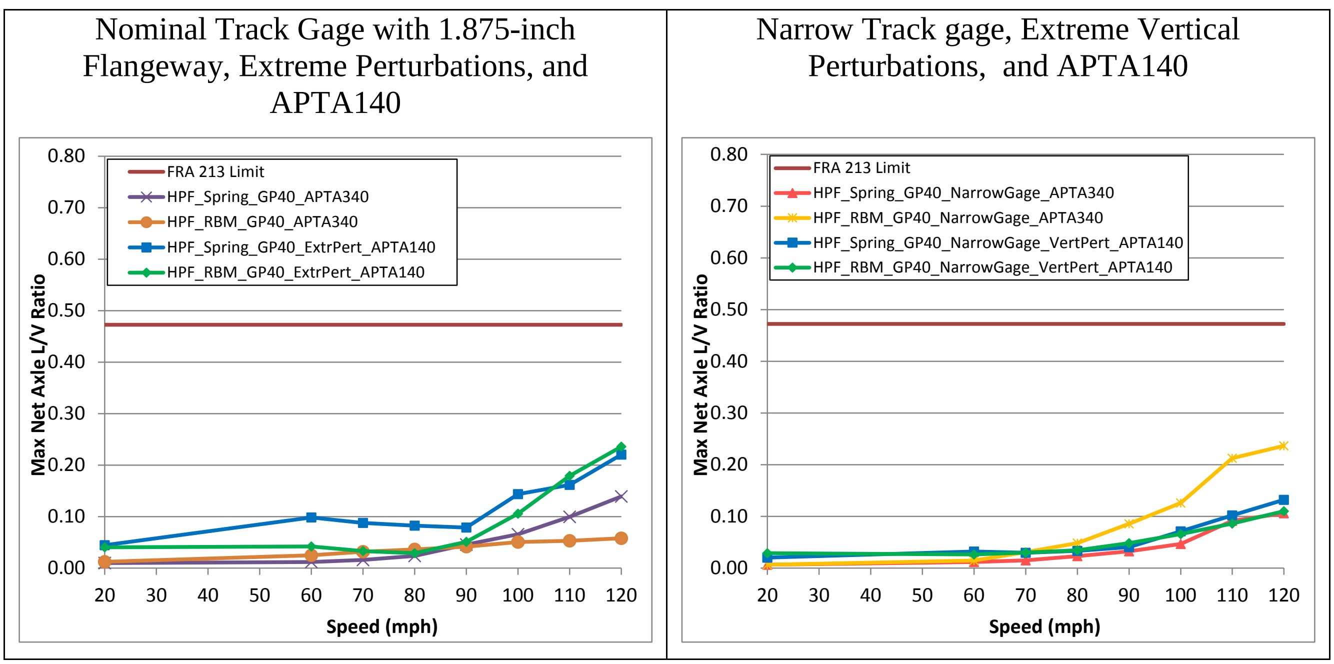

Figure 90. Maximum net axle lateral L/V ratio under the GP40 passenger locomotive - APTA140 with nominal track gage (left) and narrow track gage (right)

5.5.3 Measured HPF with T16

Figures 91–92 show results of maximum net axle lateral L/V ratio under the T16 passenger car for measured HPF with different scenarios from the parametric study.

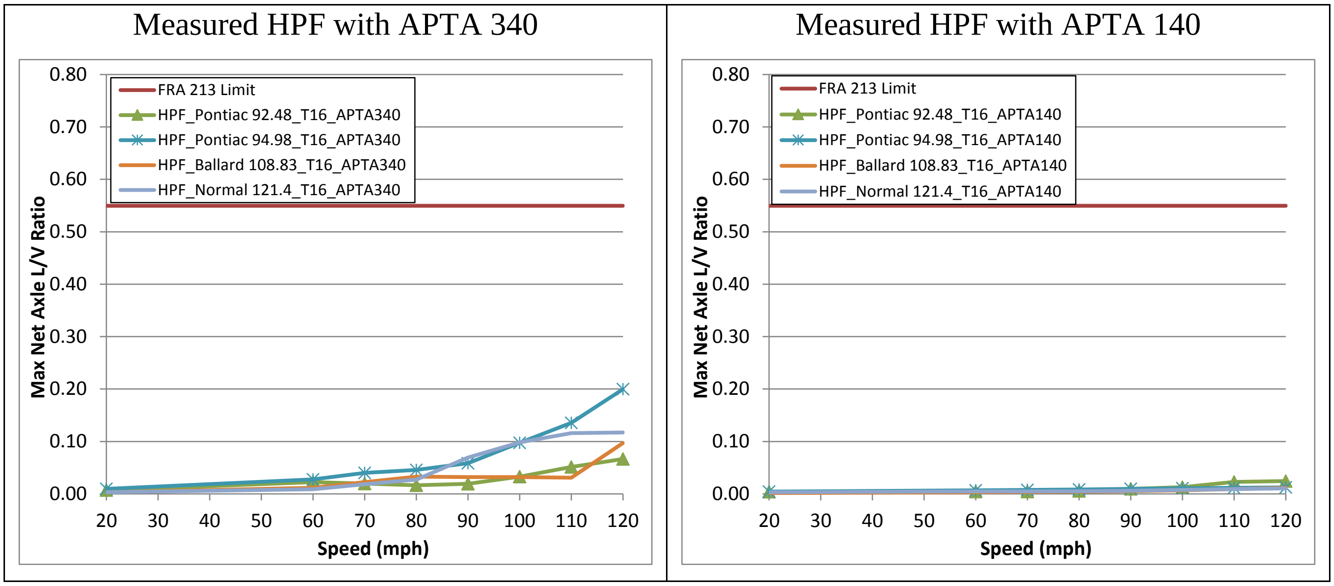

Figure 91. Maximum net axle lateral L/V ratio under the T16 passenger car - measured HPFs with wheelsets APTA 340 (left) and APTA140 (right)

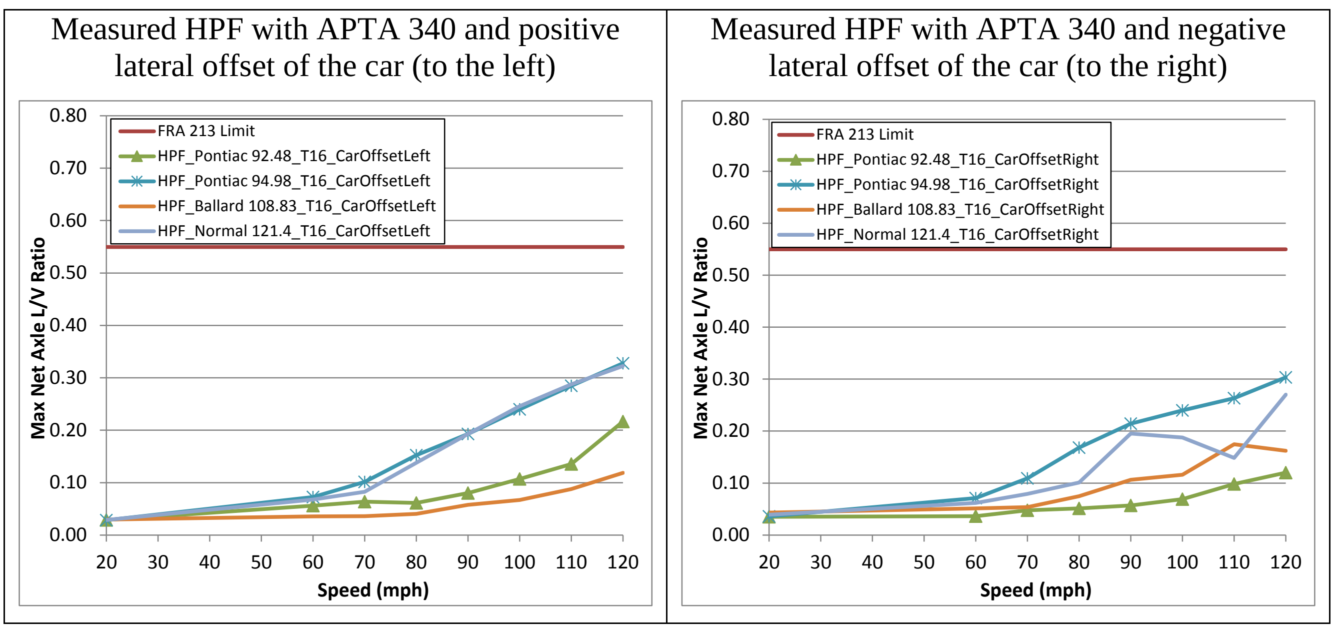

Figure 92. Maximum net axle lateral L/V ratio under the T16 passenger car - measured HPFs with positive car offset (left) and negative car offset (right)

5.5.4 Measured HPF with GP40

Figures 93–94 show results of maximum net axle lateral L/V ratio under the GP40 passenger locomotive for measured HPF with different scenarios from the parametric study.

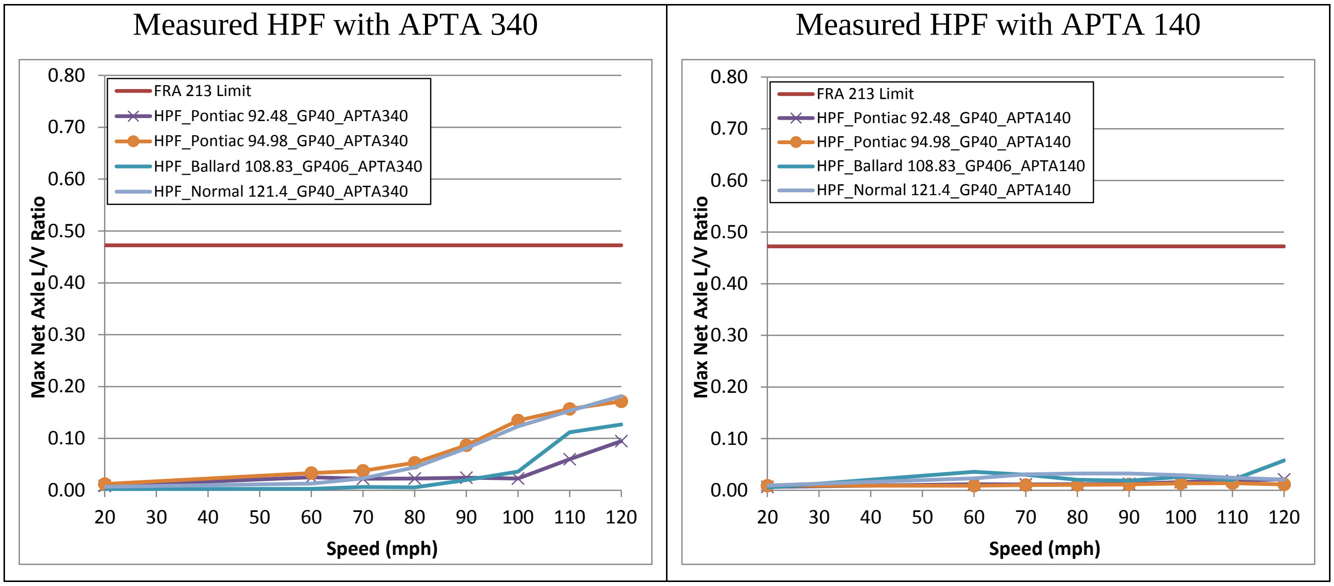

Figure 93. Maximum net axle lateral L/V ratio under the GP40 passenger locomotive - Measured HPFs with wheelsets APTA 340 (left) and APTA140 (right)

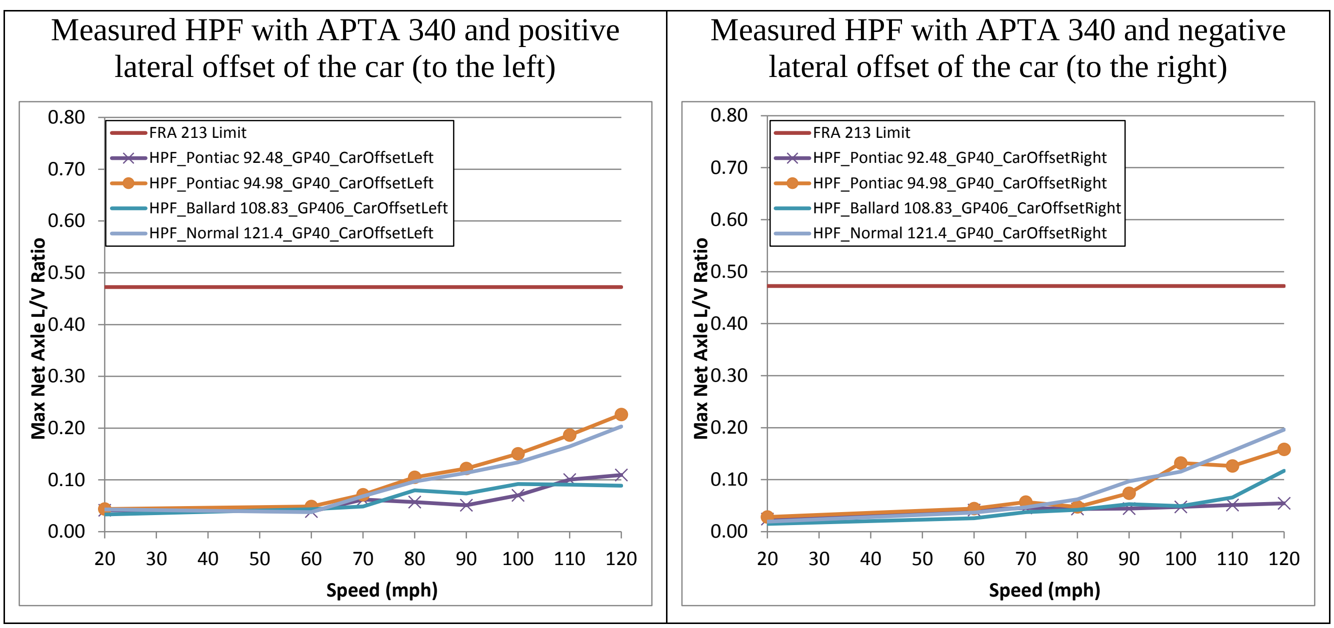

Figure 94. Maximum net axle lateral L/V ratio under the GP40 passenger locomotive - Measured HPFs with positive car offset (left) and negative car offset (right)

5.6 Maximum Truck Side L/V Ratio

5.6.1 As-designed HPF with T16

Figures 95–99 show results of maximum truck side L/V ratio under the T16 passenger car for as-designed HPF with different scenarios from the parametric study.

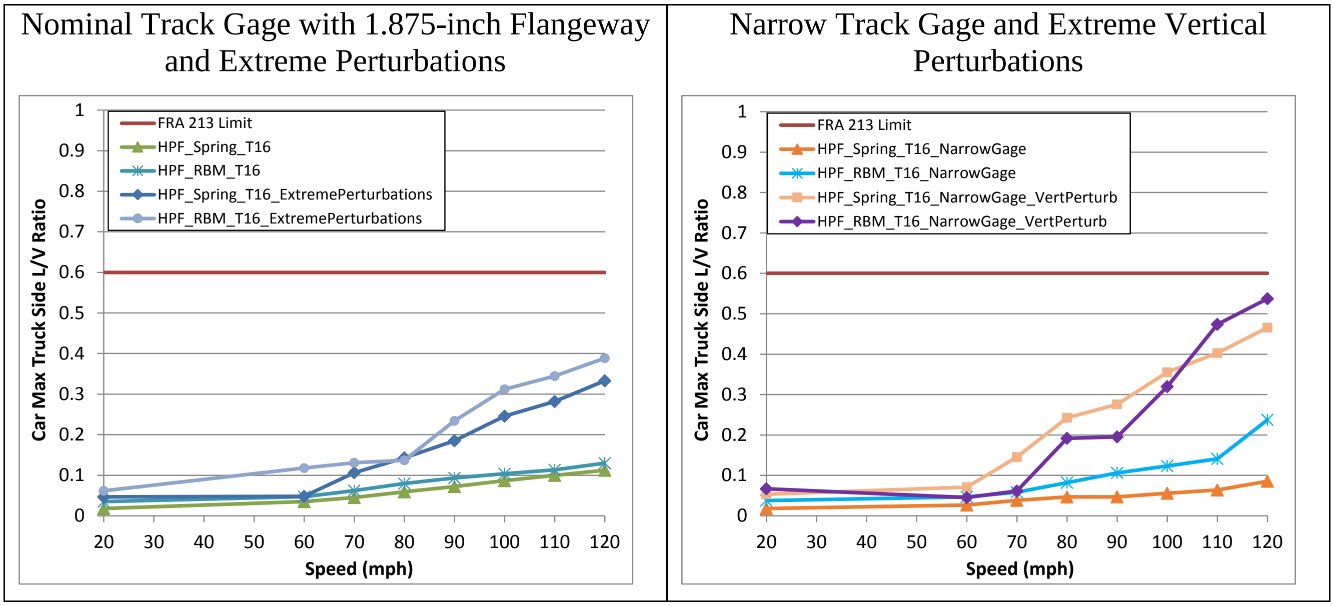

Figure 95. Maximum truck side L/V ratio under the T16 passenger car - nominal track gage (left) and narrow track gage (right)

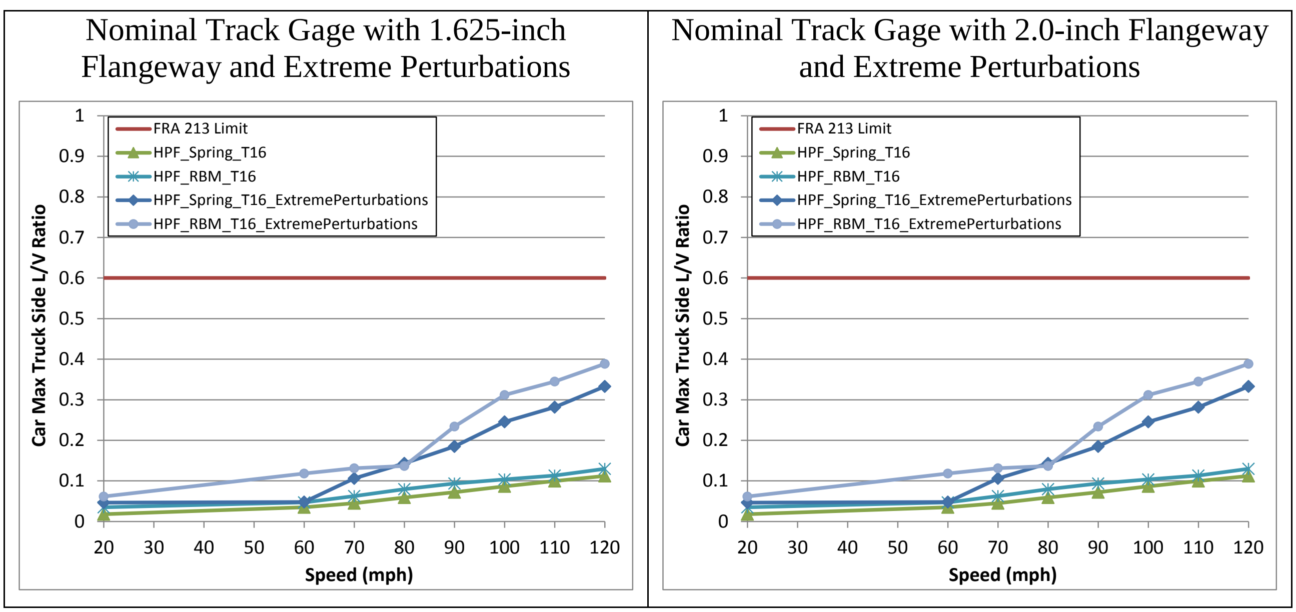

Figure 96. Maximum truck side L/V ratio under the T16 passenger car - nominal track gage with 1.625-inch flangeway (left) and 2.0-inch flangeway (right)

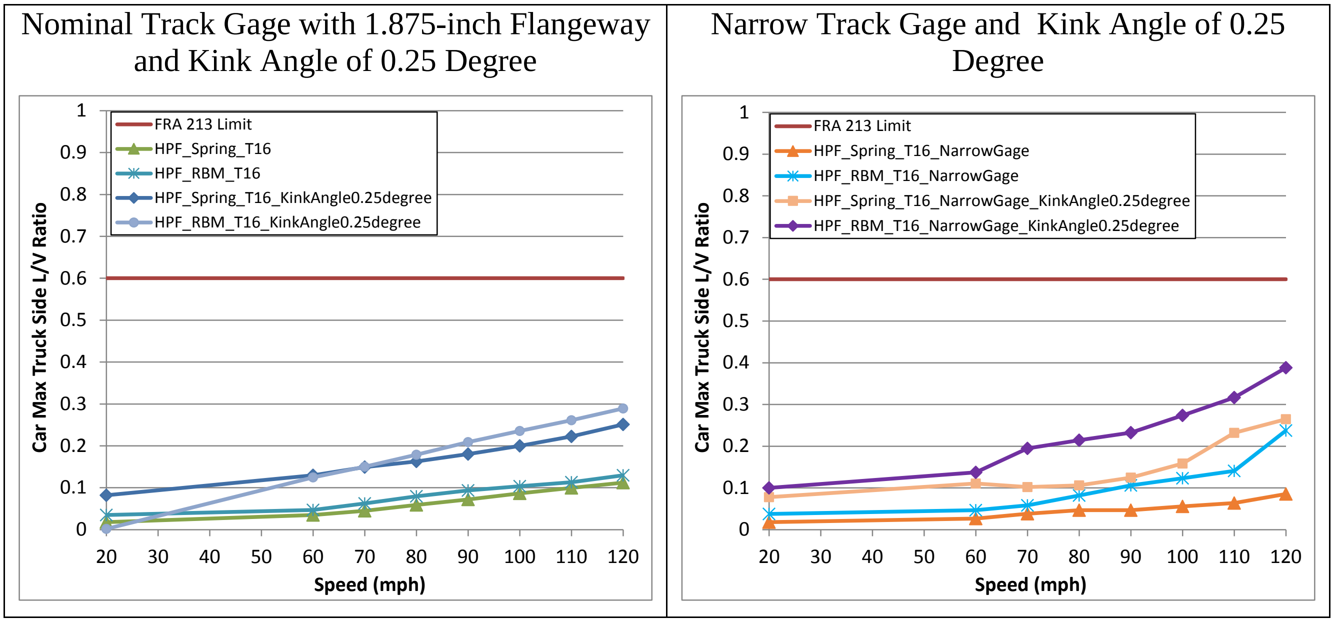

Figure 97. Maximum truck side L/V ratio under the T16 passenger car - kink angle of 0.25 degree with nominal track gage (left) and narrow track gage (right)

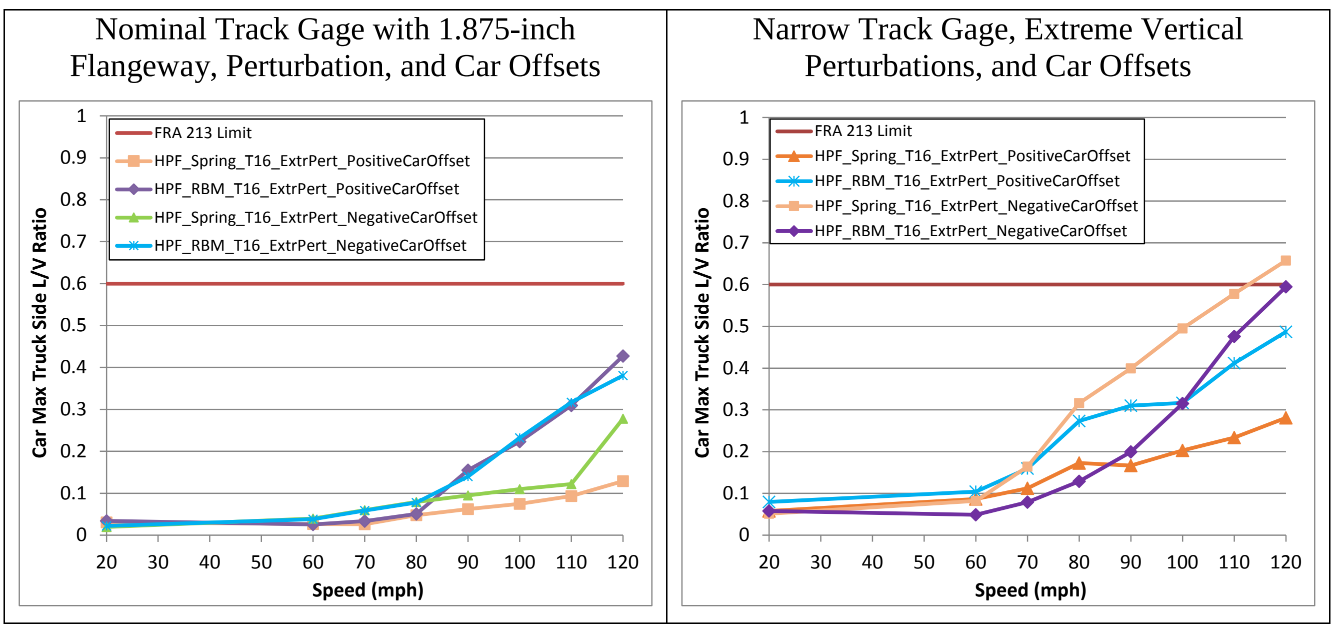

Figure 98. Maximum truck side L/V ratio under the T16 passenger car - car offsets with nominal track gage (left) and narrow track gage (right)

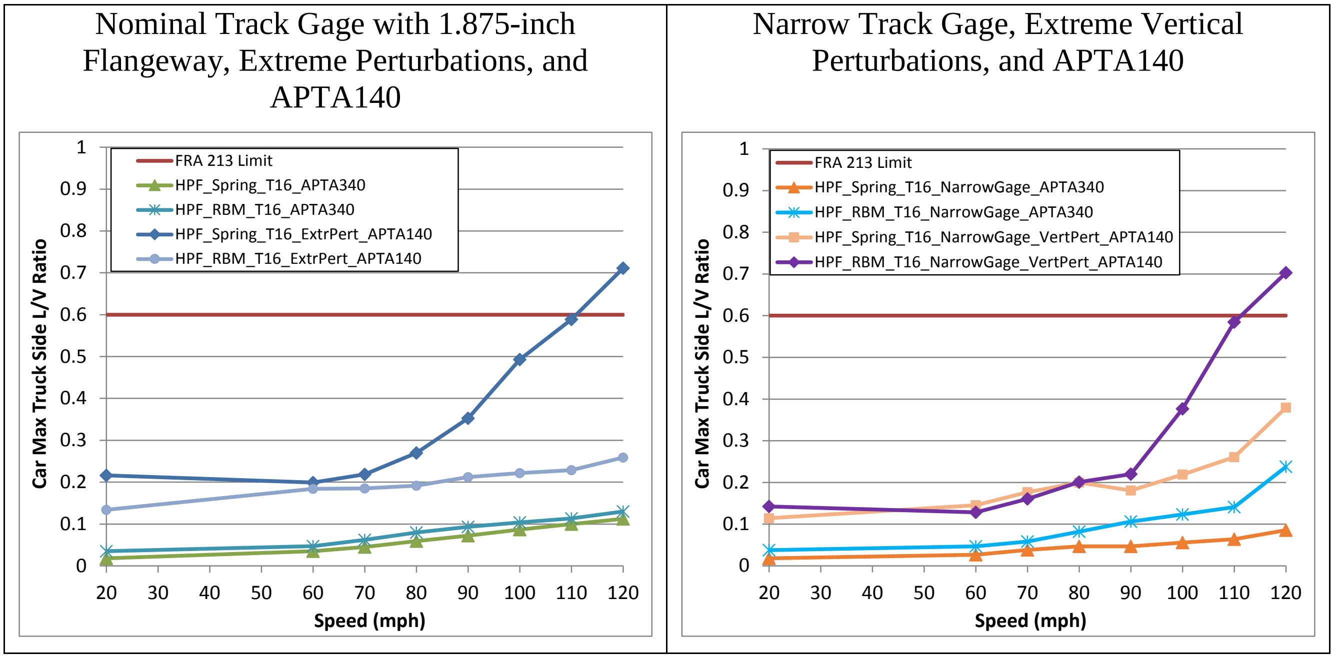

Figure 99. Maximum truck side L/V ratio under the T16 passenger car - APTA140 with nominal track gage (left) and narrow track gage (right)

5.6.2 As-designed HPF with GP40

Figures 100–104 show results of maximum truck side L/V ratio under the GP40 passenger locomotive for as-designed HPF with different scenarios from the parametric study.

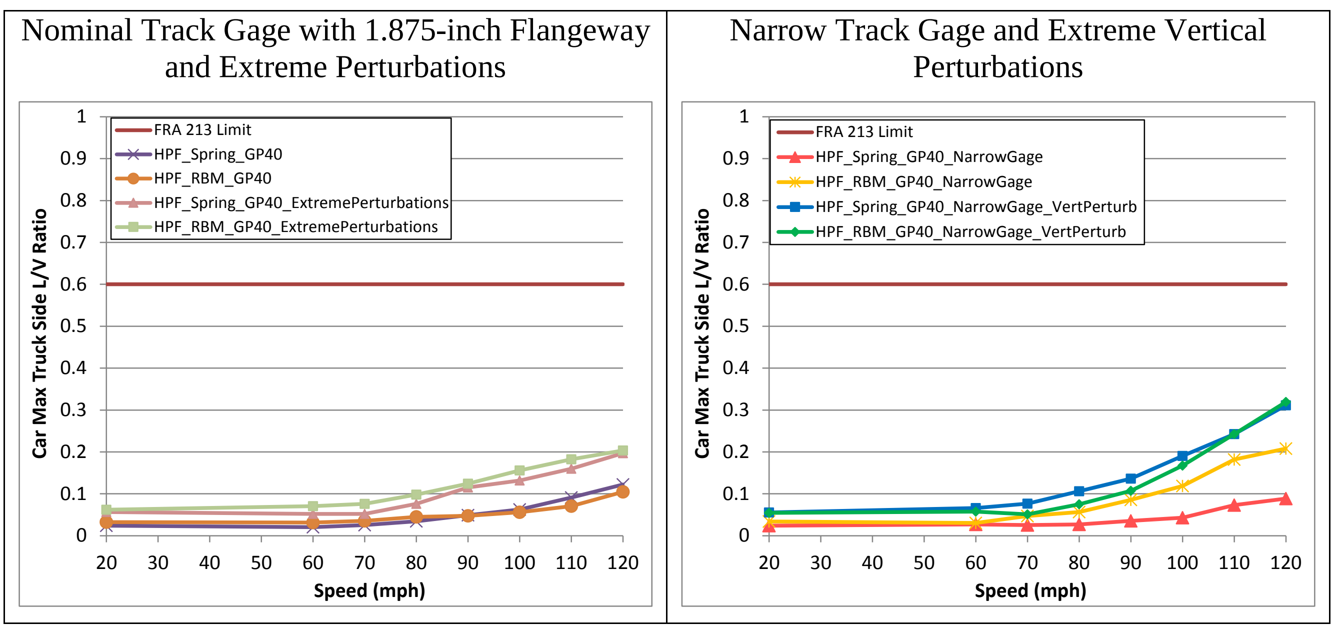

Figure 100. Maximum truck side L/V ratio under the GP40 passenger locomotive - nominal track gage (left) and narrow track gage (right)

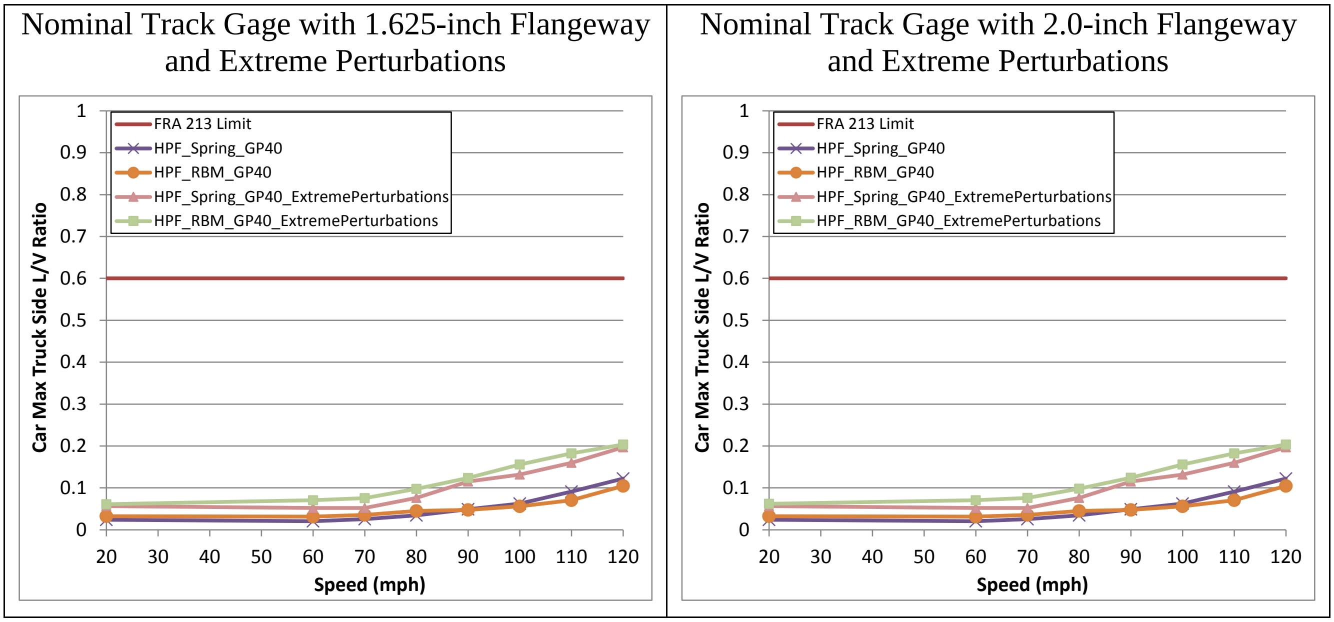

Figure 101. Maximum truck side L/V ratio under the GP40 passenger locomotive - nominal track gage with 1.625-inch flangeway (left) and 2.0-inch flangeway (right)

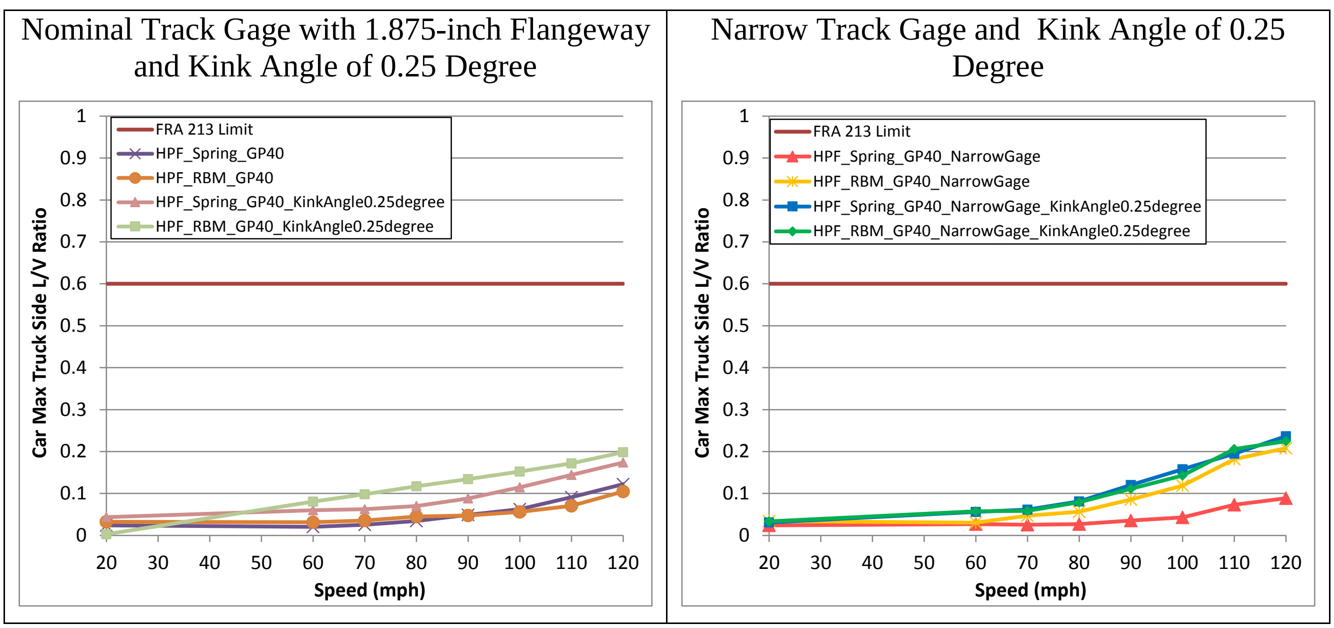

Figure 102. Maximum truck side L/V ratio under the GP40 passenger locomotive - kink angle of 0.25 degree with nominal track gage (left) and narrow track gage (right)

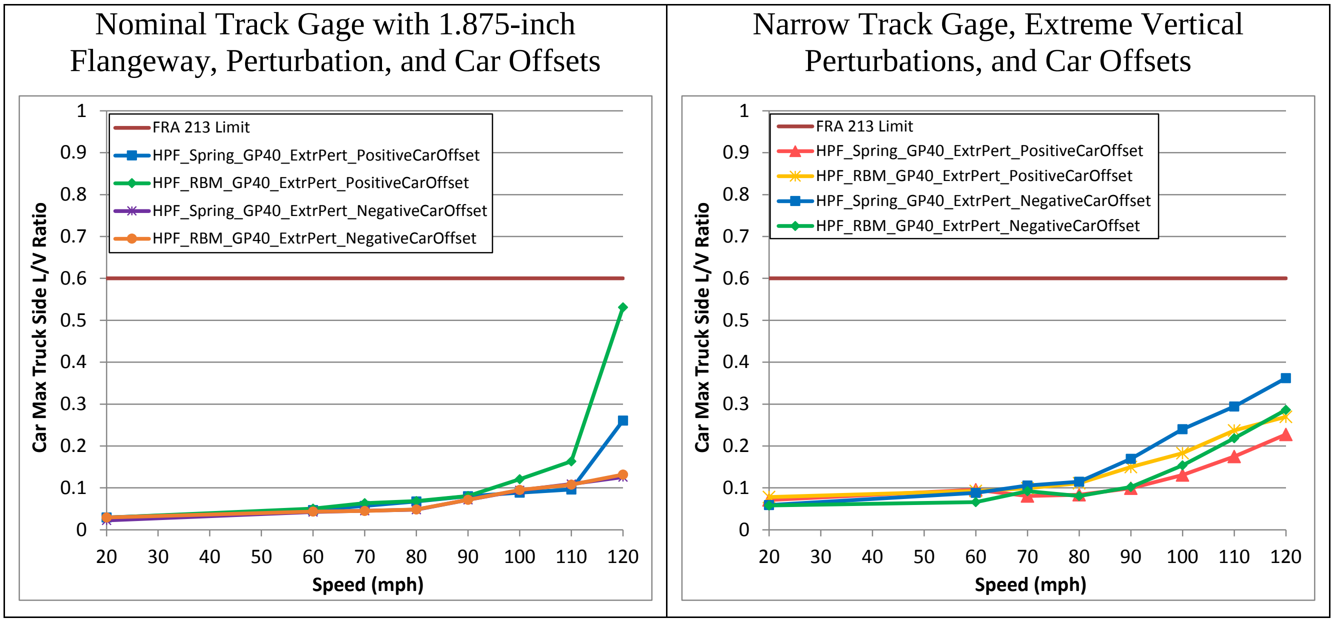

Figure 103. Maximum truck side L/V ratio under the GP40 passenger locomotive - car offsets with nominal track gage (left) and narrow track gage (right)

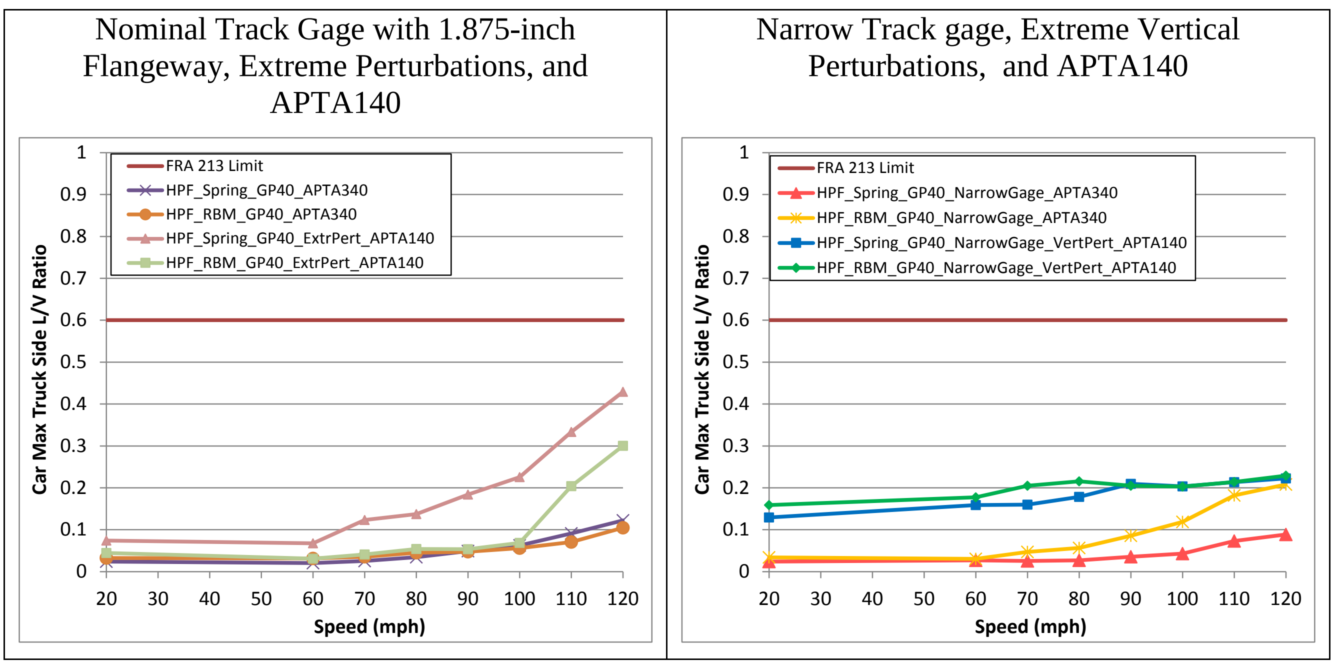

Figure 104. Maximum truck side L/V ratio under the GP40 passenger locomotive - APTA140 with nominal track gage (left) and narrow track gage (right)

5.6.3 Measured HPF with T16

Figures 105–106 show results of maximum truck side L/V ratio under the T16 passenger car for measured HPF with different scenarios from the parametric study.

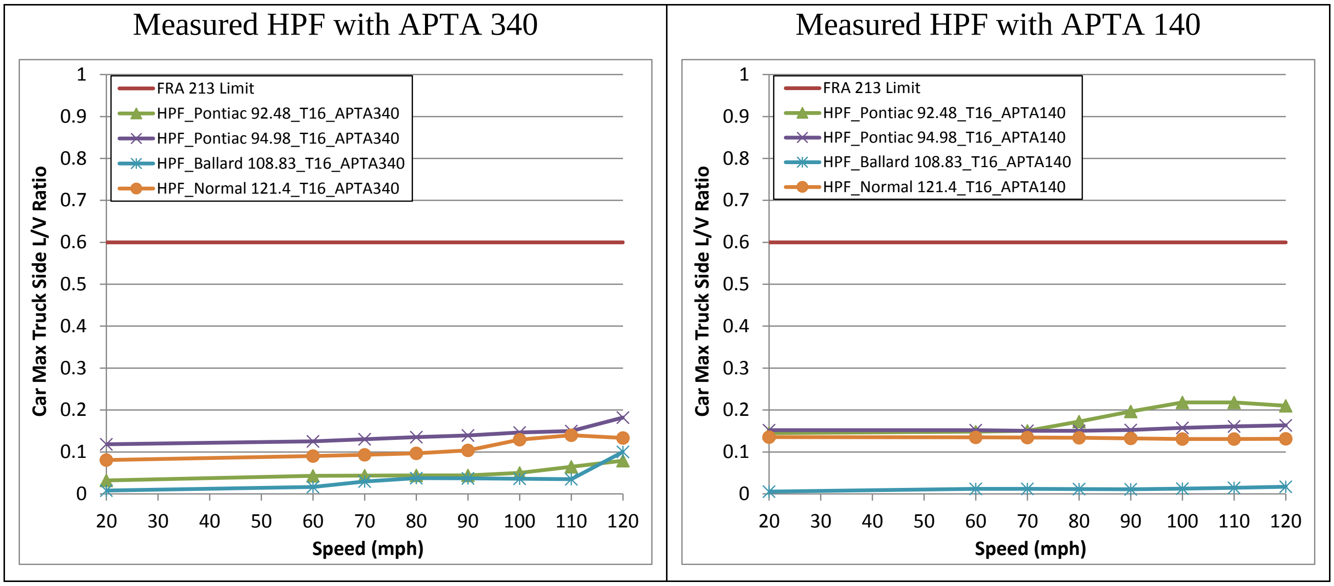

Figure 105. Maximum truck side L/V ratio under the T16 passenger car - measured HPFs with wheelsets APTA 340 (left) and APTA140 (right)

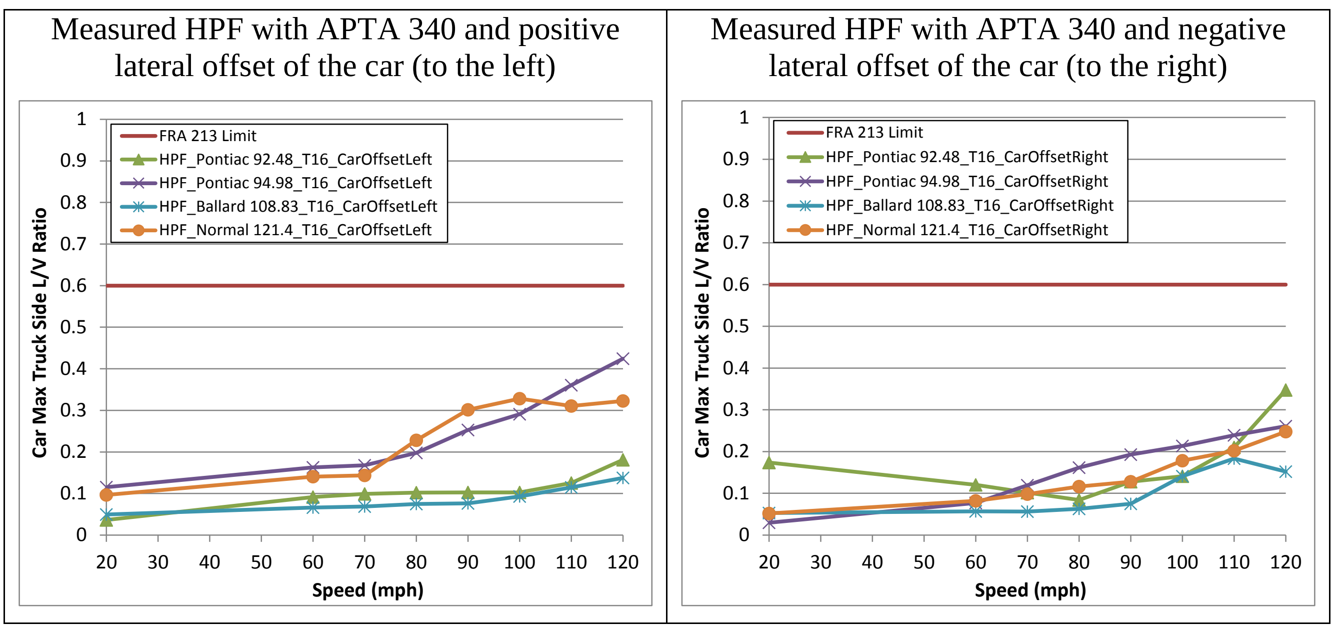

Figure 106. Maximum truck side L/V ratio under the T16 passenger car - measured HPFs with positive car offset (left) and negative car offset (right)

5.6.4 Measured HPF with GP40

Figures 107–108 show results of maximum truck side L/V ratio under the GP40 passenger locomotive for measured HPF with different scenarios from the parametric study.

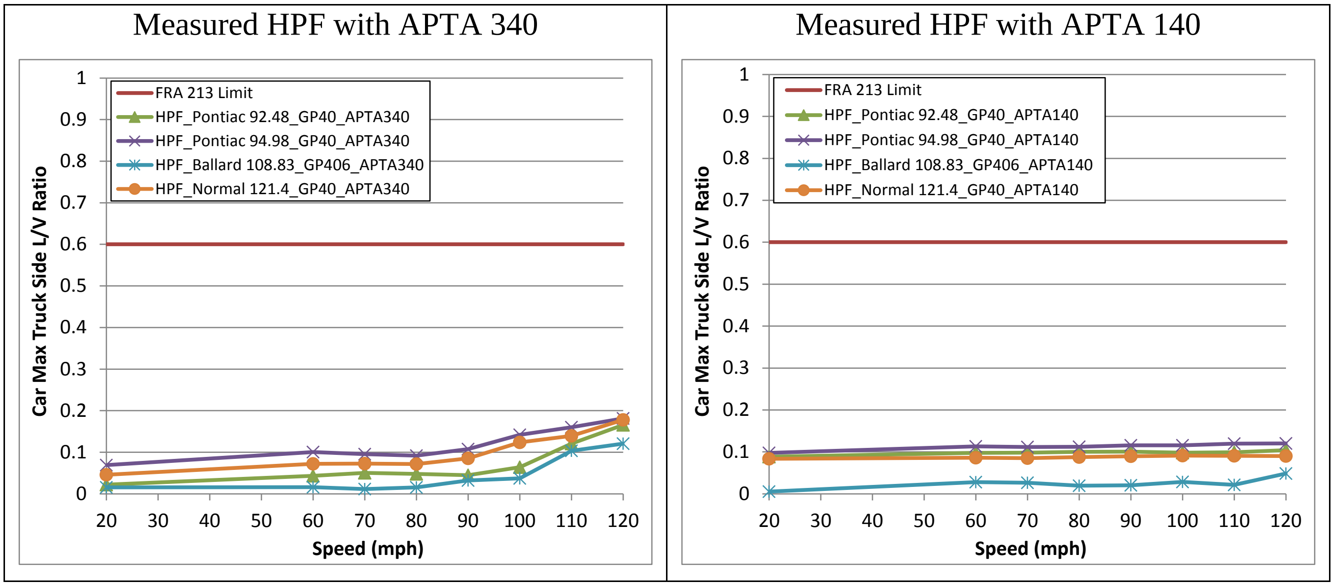

Figure 107. Maximum truck side L/V ratio under the GP40 passenger locomotive - measured HPFs with wheelsets APTA 340 (left) and APTA140 (right)

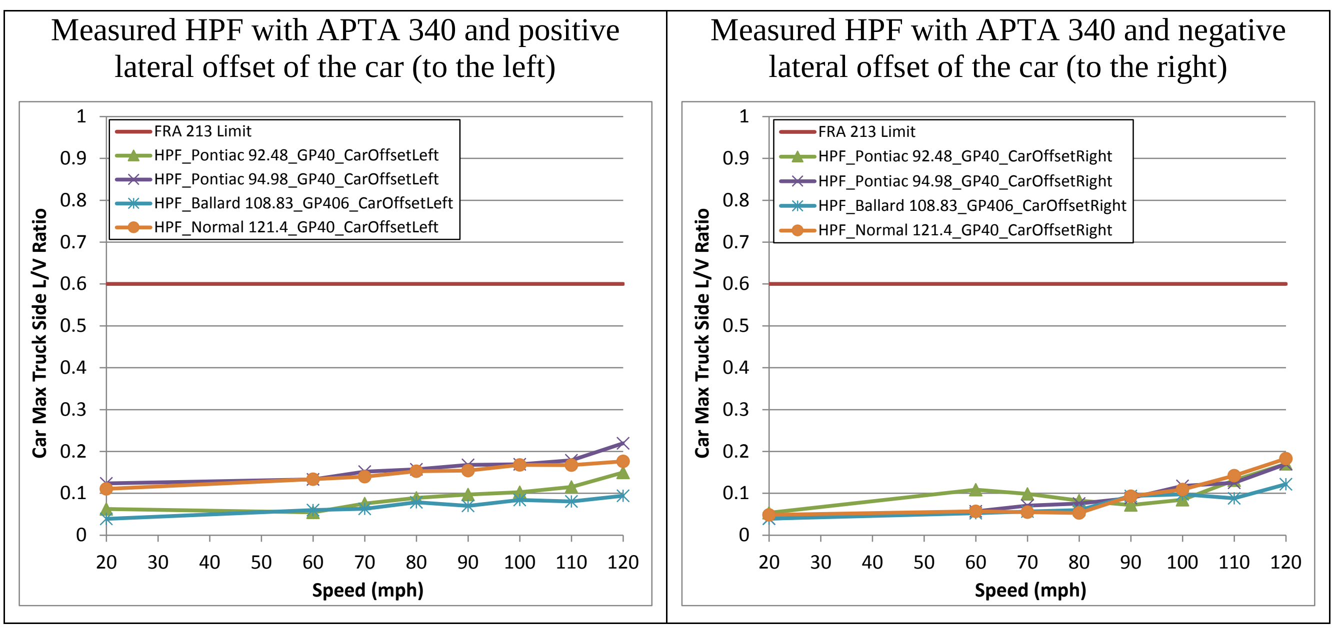

Figure 108. Maximum truck side L/V ratio under the GP40 passenger locomotive - measured HPFs with positive car offset (left) and negative car offset (right)

5.7 Comparison between Simulation and Measured Performance

The worn point frogs were measured on the Chicago – St. Louis HSR line as described in more details in Chapter 3. The MiniProf measurements of HPF were taken in October 2013. Before this project, FRA measured the performance of its DOTX-216 (i.e., the T16 car) on this same corridor. The T16 car was equipped with load measuring instrumented wheelsets (IWS) and a track geometry measurement system (TGMS). TTCI obtained the data to verify the simulation models used in this project.

The IWS test was performed at 79 mph with the test train shown in Figure 109. The following is specific information about the test:

- The train consisted of an Amtrak locomotive, two superliner cars, and the T16 car
- The train was turned in St. Louis so that the locomotive was always leading and the IWS was always on the leading truck of the T16 car
- A track geometry beam was installed on IWS truck

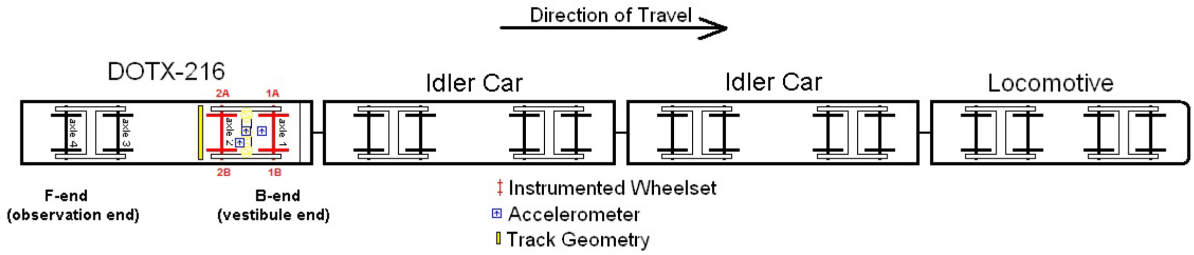

Figure 109. Train consist for IWS test

The IWS data included wheel L/V ratio for two axles on the left and right wheels and the truck side L/V ratio on the left and right sides. A simulation was conducted on measured HPFs with the T16 car at 79 mph. Simulations were performed with various scenarios of wheel profiles (APTA140 and APTA 340) and car offsets. Nominal track alinement and surface were used in the simulations, because actual track geometry data was not available until after the simulations were completed.

Table 7 compares simulated and measured wheel L/V ratios, and Table 8 compares of truck side L/V ratios. The values in red are the maximum values from all simulations and from all measurements. Figures 110 and 111 show these maximum values of wheel L/V ratio and truck side L/V ratio on clustered column charts.

Table 7. Comparison of wheel L/V ratio for T16 at 79 mph

	NUCARS® Simulations				T16 Measured Data			
	Base Case APTA340	Base Case APTA140	Car Offset Positive, APTA340	Car Offset Negative, APTA340	Axle 1 Left Wheel	Axle 1 Right Wheel	Axle 2 Left Wheel	Axle 2 Right Wheel
Pontiac 92.48	0.0194	0.1727	0.0591	0.0504	0.1842	0.2041	0.1138	0.1644
Pontiac 94.98	0.0607	0.1516	0.1277	0.1294	0.0978	0.1298	0.0508	0.1344
Ballard 108.83	0.0391	0.0134	0.0739	0.1189	0.1061	0.1348	0.0572	0.1160
Normal 121.4	0.0365	0.1335	0.0933	0.1220	0.1584	0.2592	0.0659	0.1461

Note: Maximum values from all simulations and all measurements are in red.

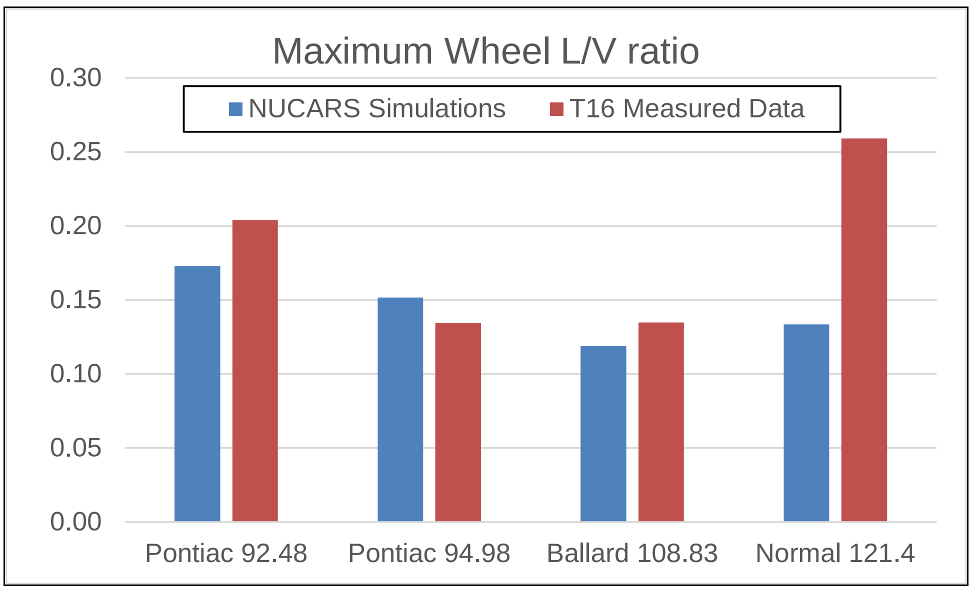

Figure 110. Comparison of maximum wheel L/V ratio for T16 at 79 mph

The comparisons show that the simulations gave reasonable estimation of the wheel and truck side L/V ratios. The simulations did not give the same values, because the condition of carbody, wheelsets, and track geometry were not simulated exactly as they were during test. However, the values from the simulations are the same magnitude as the test, which can be considered as a good validation of NUCARS® models.

Table 8. Comparison of truck side L/V ratio for T16 at 79 mph

	Truck Side L/V from Simulations				T16 Measured Data	
	Base Case APTA340	Base Case APTA140	Car Offset Positive, APTA340	Car Offset Negative, APTA340	Left Side	Right Side
Pontiac 92.48	0.0299	0.1694	0.0409	0.0486	0.1022	0.1670
Pontiac 94.98	0.1169	0.1488	0.1979	0.0826	0.0661	0.1148
Ballard 108.83	0.0378	0.0114	0.0747	0.0701	0.0641	0.1131
Normal 121.4	0.0788	0.1301	0.2281	0.0754	0.0961	0.1688

Note: Maximum values from all simulations and all measurements are in red.

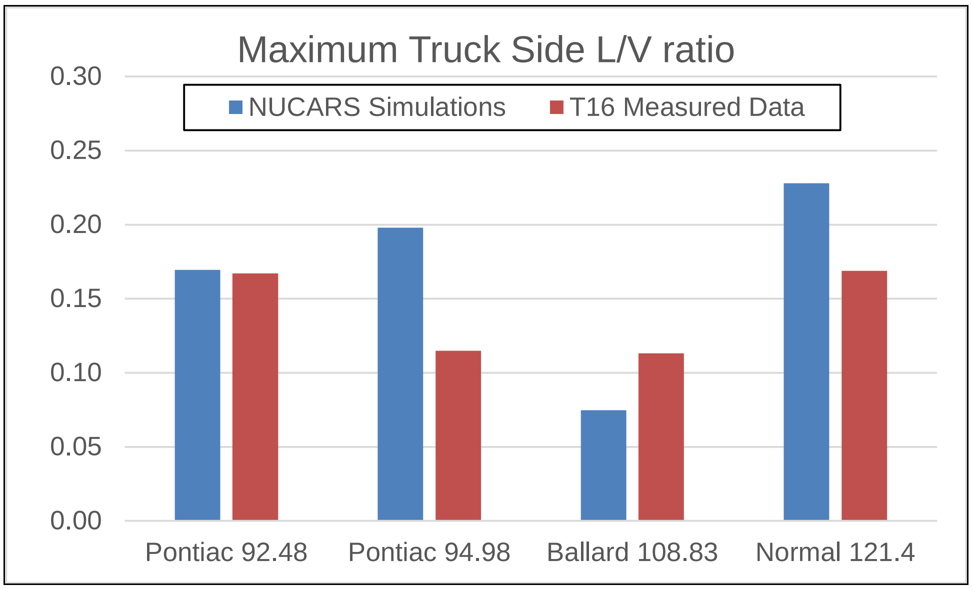

Figure 111. Comparison of maximum truck side L/V ratio for T16 at 79 mph

5.8 Summary of Results

The simulation results were compared with FRA requirements. All results satisfied VTI standards for speeds up to 110 mph. As-designed and actual frog running surface shapes were used in the simulations. Nominal and hypothetical worst-case track geometries were also used in the simulations.

The maximum speed simulated was 120 mph. For several cases with the design HPF and at this speed , the results exceeded FRA limits. These cases are as follows:

- Maximum L/V ratio under the T16 passenger car – RBM frog, nominal track gage with 1.875-inch flangeway, extreme perturbations, and positive car offset
- Maximum truck side L/V ratio under the T16 passenger car – spring frog, narrow track gage, extreme vertical perturbations, and negative car offset

- Maximum truck side L/V ratio under the T16 passenger car – Spring Frog, nominal track gage with 1.875-inch flangeway, extreme perturbations, and APTA140
- Maximum truck side L/V ratio under the T16 passenger car – RBM Frog, narrow track gage, extreme vertical perturbations, and APTA140

Figures 112–115 show wheel-rail contacts time-histories for all these four cases.

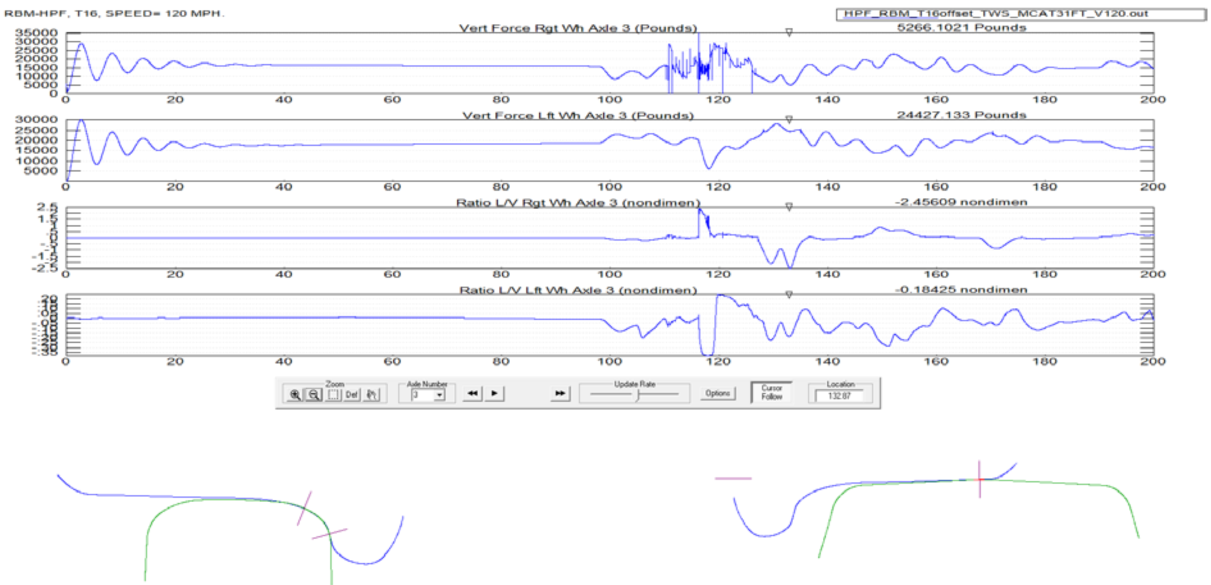

Figure 112. Time-histories simulation at 120 mph with RBM Frog, nominal track gage with 1.875-inch flangeway, extreme perturbations, and positive car offset

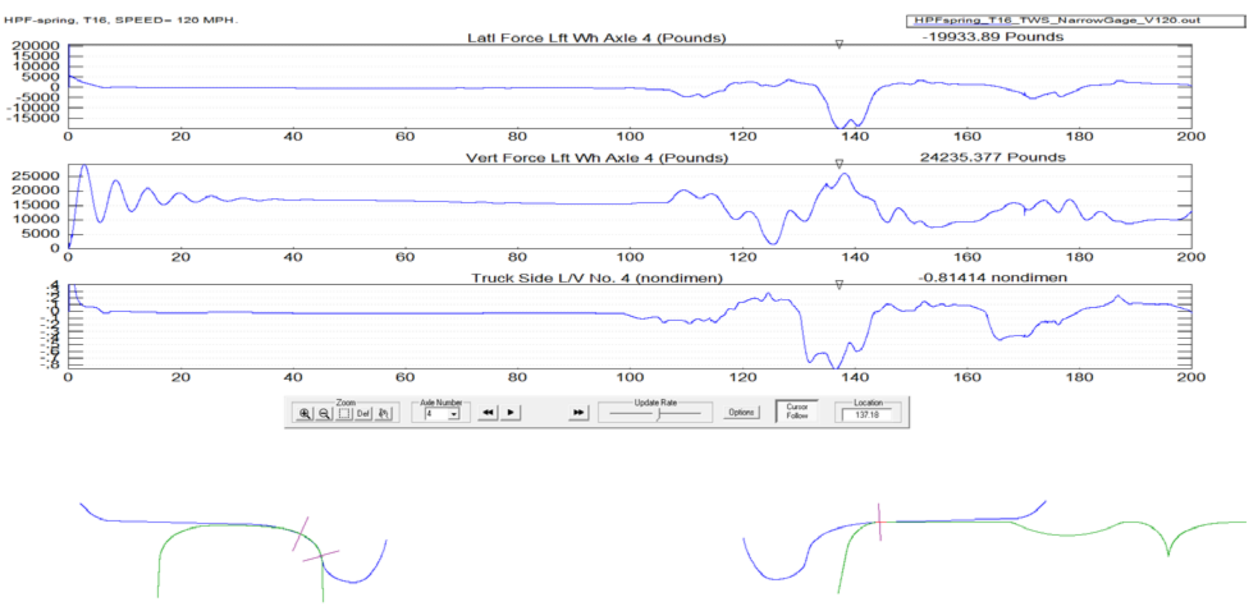

Figure 113. Time-histories from simulation at 120 mph with spring frog, narrow track gage, extreme vertical perturbations, and negative car offset

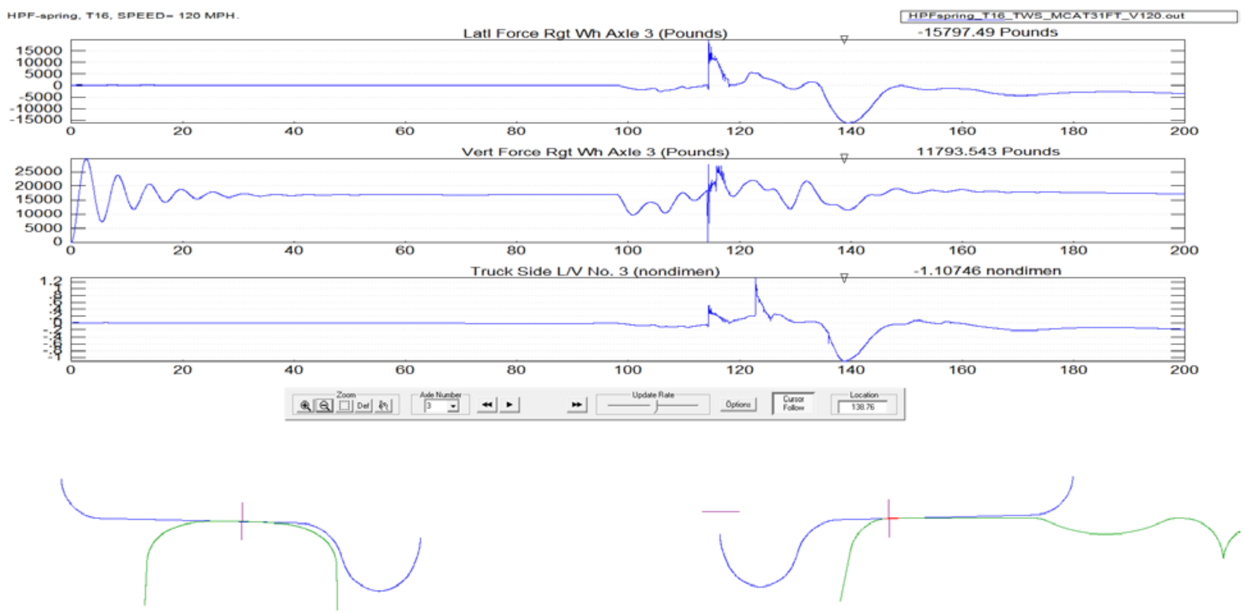

Figure 114. Time-histories from simulation at 120 mph with spring frog, nominal track gage with 1.875-inch flangeway, extreme perturbations, and APTA140

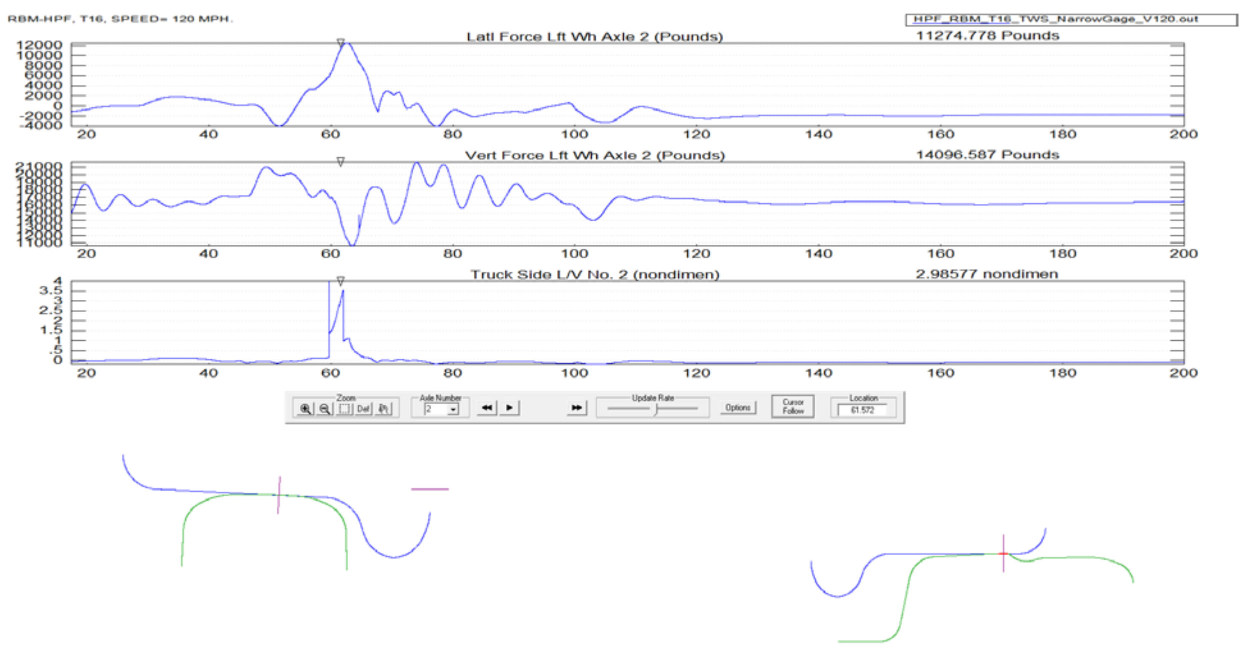

Figure 115. Time-histories from simulation at 120 mph with RBM frog, narrow track gage, extreme vertical perturbations, and APTA140

The time histories and wheel-rail contacts presented in Figures 112–115 show that the larger values of the wheel L/V and truck side L/V occur on the guard rail or on the wing. However, the occurrences on the wing rail may be beyond the heel end of the frog flangeway, because they occurred about 20 feet behind the frog point.

FRA criteria for wheel L/V and truck side L/V are developed for typical wheel-rail contact conditions. However, wheel-rail contact on the frog-wing and guard rail is different from these typical conditions. A higher L/V ratio for wheel climbing on a frog wing could be allowed, because the rail on the opposite side prevents the axle from further climbing. A higher truck side L/V ratio for frogs could also be allowed, because the wider frog bottom resists rail roll.

Further research is recommended to examine the influences of the actual wing shape as well as flangeway widening behind the frog.

6. Conclusion

More than 700 simulations of passenger vehicles running through HPF at speeds up to 120 mph were conducted. Various types of HPFs were considered including brand new RBM frog and spring frog as well as worn spring frogs measured on the Chicago – St. Louis HSR line. The wheel-rail contact conditions were examined and results from all cases provide confirmation that HPF design can be used for train operations up to 110 mph.

The simulation results were evaluated using FRA 213 VTI Safety Standard. All results for design HPFs satisfied FRA VTI standards for speeds up to 110 mph. Results of simulations with measured HPF gave even better results, and they satisfied all FRA requirements. Performance through the measured HPF was better than through the as-designed HPF because the latter had less favorable geometry conditions at the frog point.

The measured HPFs were simulated with positive and negative car offsets and two wheelsets: APTA340 with 53.3750 inches back-to-back spacing and APTA140 with 53 inches back-to-back spacing. During simulations for the as-designed HPFs, many parameters related to the track gage, flangeway, track perturbations, and car offsets were varied. Two track gages were considered: nominal 56.5 inches and narrow track gage of 56.0 inches. For nominal gage, various flangeway were simulated: 1.625 inches, 1.875 inches (nominal dimension) and 2.0 inches.

The perturbations used for simulations of design HPFs represent the worst-case scenario for Class 6 track. These perturbations are allowed by FRA standards on Class 6 track; however, they are not likely to be located close to the HPFs. All No. 24 HPFs on the modeled route were built with concrete ties at the factory, giving additional assurance that the gage, surface, and alignment of the frog was correct when installed in track.

From the parametric study of track conditions modeled, the gage line deviation caused by the HPF was less severe than allowable track perturbations for Class 6 track. In the simulations, the combination of running surface profile changes due to the frog and allowable track geometry deviations produced vehicle performance within the allowable limits. This suggests that the allowable limits are appropriate for turnout frogs as well as for open track.

Also, from the parametric study and the field performance measurements, it is apparent that the frog with some wearing will likely give better performance than a new frog. As components wear, guard face gage will move toward compliance and guard check gage will likely also move toward compliance (as the frog wears faster than the guard rail).

The research shows the advantages of wheelset contact with the guard rail before flange contact with the frog point. For operations with HPFs, a thorough review of the positioning of the guard rail opposite the frog is recommended. This review should include the dimensions of equipment to be operated, especially the wheel profiles, and back-to-back spacing. With this information, adjustments of the guard rail position relative to the running rail can be made.

6.1 Future Work

The limited test data obtained on the Chicago – St. Louis HSR line provided reasonable validation of NUCARS® models. The simulations did not give exactly the same values as the test; however, the values from the simulations are of the same order as the test, and this is considered as a good benchmark of NUCARS® modeling. Since the T16 test was run at 79 mph, it is recommended to perform dynamic testing with passenger equipment going through the HPFs at speeds up to 110 mph.

Further research is recommended to examine the influences of the wing shape and flangeway widening behind the frog.

7. References

1. Walker, R., Maram, R., and Klopp, A. unpublished. "Interim Report: FRA Task Order 326 DOTX 216 Characterization Test Report." DOT/FRA/ORD-14/XXX. U.S. Department of Transportation, Office of Railroad Policy and Development, Federal Railroad Administration, Washington, D.C.
2. Federal Railroad Administration. Code of Federal Regulations, 49 CFR 213 – Track Safety Standard, available from http://www.ecfr.gov/cgi-bin/text-idx?c=ecfr&sid=f09164a19ca78bafbcaf4b04b8574672&rgn=div6&view=text&node=49:4.1.1.1.8.7&idno=49
3. Greenwood Engineering, available from: http://www.greenwood.dk/miniprof.php http://www.railway-technology.com/contractors/track/greenwood/
4. Sasaoka, C., Davis, D., Singh, S., and Guillen, D. July 2002. "Improved Running Surface Profile for No. 20 Frogs." *Technology Digest* TD-02-017, Association of American Railroads, Transportation Technology Center, Inc., Pueblo, CO

Appendix A
Comparison of Design RBM and Spring HPFs

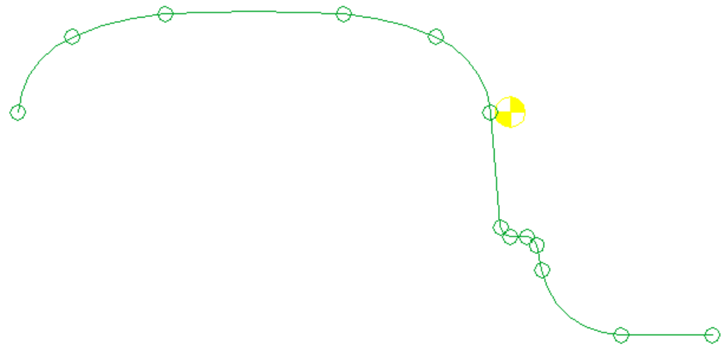	**A-1**: Sections 72 inches in front of the 0.5-inch point of frog
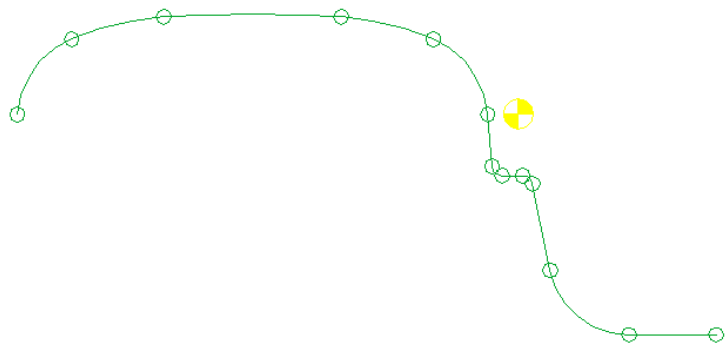	**A-2**: Sections 71 inches in front of the 0.5-inch point of frog
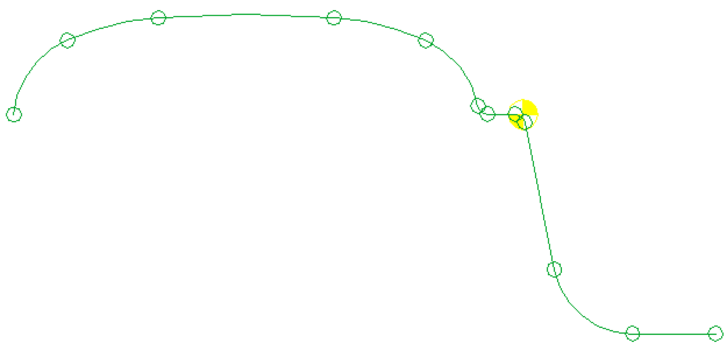	**A-3**: Sections 70 inches in front of the 0.5-inch point of frog
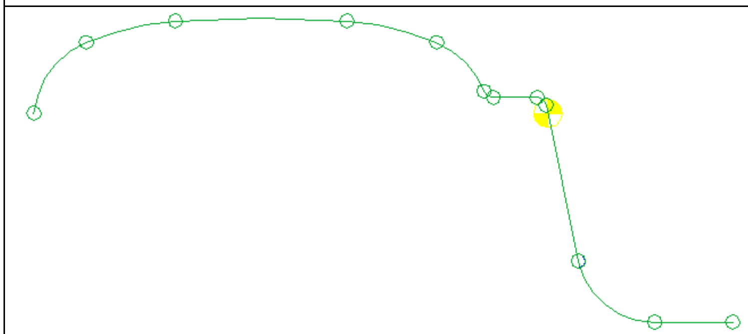	**A-4**: Sections 69 inches in front of the 0.5-inch point of frog
No. 24 (Blue) RBM frog with a conformal running surface No. 24 (Green) RBM frog with a flat running surface	

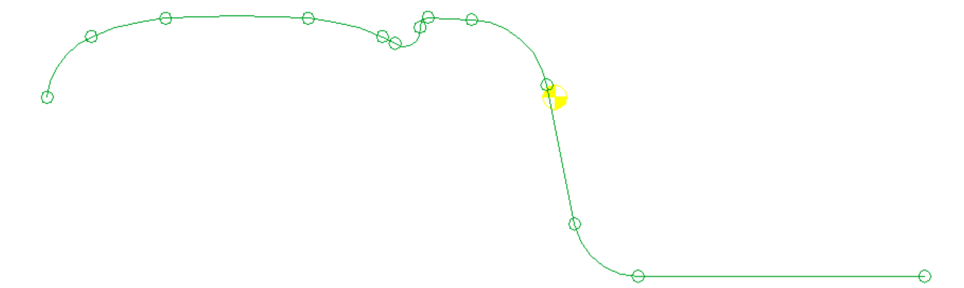	**A-5**: Sections 64 inches in front of the 0.5-inch point of frog
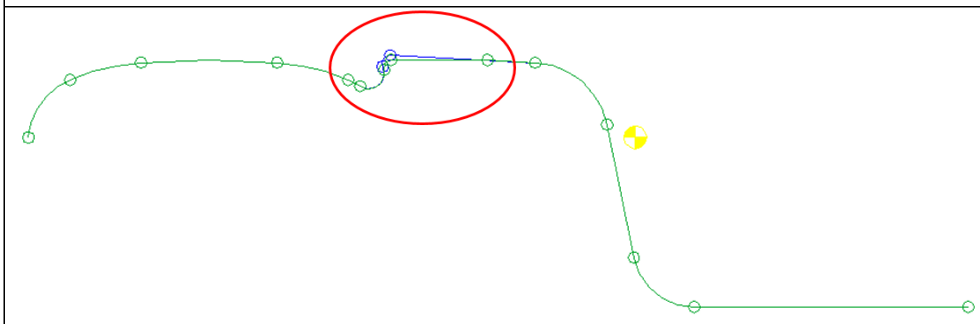	**A-6**: Sections 56 inches in front of the 0.5-inch point of frog
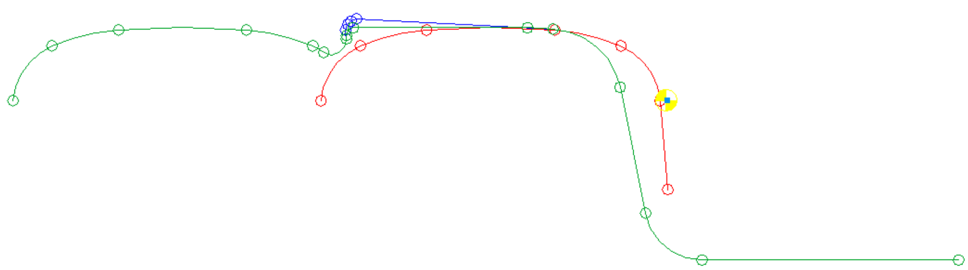	**A-7**: Sections 48 inches in front of the 0.5-inch point of frog
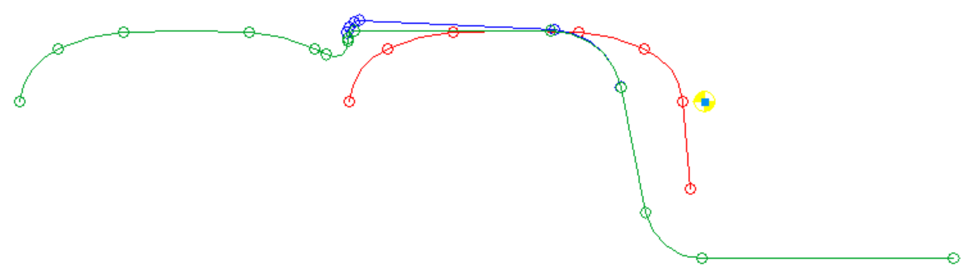	**A-8**: Sections 40 inches in front of the 0.5-inch point of frog
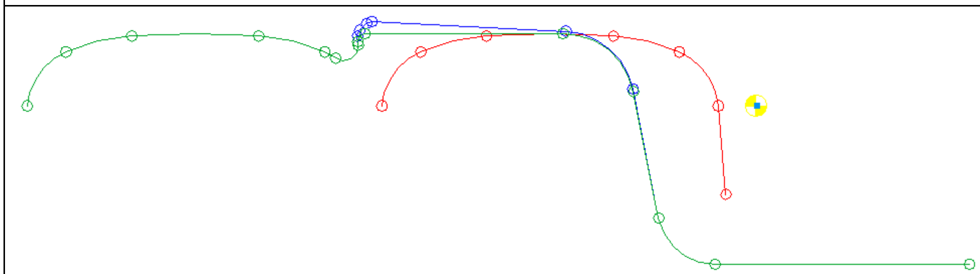	**A-9**: Sections 32 inches in front of the 0.5-inch point of frog
No. 24 (Red) Spring HPF No. 24 (Blue) RBM frog with a conformal running surface No. 24 (Green) RBM frog with a flat running surface	

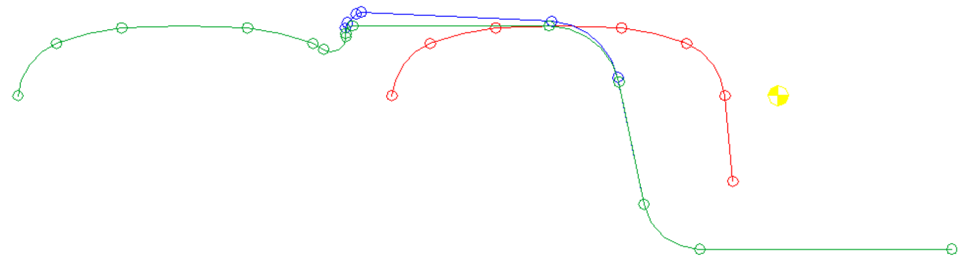	**A-10**: Sections 24 inches in front of the 0.5-inch point of frog
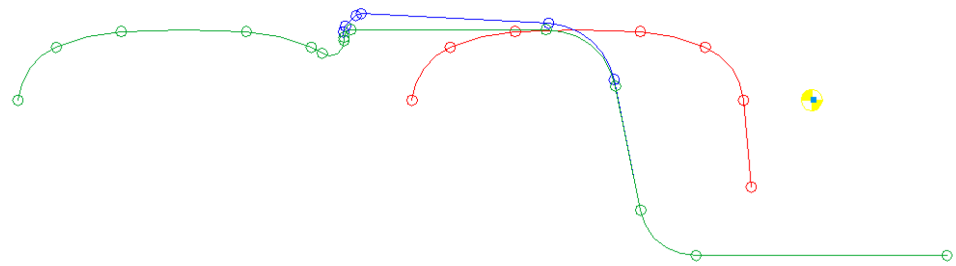	**A-11**: Sections 16 inches in front of the 0.5-inch point of frog
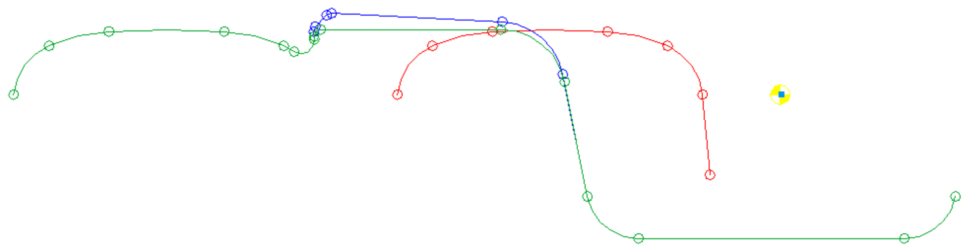	**A-12**: Sections 8 inches in front of the 0.5-inch point of frog
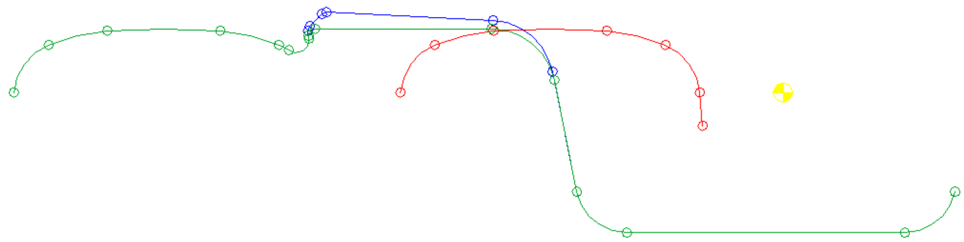	**A-13**: Sections 4 inches in front of the 0.5-inch point of frog
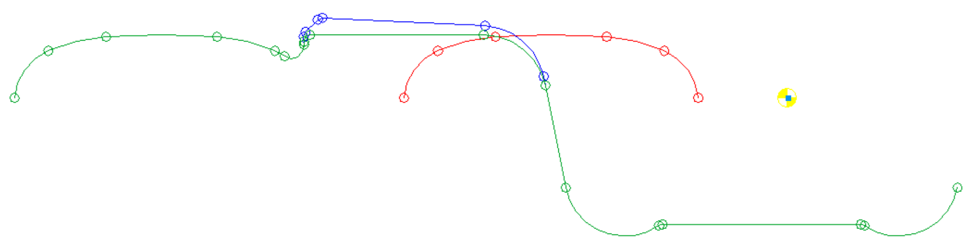	**A-14**: Sections of the 0.5-inch point of frog

No. 24 (Red) Spring HPF

No. 24 (Blue) RBM frog with a conformal running surface

No. 24 (Green) RBM frog with a flat running surface

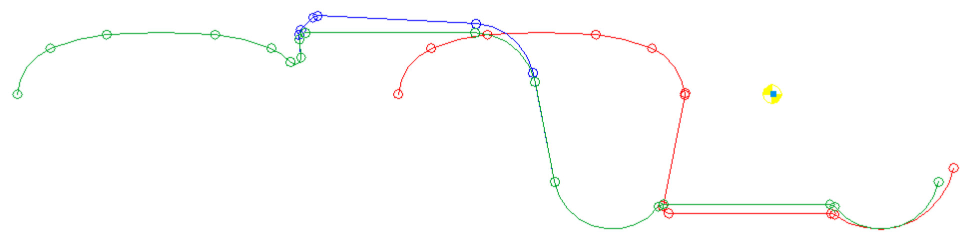	**A-15**: Sections 0.5 inch behind the 0.5-inch point of frog
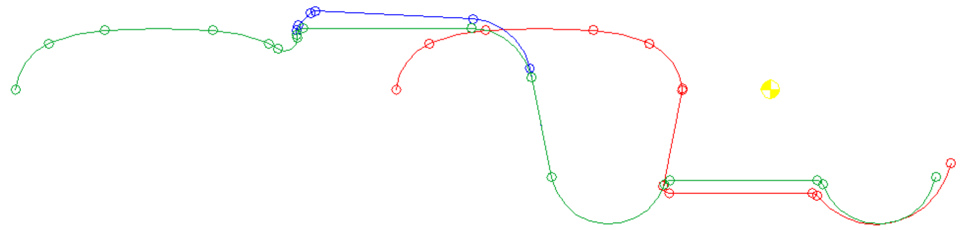	**A-16**: Sections 1 inch behind the 0.5-inch point of frog
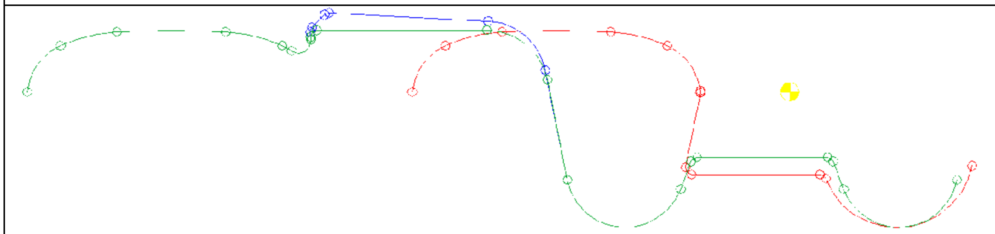	**A-17**: Sections 1.5 inches behind the 0.5-inch point of frog
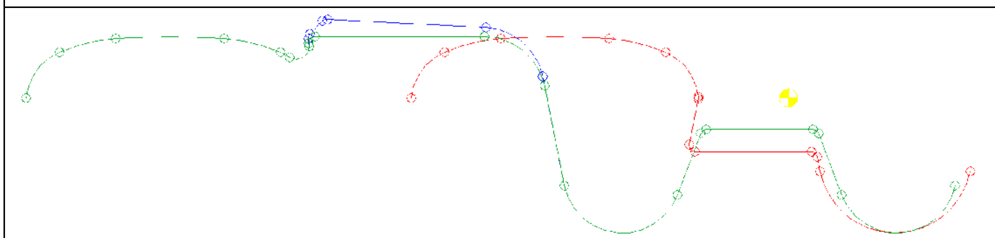	**A-18**: Sections 2 inches behind the 0.5-inch point of frog
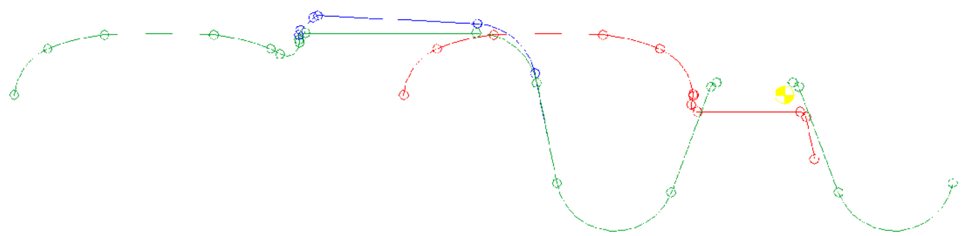	**A-19**: Sections 2.5 inches behind the 0.5-inch point of frog

No. 24 (Red) Spring HPF

No. 24 (Blue) RBM frog with a conformal running surface

No. 24 (Green) RBM frog with a flat running surface

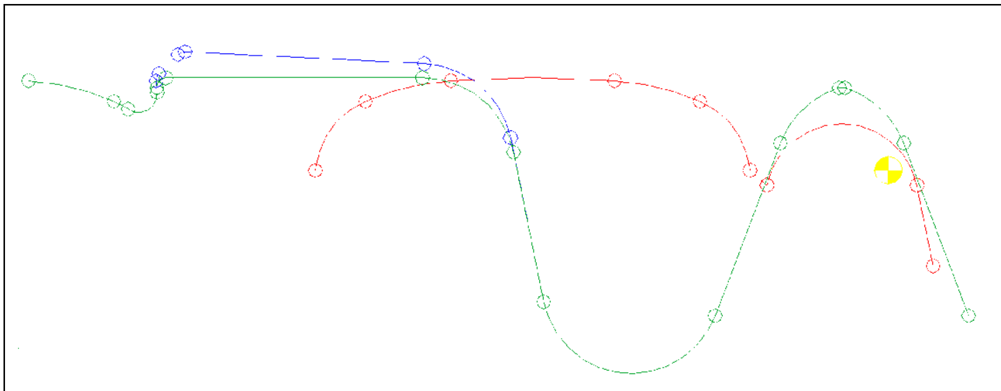	**A-20**: Sections 3 inches behind the 0.5-inch point of frog
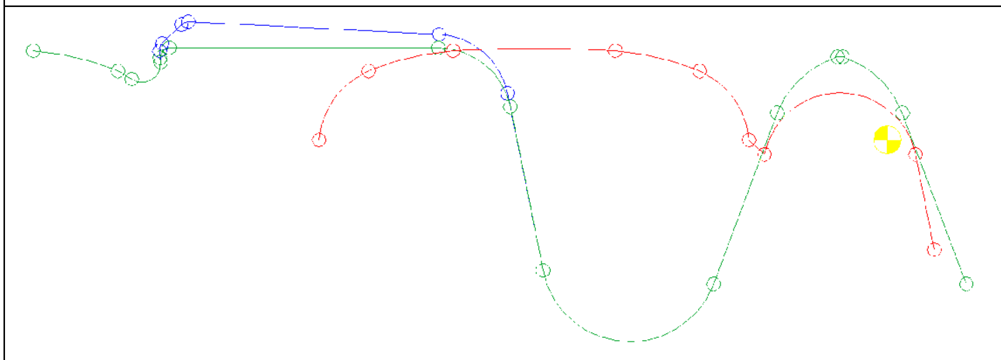	**A-21**: Sections 3.5 inches behind the 0.5-inch point of frog
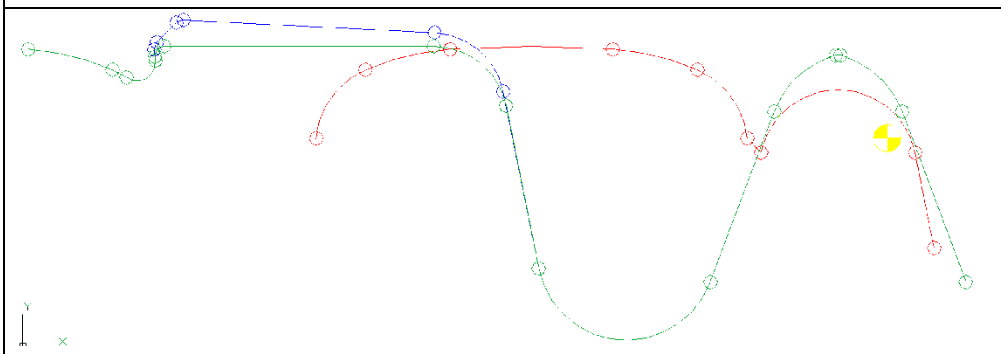	**A-22**: Sections 4 inches behind the 0.5-inch point of frog
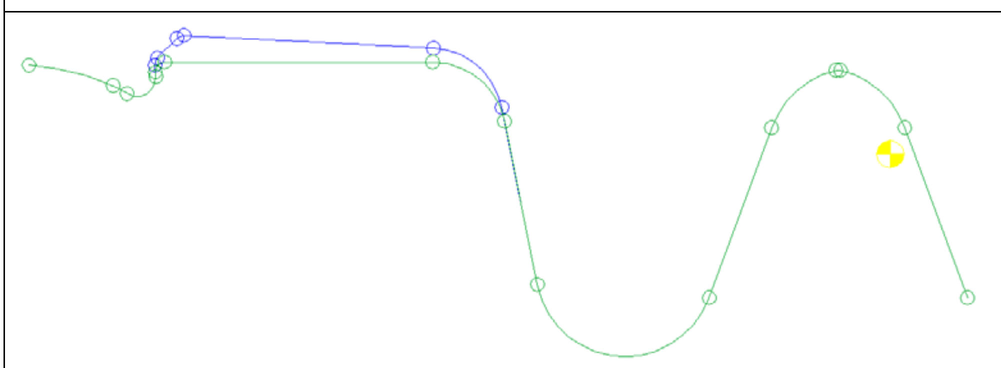	**A-23**: Sections 5 inches behind the 0.5-inch point of frog

No. 24 (Red) Spring HPF

No. 24 (Blue) RBM frog with a conformal running surface

No. 24 (Green) RBM frog with a flat running surface

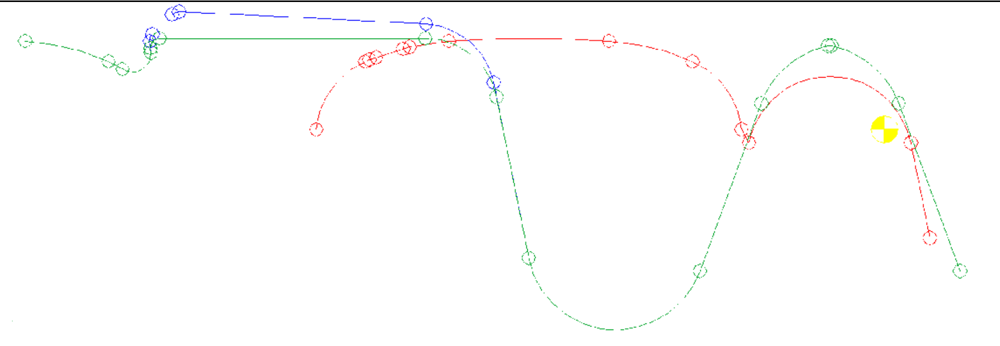	**A-24**: Sections 6 inches behind the 0.5-inch point of frog
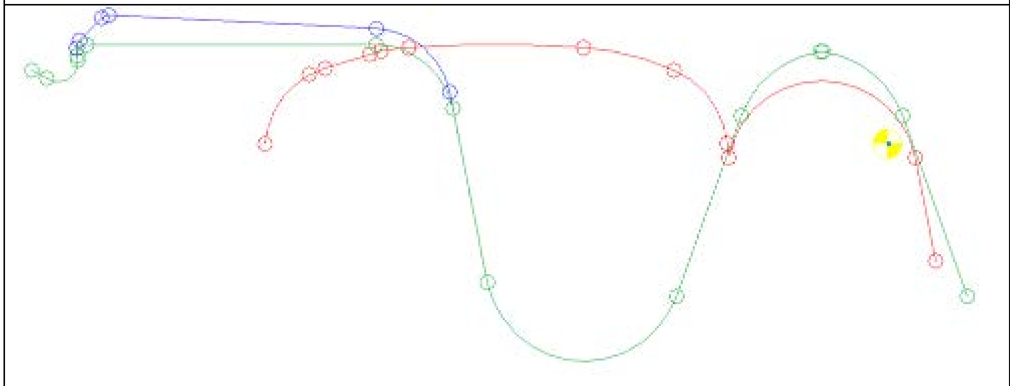	**A-25**: Sections 8 inches behind the 0.5-inch point of frog
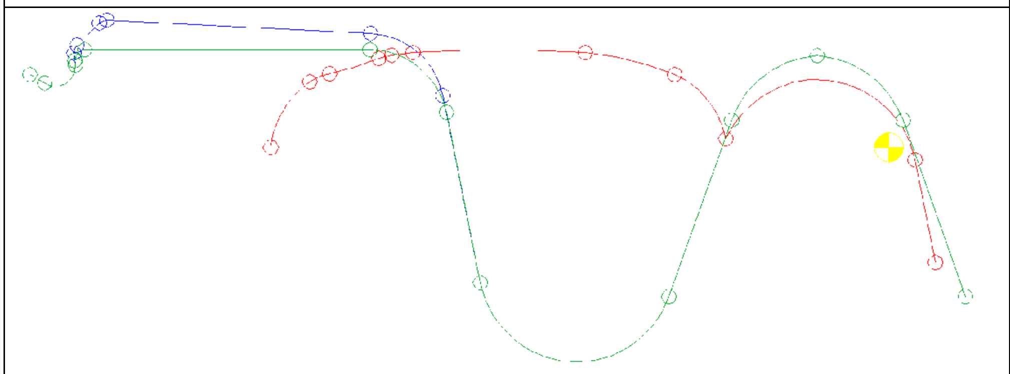	**A-26**: Sections 10 inches behind the 0.5-inch point of frog
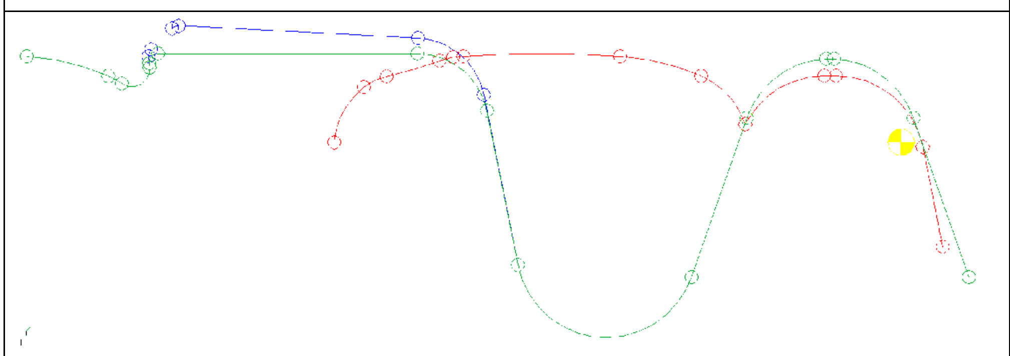	**A-27**: Sections 12 inches behind the 0.5-inch point of frog

No. 24 (Red) Spring HPF

No. 24 (Blue) RBM frog with a conformal running surface

No. 24 (Green) RBM frog with a flat running surface

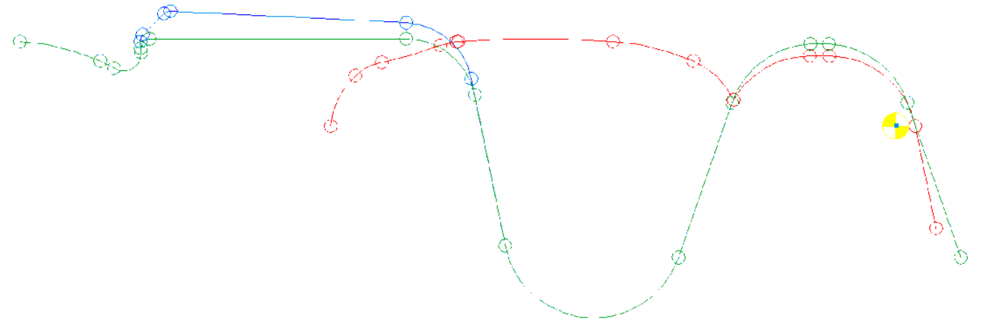	**A-28**: Sections 14 inches behind the 0.5-inch point of frog
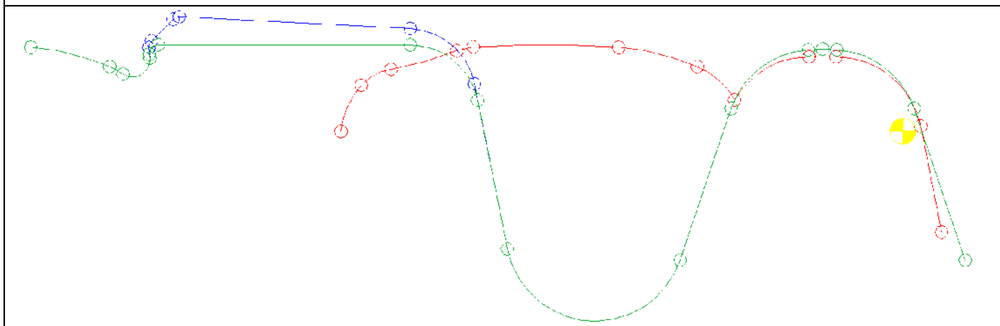	**A-29**: Sections 16 inches behind the 0.5-inch point of frog
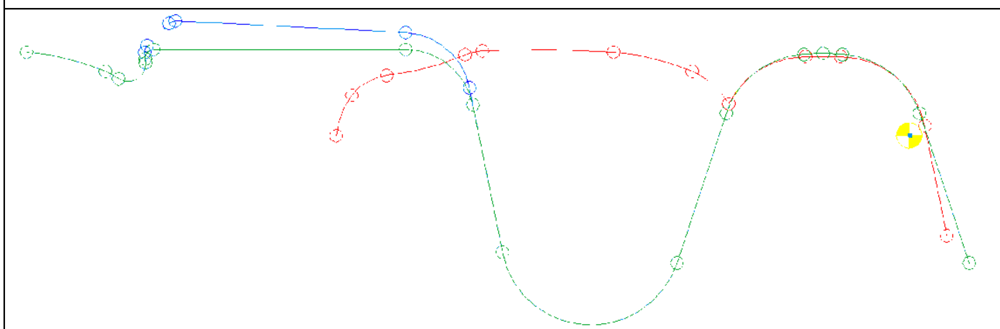	**A-30**: Sections 18 inches behind the 0.5-inch point of frog
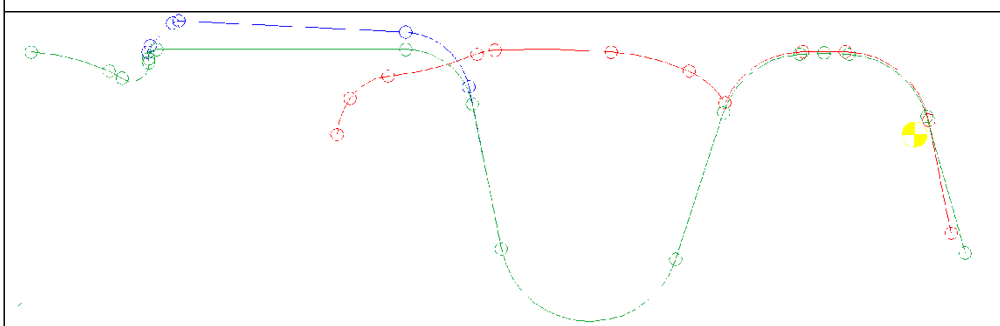	**A-31**: Sections 20 inches behind the 0.5-inch point of frog

No. 24 (Red) Spring HPF

No. 24 (Blue) RBM frog with a conformal running surface

No. 24 (Green) RBM frog with a flat running surface

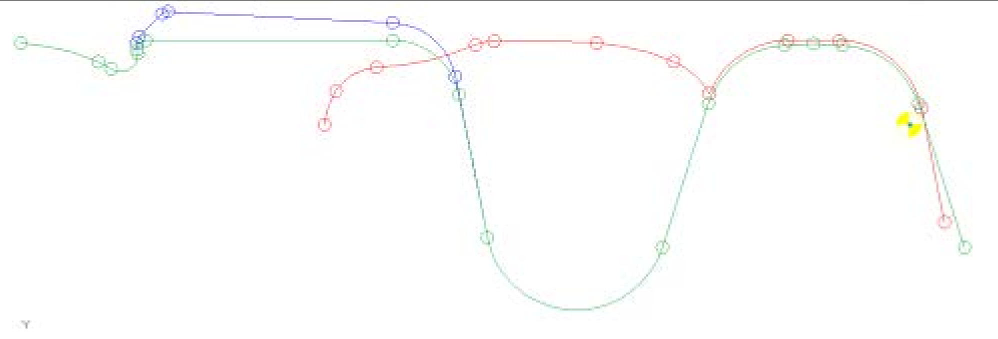	**A-32**: Sections 22 inches behind the 0.5-inch point of frog
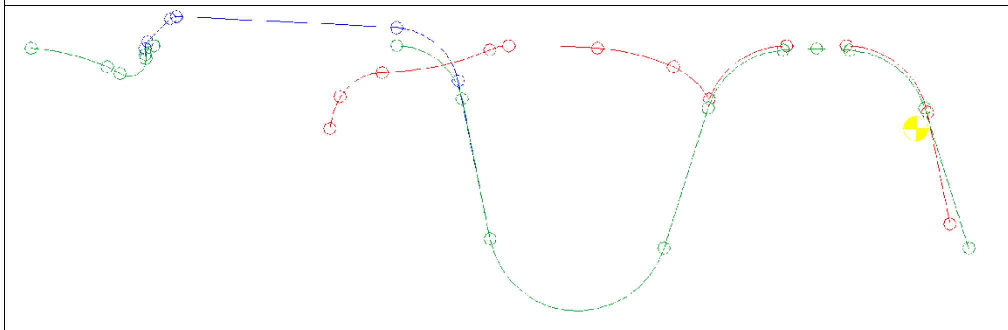	**A-33**: Sections 24 inches behind the 0.5-inch point of frog
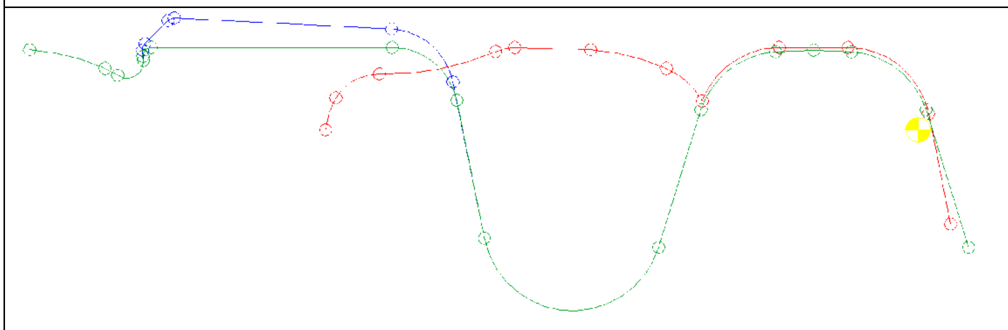	**A-34**: Sections 26 inches behind the 0.5-inch point of frog
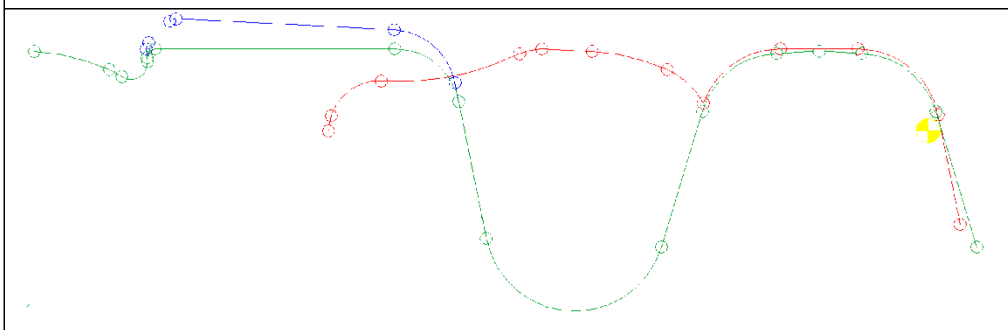	**A-35**: Sections 28 inches behind the 0.5-inch point of frog

No. 24 (Red) Spring HPF

No. 24 (Blue) RBM frog with a conformal running surface

No. 24 (Green) RBM frog with a flat running surface

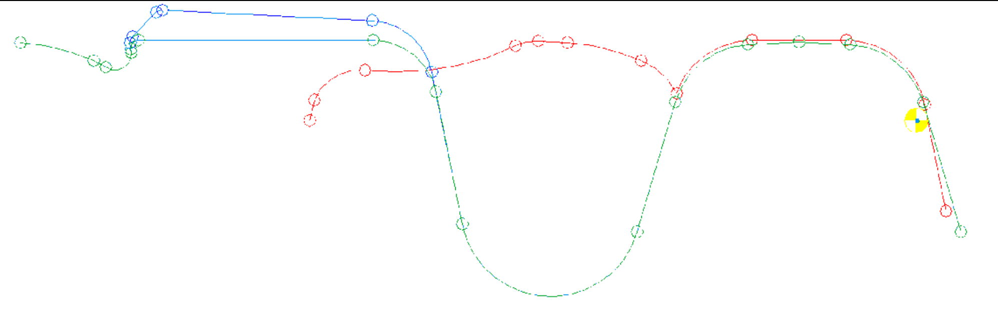	**A-36**: Sections 32 inches behind the 0.5-inch point of frog
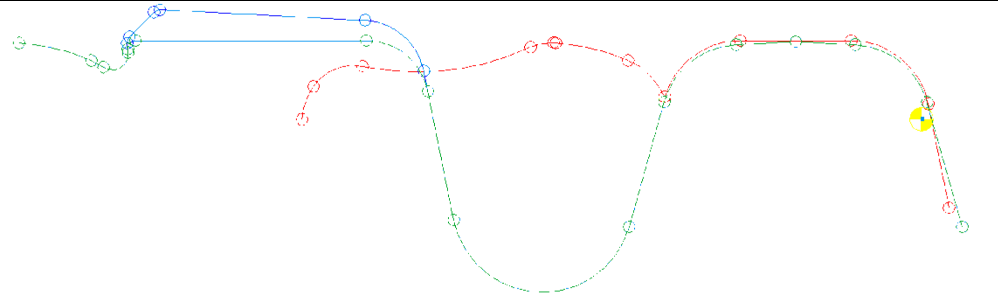	**A-37**: Sections 36 inches behind the 0.5-inch point of frog
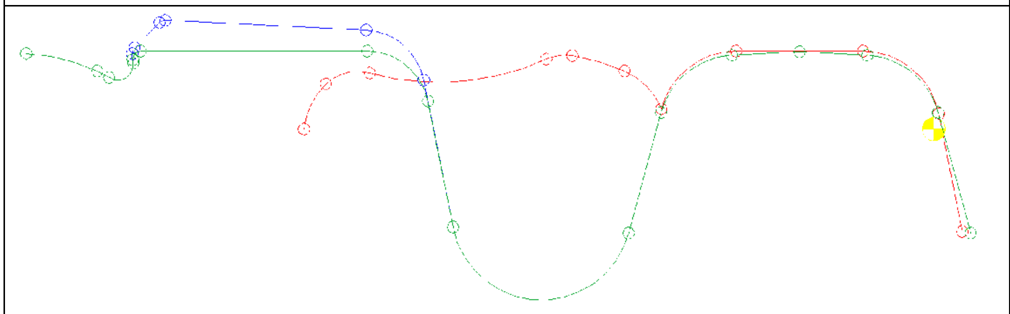	**A-38**: Sections 40 inches behind the 0.5-inch point of frog
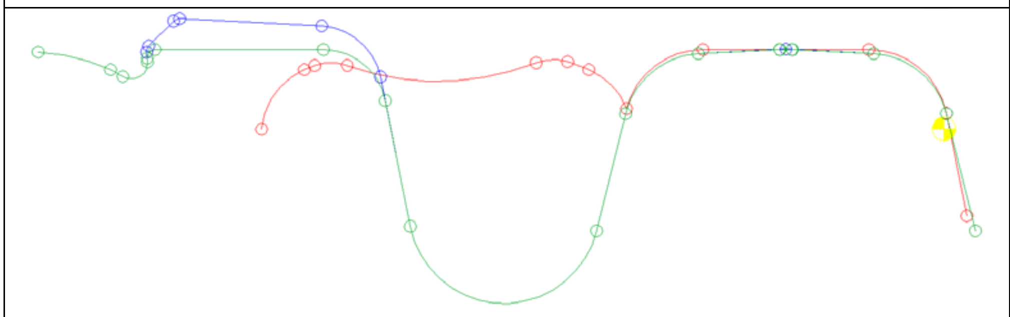	**A-39**: Sections 48 inches behind the 0.5-inch point of frog

No. 24 (Red) Spring HPF

No. 24 (Blue) RBM frog with a conformal running surface

No. 24 (Green) RBM frog with a flat running surface

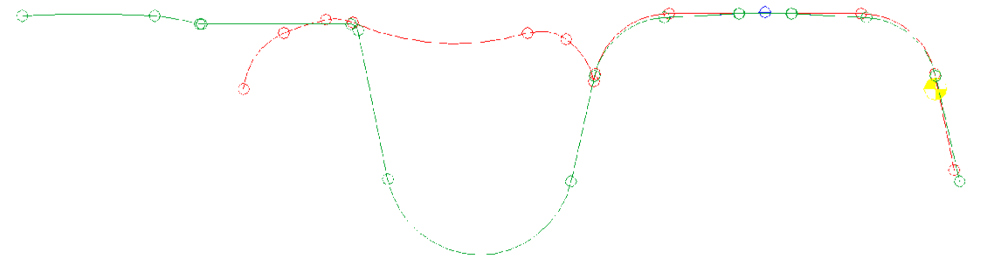	**A-40**: Sections 56 inches behind the 0.5-inch point of frog
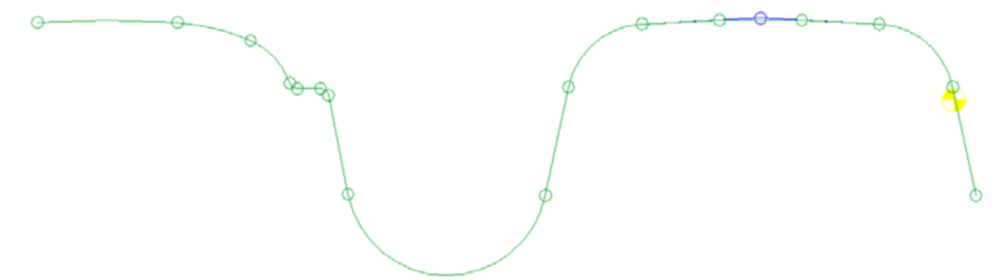	**A-41**: Sections 61 inches behind the 0.5-inch point of frog
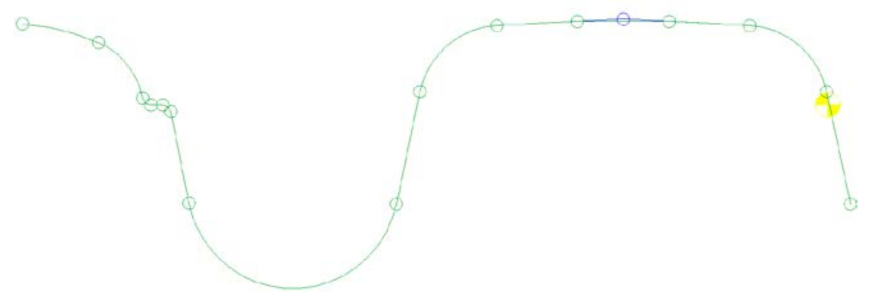	**A-42**: Sections 62 inches behind the 0.5-inch point of frog
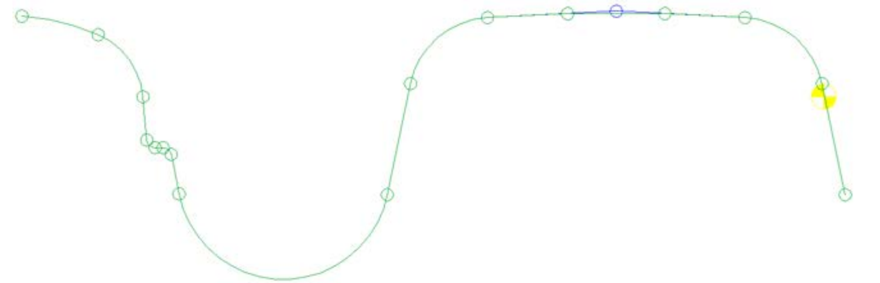	**A-43**: Sections 63 inches behind the 0.5-inch point of frog

No. 24: (Red) Spring HPF

No. 24: (Blue) RBM frog with a conformal running surface

No. 24: (Green) RBM frog with a flat running surface

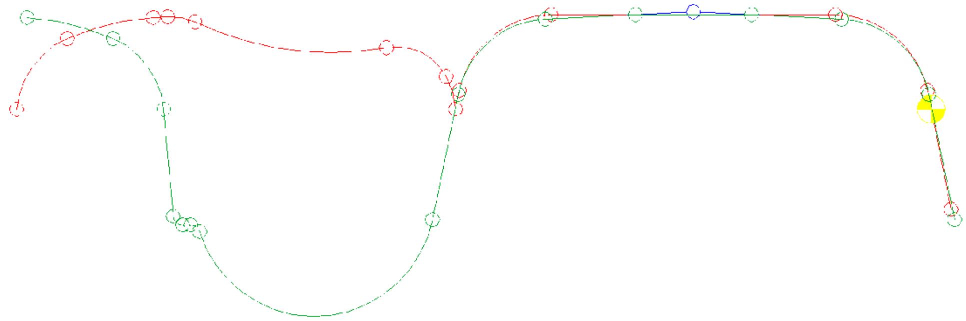	**A-44**: Sections 64 inches behind the 0.5-inch point of frog
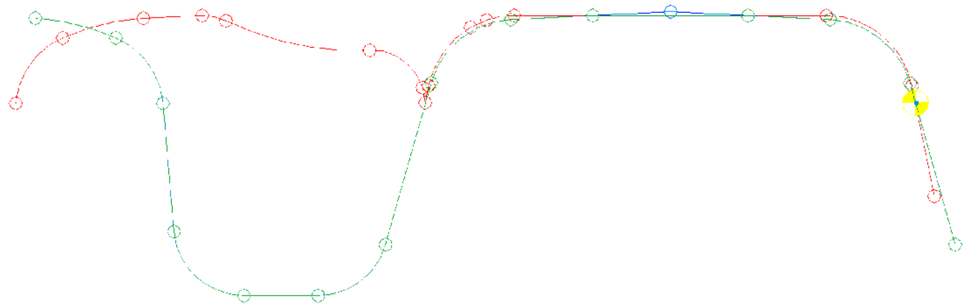	**A-45**: Sections 72 inches behind the 0.5-inch point of frog
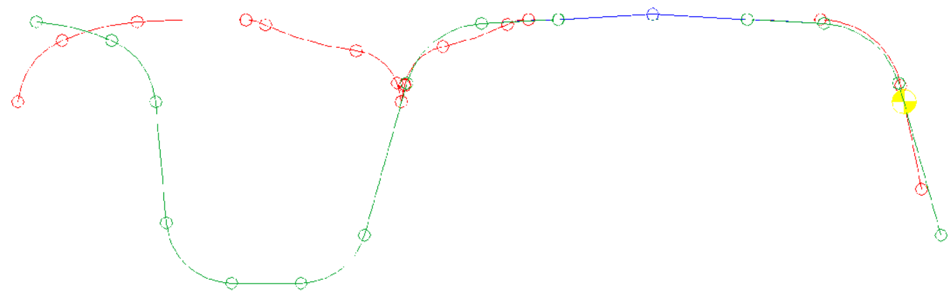	**A-46**: Sections 80 inches behind the 0.5-inch point of frog
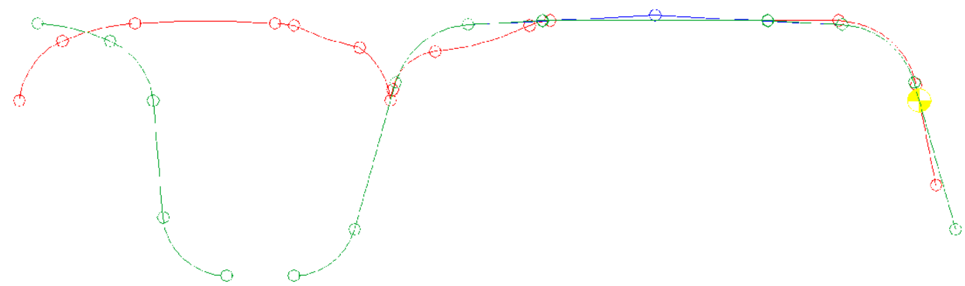	**A-47**: Sections 88 inches behind the 0.5-inch point of frog

No. 24: (Red) Spring HPF

No. 24: (Blue) RBM frog with a conformal running surface

No. 24: (Green) RBM frog with a flat running surface

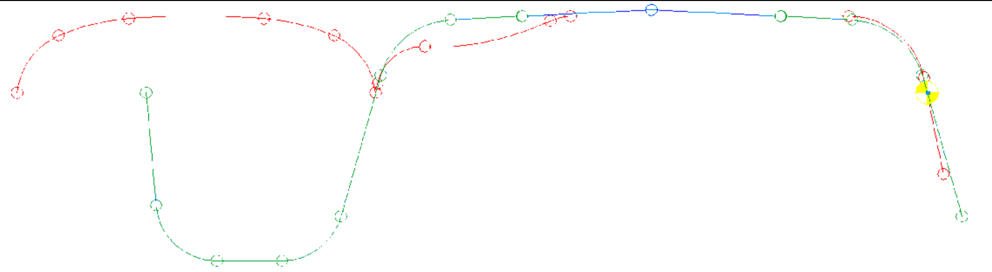	**A-48**: Sections 96 inches behind the 0.5-inch point of frog
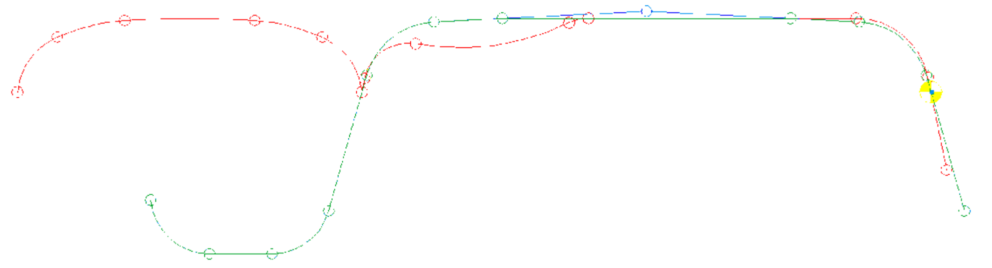	**A-49**: Sections 104 inches behind the 0.5-inch point of frog
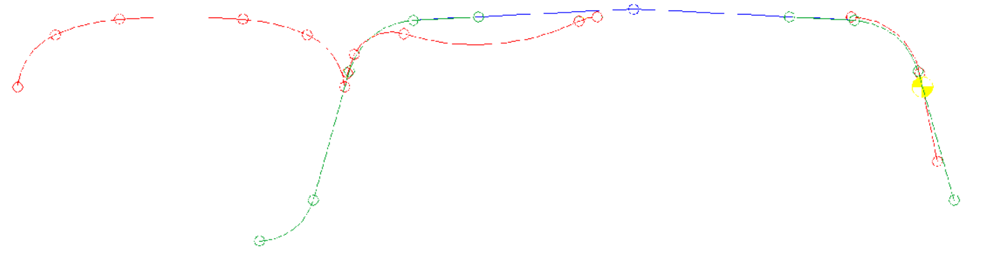	**A-50**: Sections 112 inches behind the 0.5-inch point of frog
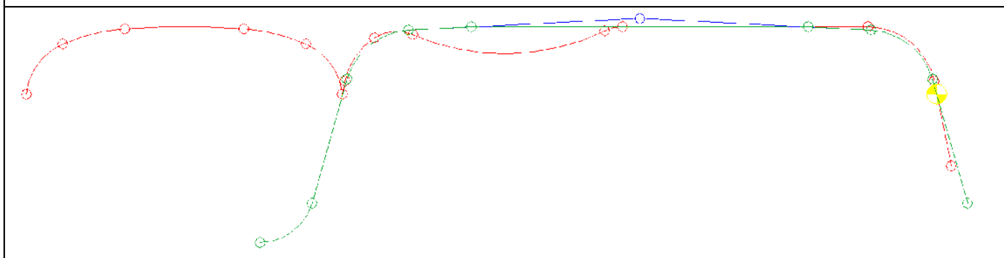	**A-51**: Sections 120 inches behind the 0.5-inch point of frog
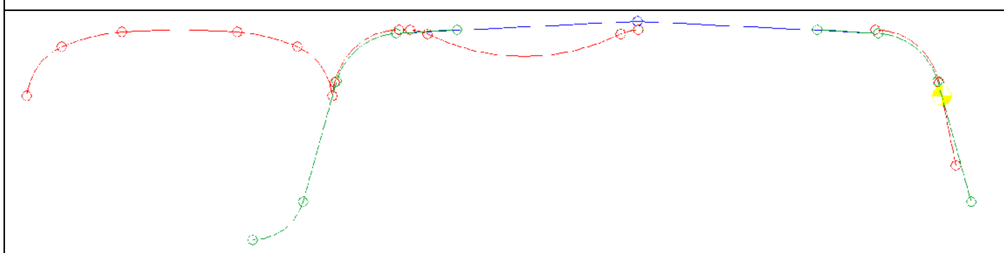	**A-52**: Sections 128 inches behind the 0.5-inch point of frog
No. 24: (Red) Spring HPF No. 24: (Blue) RBM frog with a conformal running surface No. 24: (Green) RBM frog with a flat running surface	

Appendix B
Setup of Design RBM and Spring HPFs

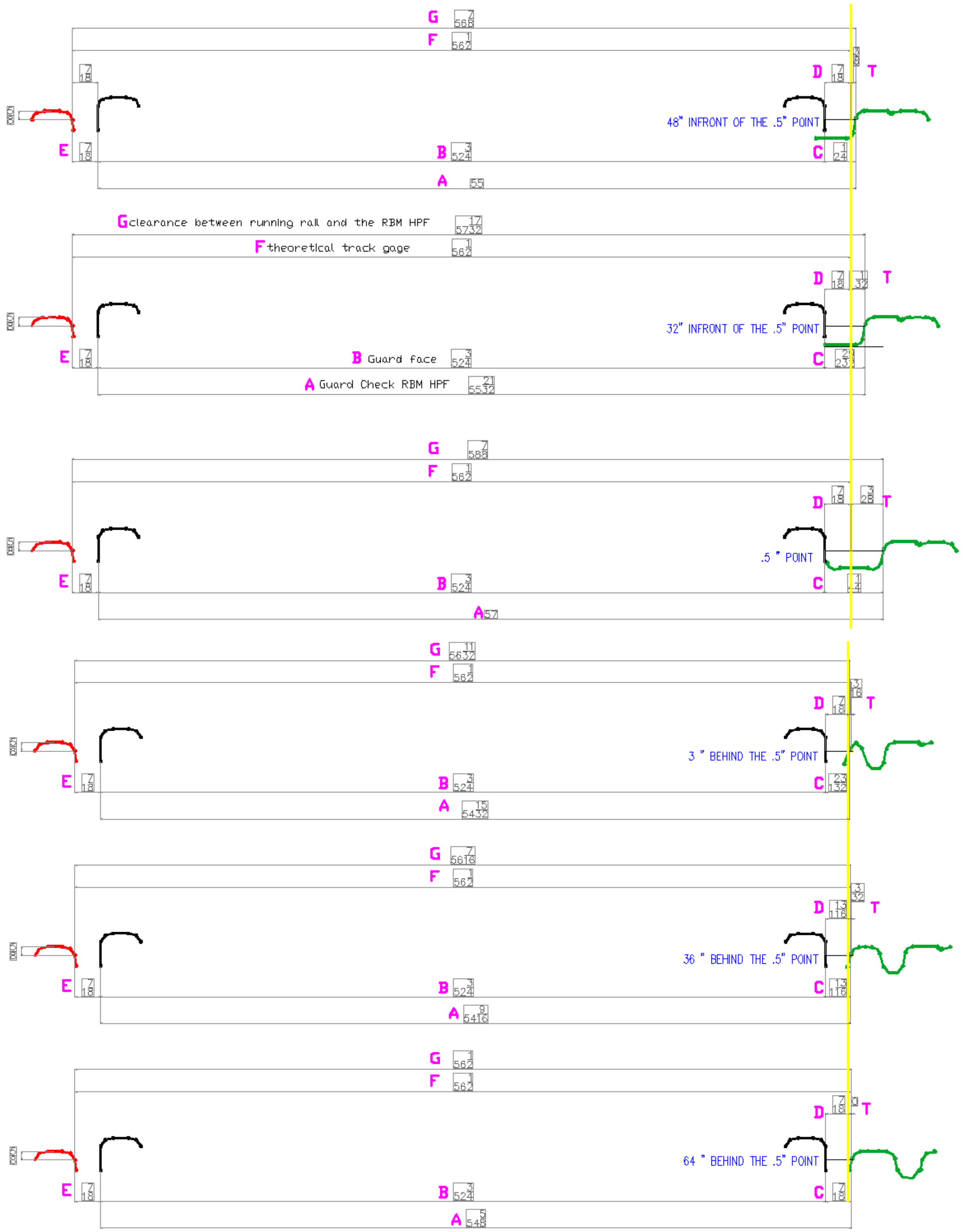

	RBM							
Section	Theoretical point to surface	Running rail to guard rail	HPF wing to theoretical gage	Clearance between the HPF point and wing	Theoretical track gage	Clearance between running rail and the point	Guard check	Guard face
	T	**E**	**D**	**C=D+T**	**F**	**G=F+T**	**A**	**B**
72" in front	0.12339	1.875	1.875	1.99839	56.5	56.62	54.75	52.75
71" in front	0.19313	1.875	1.875	2.06813	56.5	56.69	54.82	52.75
70" in front	0.22402	1.875	1.875	2.09902	56.5	56.72	54.85	52.75
69" in front	0	1.875	1.875	1.875	56.5	56.50	54.63	52.75
64" in front	0.04687	1.875	1.875	1.92187	56.5	56.55	54.67	52.75
56" in front	0.21607	1.875	1.875	2.09107	56.5	56.72	54.84	52.75
48" in front	0.39004	1.875	1.875	2.26504	56.5	56.89	55.02	52.75
40" in front	0.72688	1.875	1.875	2.60188	56.5	57.23	55.35	52.75
32" in front	1.06359	1.875	1.875	2.93859	56.5	57.56	55.69	52.75
24" in front	1.39993	1.875	1.875	3.27493	56.5	57.90	56.02	52.75
16" in front	1.73645	1.875	1.875	3.61145	56.5	58.24	56.36	52.75
8" in front	2.07296	1.875	1.875	3.94796	56.5	58.57	56.70	52.75
4" in front	2.24122	1.875	1.875	4.11622	56.5	58.74	56.87	52.75
POINT	2.40944	1.875	1.875	4.28444	56.5	58.91	57.03	52.75
0.5" behind	2.43048	1.875	1.875	4.30548	56.5	58.93	57.06	52.75
1" behind	2.4515	1.875	1.875	4.3265	56.5	58.95	57.08	52.75
1.5" behind	2.47214	1.875	1.875	4.34714	56.5	58.97	57.10	52.75
2" behind	2.49317	1.875	1.875	4.36817	56.5	58.99	57.12	52.75
2.5" behind	-0.17331	1.875	1.875	1.70169	56.5	**56.33**	**54.45**	52.75
3" behind	-0.17201	1.875	1.875	1.70299	56.5	**56.33**	**54.45**	52.75
3.5" behind	-0.17065	1.875	1.875	1.70435	56.5	**56.33**	**54.45**	52.75
4" behind	-0.16928	1.875	1.875	1.70572	56.5	**56.33**	**54.46**	52.75
5" behind	-0.16655	1.875	1.875	1.70845	56.5	**56.33**	**54.46**	52.75
6" behind	-0.16382	1.875	1.875	1.71118	56.5	**56.34**	**54.46**	52.75
8" behind	-0.15836	1.875	1.875	1.71664	56.5	**56.34**	**54.47**	52.75
10" behind	-0.15289	1.875	1.875	1.72211	56.5	**56.35**	**54.47**	52.75
12" behind	-0.14743	1.875	1.875	1.72757	56.5	**56.35**	**54.48**	52.75
14" behind	-0.14197	1.875	1.875	1.73303	56.5	**56.36**	**54.48**	52.75
16" behind	-0.13651	1.875	1.875	1.73849	56.5	**56.36**	**54.49**	52.75
18" behind	-0.13104	1.875	1.875	1.74396	56.5	**56.37**	**54.49**	52.75
20" behind	-0.12556	1.875	1.875	1.74944	56.5	**56.37**	**54.50**	52.75
22" behind	-0.12012	1.875	1.875	1.75488	56.5	**56.38**	**54.50**	52.75
24" behind	-0.11466	1.875	1.875	1.76034	56.5	**56.39**	**54.51**	52.75
26" behind	-0.1092	1.875	1.875	1.7658	56.5	**56.39**	**54.52**	52.75
28" behind	-0.10375	1.875	1.875	1.77125	56.5	**56.40**	**54.52**	52.75
32" behind	-0.09281	1.875	1.875	1.78219	56.5	**56.41**	**54.53**	52.75
36" behind	-0.08189	1.875	1.875	1.79311	56.5	**56.42**	**54.54**	52.75
40" behind	-0.07097	1.875	1.875	1.80403	56.5	**56.43**	**54.55**	52.75
48" behind	-0.04913	1.875	1.875	1.82587	56.5	**56.45**	**54.58**	52.75
56" behind	-0.02481	1.875	1.875	1.85019	56.5	**56.48**	**54.60**	52.75
61" behind	0	1.875	1.875	1.875	56.5	56.50	54.63	52.75
62" behind	0	1.875	1.875	1.875	56.5	56.50	54.63	52.75

63" behind	0	1.875	1.875	1.875	56.5	56.50	54.63	52.75
64" behind	0	1.875	1.875	1.875	56.5	56.50	54.63	52.75
72" behind	0	1.938	1.875	1.875	56.5	56.50	54.56	52.69
80" behind	0	2.094	1.875	1.875	56.5	56.50	54.41	52.53
88" behind	0	2.250	1.875	1.875	56.5	56.50	54.25	52.38
96" behind	0	2.406	1.875	1.875	56.5	56.50	54.09	52.22
104" behind	0	2.594	1.875	1.875	56.5	56.50	53.91	52.03
112" behind	0	2.750	1.875	1.875	56.5	56.50	53.75	51.88
120" behind	0	2.906	1.875	1.875	56.5	56.50	53.59	51.72
128" behind	0	3.063	1.875	1.875	56.5	56.50	53.44	51.56
							≥ 54.5"	**≤ 53"**
					min	56.33	53.44	51.56
					max	58.99	57.12	52.75

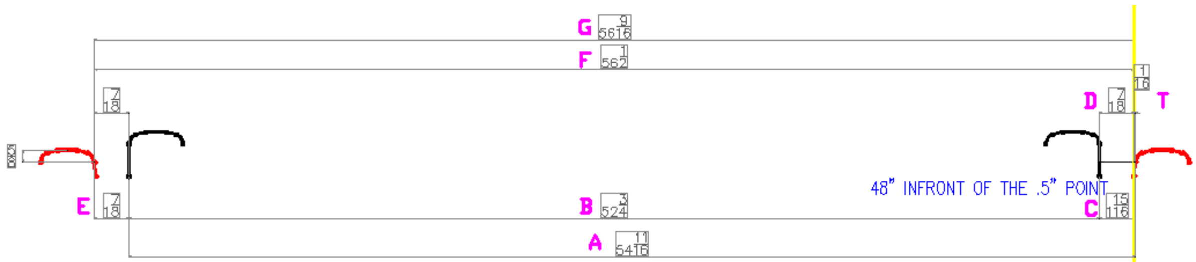
G 56 9/16
F 56 1/2
7/16
D 7/16
1/16
T
E 7/16
B 52 3/4
48" INFRONT OF THE .5" POINT
C 1 15/16
A 54 11/16

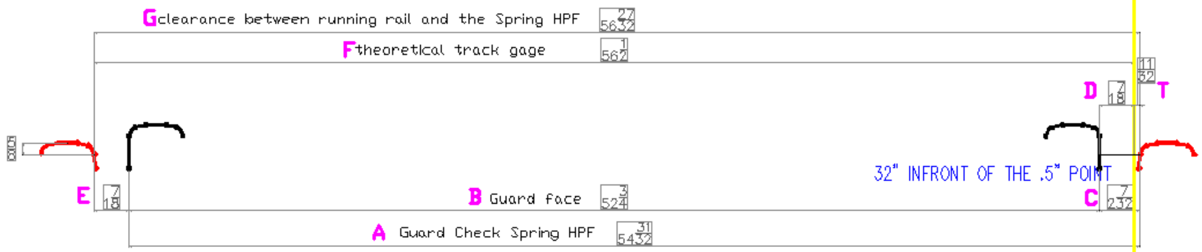
G clearance between running rail and the Spring HPF 56 27/32
F theoretical track gage 56 1/2
11/32
D 7/16
T
E 7/16
B Guard face 52 3/4
32" INFRONT OF THE .5" POINT
C 2 7/32
A Guard Check Spring HPF 54 31/32

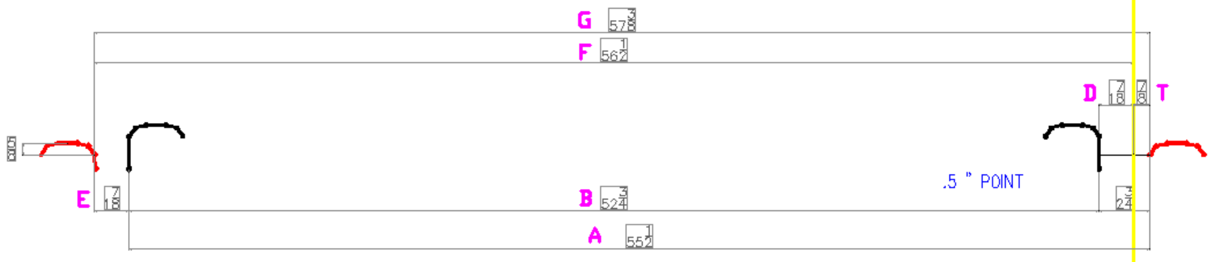
G 57 3/8
F 56 1/2
D 7/16
7/8
T
E 7/16
B 52 3/4
.5 " POINT
2 3/4
A 55 1/2

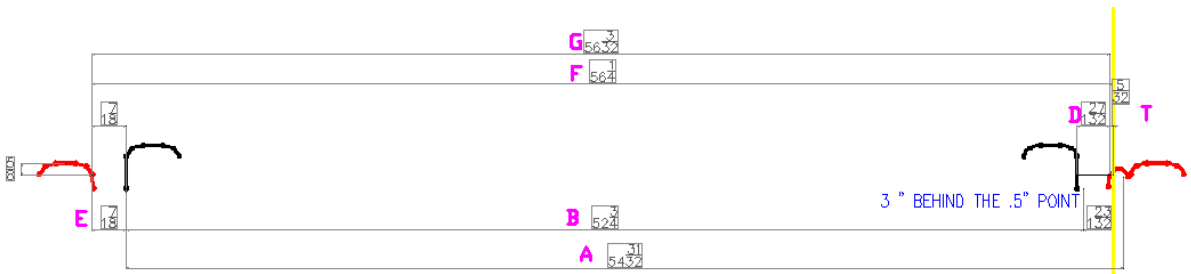
G 56 3/32
F 56 1/4
7/16
5/32
D 1 27/32
T
E 7/16
B 52 3/4
3 " BEHIND THE .5" POINT
1 23/32
A 54 31/32

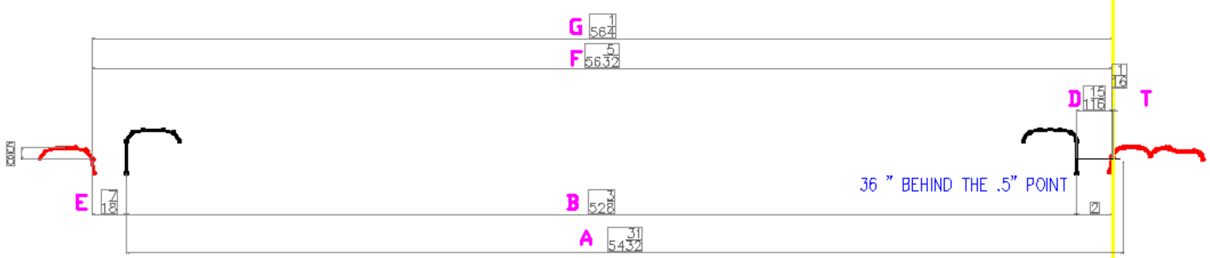
G 56 1/4
F 56 5/32
1/16
D 1 15/16
T
E 7/16
B 52 3/8
36 " BEHIND THE .5" POINT
2
A 54 31/32

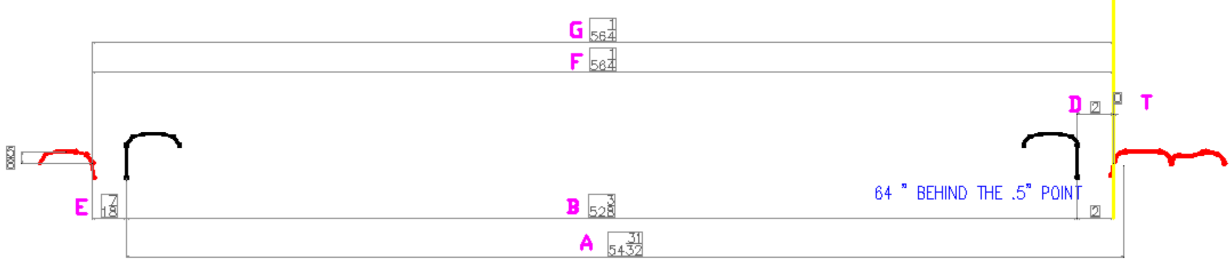
G 56 1/4
F 56 1/4
D 2
0
T
E 7/16
B 52 3/8
64 " BEHIND THE .5" POINT
2
A 54 31/32

	Spring Frog							
Section	theoretical point to surface	running rail to guard rail	HPF wing to theoretical gage	clearance between the HPF point and wing	theoretical track gage	clearance between running rail and the point	Guard check	Guard face
	T	**E**	**D**	**C=D+T**	**F**	**G=F+T**	**A**	**B**
48" in front	0.05448	1.875	2	2.05448	56.5	56.55	54.68	52.63
40" in front	0.19152	1.875	2	2.19152	56.5	56.69	54.82	52.63
32" in front	0.32936	1.875	2	2.32936	56.5	56.83	54.95	52.63
24" in front	0.46703	1.875	2	2.46703	56.5	56.97	55.09	52.63
16" in front	0.60479	1.875	2	2.60479	56.5	57.10	55.23	52.63
8" in front	0.74255	1.875	2	2.74255	56.5	57.24	55.37	52.63
4" in front	0.81215	1.875	2	2.81215	56.5	57.31	55.44	52.63
POINT	0.88039	1.875	2	2.88039	56.5	57.38	55.51	52.63
2" behind	0.91483	1.875	2	2.91483	56.5	57.41	55.54	52.63
4" behind	-0.15889	1.875	2	1.84111	56.5	**56.34**	**54.47**	52.63
6" behind	-0.15503	1.875	2	1.84497	56.5	**56.34**	**54.47**	52.63
8" behind	-0.15084	1.875	2	1.84916	56.5	**56.35**	**54.47**	52.63
10" behind	-0.14641	1.875	2	1.85359	56.5	**56.35**	**54.48**	52.63
12" behind	-0.14511	1.875	2	1.85489	56.5	**56.35**	**54.48**	52.63
14" behind	-0.14015	1.875	2	1.85985	56.5	**56.36**	**54.48**	52.63
16" behind	-0.13465	1.875	2	1.86535	56.5	**56.37**	**54.49**	52.63
18" behind	-0.12894	1.875	2	1.87106	56.5	**56.37**	**54.50**	52.63
20" behind	-0.12322	1.875	2	1.87678	56.5	**56.38**	**54.50**	52.63
22" behind	-0.1175	1.875	2	1.8825	56.5	**56.38**	**54.51**	52.63
24" behind	-0.11178	1.875	2	1.88822	56.5	**56.39**	**54.51**	52.63
26" behind	-0.10605	1.875	2	1.89395	56.5	**56.39**	**54.52**	52.63
28" behind	-0.10032	1.875	2	1.89968	56.5	**56.40**	**54.52**	52.63
32" behind	-0.09375	1.875	2	1.90625	56.5	**56.41**	**54.53**	52.63
36" behind	-0.07741	1.875	2	1.92259	56.5	**56.42**	**54.55**	52.63
40" behind	-0.06596	1.875	2	1.93404	56.5	**56.43**	**54.56**	52.63
48" behind	-0.04303	1.875	2	1.95697	56.5	**56.46**	**54.58**	52.63
56" behind	-0.02011	1.875	2	1.97989	56.5	**56.48**	**54.60**	52.63
64" behind	0	1.875	2	2	56.5	56.50	54.63	52.63
72" behind	0	1.938	2	2	56.5	56.50	54.56	52.56
80" behind	0	2.094	2	2	56.5	56.50	54.41	52.41
88" behind	0	2.250	2	2	56.5	56.50	54.25	52.25
96" behind	0	2.406	2	2	56.5	56.50	54.09	52.09
104" behind	0	2.594	2	2	56.5	56.50	53.91	51.91
112" behind	0	2.750	2	2	56.5	56.50	53.75	51.75
120" behind	0	2.906	2	2	56.5	56.50	53.59	51.59
128" behind	0	3.063	2	2	56.5	56.50	53.44	51.44
							≥ 54.5"	**≤ 53"**
					min	56.34	53.44	51.44
					max	57.41	55.54	52.63

Abbreviations and Acronyms

AAR	Association of American Railroads
APTA	American Public Transportation Association
CFR	Code of Federal Regulations
FRA	Federal Railroad Administration
HPF	heavy point frog
HSR	high-speed rail
IDOT	Illinois Department of Transportation
IWS	instrumented wheelset
L/V	lateral/vertical ratio
MP	mile post
RBM	rail-bound manganese
TTC	Transportation Technology Center (the facility)
TTCI	Transportation Technology Center, Inc. (the company)
VTI	Vehicle Track Interaction
W/R	wheel/rail